# STUDIES ON STRUCTURAL RELATIONS IN CRYSTALLINE AND VITREOUS COMPOUNDS

FINAL TECHNICAL REPORT

by

PEDER KIERKEGAARD
STIG AXRUP
GUNILLA BARVLING
KAIJA EISTRAT
LARS-OVE HAGMAN
MATS ISRAELSSON
LARS KIHLBORG
ANN KOPWILLEM
BARBRO LINNROS
MADELEINE SELEBORG



March 1968
EUROPEAN RESEARCH OFFICE
UNITED STATES ARMY

Contract Number DAJA37-67-C-0421

UNIVERSITY OF STOCKHOLM
INSTITUTE OF INORGANIC AND PHYSICAL CHEMISTRY
STOCKHOLM, SWEDEN

AD .

# STUDIES ON STRUCTURAL RELATIONS IN CRYSTALLINE AND VITREOUS COMPOUNDS

FINAL TECHNICAL REPORT

By

PEDER KIERKEGAARD

STIG AXRUP
GUNILLA BARVLING
KAIJA EISTRAT
LARS-OVE HAGMAN
MATS ISRAELSSON
LARS KIHLBORG
ANN KOPWILLEM
BARBRO LINNROS
MADELEINE SELEBORG

March 1968

EUROPEAN RESEARCH OFFICE
UNITED STATES ARMY

Contract number DAJA37-67-C-0421

UNIVERSITY OF STOCKHOLM
INSTITUTE OF INORGANIC AND PHYSICAL CHEMISTRY
STOCKHOLM, SWEDEN

BLANK PAGE

CONTENTS

ABSTRACT

The work reported in this document is a continuation of studies on structural relations in crystalline and vitreous compounds containing hexacoordinating and tetracoordinating elements.

Studies on the structural properties of crystalline and vitreous polymolybdates and polywolframates have been performed. Results obtained from X-ray studies on sodium dimolybdate and diwolframate are reported and discussed. Details of the structural investigation of dipotassium tetrawolframate are given.

The research work has also comprised some studies on glasses and crystalline substances on arsenate molybdate (wolframate) basis containing alkali or silver atoms.

Structural data are given for the crystalline compounds $NaZr_2(PO_4)_3$ and $U(PO_3)_4$.

Studies on the structural conditions in the ternary oxide systems containing vanadium and molybdenum or wolfram have been performed. Description of the structures are given for the crystalline phases $(Mo_{0.93}V_{0.07})_5O_{14}$, $W_{0.375}V_{0.625}O_{2.5}$ and $W_{0.35}O_{0.65}O_{2.5}$.

Preliminary results are given for investigations of copper wolfram oxides. X-ray investigations have been performed on the compounds $CuWO_{4-x}$ and $Cu_3WO_6$.

The preparation and properties of amorphous molybdenum trioxide are described.

A summary of the types of calculations carried out by computer within this research project is given.

Apparatus and measuring techniques for studies of magnetic susceptibility of vitreous and crystalline specimens have been developed. Measurements over the temperature region $90^{\circ}K$ - $298^{\circ}K$ have been performed on the crystalline compounds

$MoOPO_4$ and $W_2O_3(PO_4)_2$ and glasses prepared from these phases. The crystals of $MoOPO_4$ have been found to be paramagnetic while the other compounds are diamagnetic.

Plans for further research within this field are outlined.

## 1. INTRODUCTION AND BACKGROUND OF THE RESEARCH

The research reported in this document has been carried out during the third year of a research program sponsored by the U.S. Department of Army, through its European Research Office. The results obtained during the previous two years have been communicated in two annual reports and also described in a series of published articles and in several papers to be published, viz.:

"Structural Studies on Vitreous Compounds." Contract number DA-91-591-EUC-3635. Final Technical Report (April 1966). (P. Kierkegaard, K. Eistrat, K. Gustafsson, K.-E. Johansson and A. Skancke)

"Studies on Structural Relations in Crystalline and Vitreous Compounds." Contract number DA-91-591-EUC-3980. Final Technical Report (March 1967). (P. Kierkegaard, S. Axrup, B. Linnros, M. Nygren, M. Seleborg, K. Eistrat and M. Sundbäck)

"The Crystal Structure of Dipotassium Trimolybdate." Acta Chem. Scand. 20 (1966) 2195-2201. (M. Seleborg)

"A Refinement of the Crystal Structure of Disodium Dimolybdate." Acta Chem. Scand. 21 (1967) 499-504. (M. Seleborg)

"X-Ray Studies on Some Wolfram Oxide Phosphate Glasses." Arkiv Kemi 27 (1967) 197-212. (A. Skancke and P. Kierkegaard)

"Tunnel Structure of $K_2W_4O_{13}$." Chem. Comm. (1967) 1126-1127. (M. Seleborg)

"The Crystal Structure of $(Mo_{0.3}W_{0.7})_2O_5$ of $\underline{R}$-$Nb_2O_5$ Type and a Comparison with the Structures of $V_2O_5$ and $V_2MoO_8$." Acta Chem. Scand. 21 (1967) 2495-2502. (L. Kihlborg)

"Tracing Phase Transitions by Means of High Frequency ac Measurements Using a Q-meter." Arkiv Kemi 28 (1968) 2217-2221. (M. Nygren and A. Magnéli)

"The Crystal Structure of $NaMe^{IV}_2(PO_4)_3$, $\underline{Me}^{IV}$ = Ge, Ti, Zr." Accepted for publication in Acta Chem. Scand. (L.-O. Hagman and P. Kierkegaard)

"An X-Ray Diffractometer for Investigations of Vitreous and Liquid Materials at Room and Elevated Temperatures." (P. Kierkegaard and K.-E. Johansson)

"Crystal Structure of a New Copper Wolfram Oxide, $Cu_3WO_6$." (E. Gebert and L. Kihlborg)

"The Crystal Structure of $CuWO_{4-\underline{x}}$." (L. Kihlborg and E. Gebert)

"A Structural Investigation of Uranium(IV) Metaphosphate." (P. Kierkegaard and A. Kopwillem)

Accounts of recent scientific activities have been submitted this year as the following Special and Technical Scientific Reports:

ST & SR No. I: "Tunnel Structure of $K_2W_4O_{13}$."

ST & SR No. II: "Tracing Phase Transitions by Means of High Frequency as Measurements Using a Q-meter."

ST & SR No. III: "The Crystal Structure of $(Mo_{0.3}V_{0.7})_2O_5$ of $\underline{R}$-$Nb_2O_5$ Type and a Comparison with the Structures of $V_2O_5$ and $V_2MoO_8$."

ST & SR No. IV: "The Crystal Structure of $NaMe^{IV}_2(PO_4)_3$, $\underline{Me}^{IV}$ = Ge, Ti, Zr."

The reports No. I, III and IV are attached to this document as Appendices.

(N.B.: Report No. II is not included here, as it was presented as Appendix IV of the Annual Report delivered in 1967.)

Additional Appendices attached to the present document include

II. "Derivation of the Radial Distribution Function for Crystalline Materials from X-Ray Powder Data."

V. "The Crystal Structure of a New Copper Wolfram Oxide, $Cu_3WO_6$."

The research has been directed by Peder Kierkegaard, who is also the main author of this report. The members of the group have contributed to the research as indicated in the headings of the various sections of the report.

## 2. EXPERIMENTAL METHODS AND DEVELOPMENT WORK

In the research reported in this document extensive use has been made of several techniques suitable for the acquisition of information about the constitution of crystalline and vitreous compounds. The methods thus applied have been described in the two previous annual reports (1,2) and, therefore, only some complementary notes are given in this report. The work has, however, also required the application of some other methods which are described below.

### 2.1. A SIMPLE DEVICE FOR PREPARATION OF AMORPHOUS SUBSTANCES BY VAPOUR DEPOSITION (Lars Kihlborg)

Most vitreous materials investigated within this program have been obtained by quenching from the molten state. An alternative way of preparing amorphous or vitreous substances is by deposition of a vapour on a cool surface. This method is of course restricted to materials which can be heated to give a comparatively high vapour pressure. This is, however, the case for several substances of interest within the present program.

Fig. 1 shows a simple device which has now been successfully applied for the preparation of e.g. molybdenum trioxide in an X-ray amorphous state (cf. sec. 4.2.1). The apparatus consists of an outer glassjacket provided with an outlet to be connected to an evacuating pump via a cold trap. The sample is placed on a platinum strip which can be electrically heated. The deposition of the vapour takes place on the nickel or silver plated closed end of a tube containing the cooling agent (e.g. liquid air). The distance between the sample and the cool surface can be varied. The leads to the heating element are introduced through the insulating ring between the jacket and a metal Dewar surrounding the upper part of the cooling agent reservoir.

### 2.2. X-RAY DIFFRACTION TECHNIQUES

In the research work described in this report X-ray diffraction techniques have been extensively applied. These methods have been applied for investigations of crystalline materials as well as vitreous compounds. Most

Legend to Figure 1

1. Connection to vacuum pump.
2. Brass rods, acting as electrical connection for the strip furnace.
3. O-ring sealings.
4. Connection to cold trap and vacuum pump.
5. Reservoir for cooling agent.
6. Surface where vapour deposition takes place.
7. Electrically heated sample holder made from a platinum strip.
8. Glass tube.

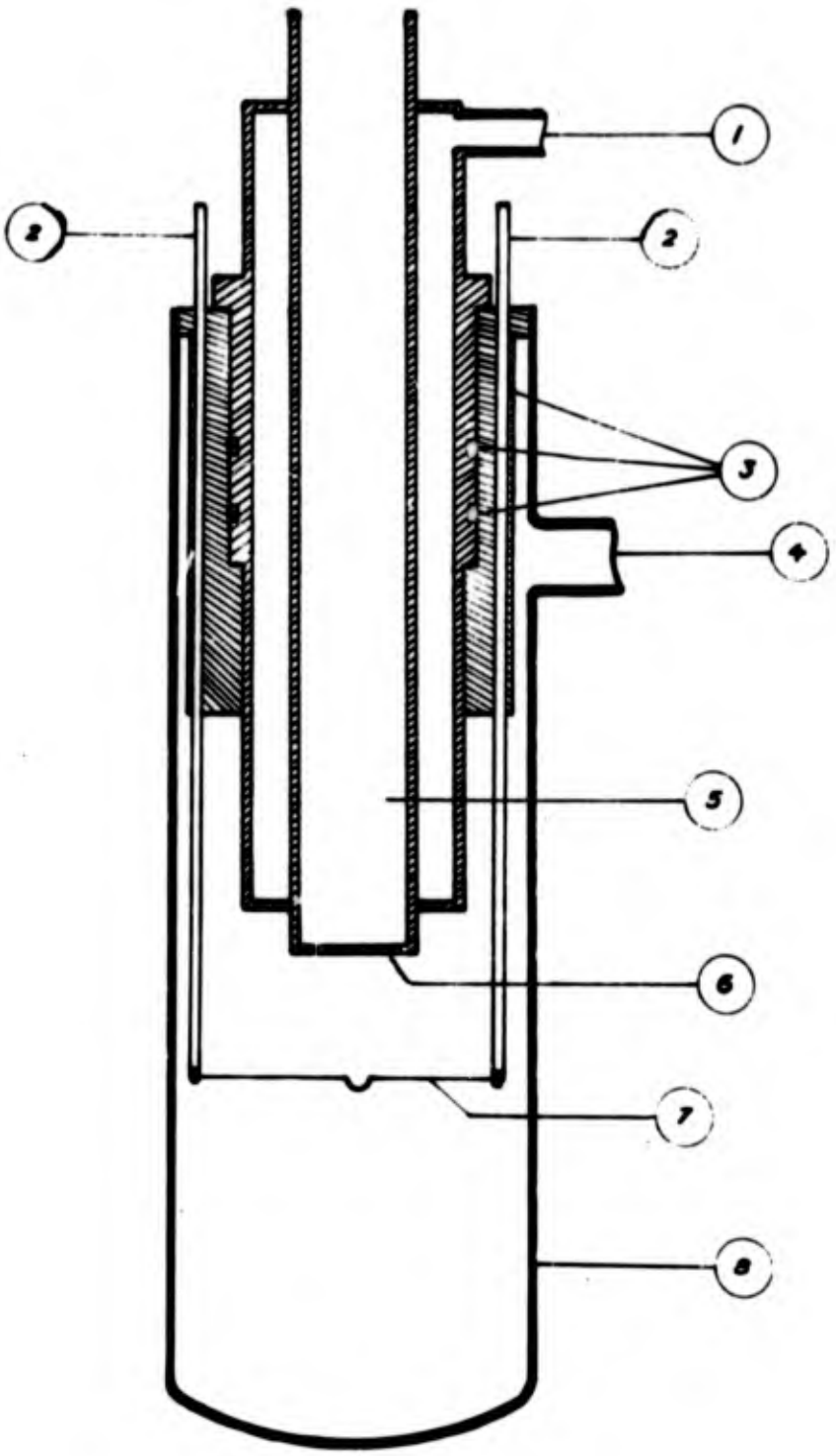


Figure 1. Device for vapour deposition experiments.

of the work has been conducted with well known procedures and commercial or other instrumentation already present at this Institute and also described in the previous annual reports (1,2).

2.2.1. Phase analysis and crystal structure studies

Powder photographs were taken with a Guinier-Hägg focusing camera of 80 mm diameter using quartz ($10\bar{1}1$ plane) crystal monochromatized $CuK\alpha_1$ radiation.

Most intensity data from single crystals have been recorded with conventional multiple film technique, on Nonius Weissenberg camera (Cu or Mo radiation). More accurate data have been registered with a scintillation counter on a General Electric SPG Spectrogoniometer equipped with a full-circle single crystal orienter (Goniostat). This arrangement permits investigation of almost the whole of the reciprocal space up to $2\theta \approx 140^{\circ}$. For a technical description of the instrument, see (3a).

2.2.2. Studies on vitreous materials

The use of a special diffractometer, designed and built at this Institute, for X-ray diffraction studies of vitreous materials has been described in considerable detail in Refs. (1,2). In order to meet the special needs for investigation of melts of alkali isopolywolframates, which have been found to be somewhat aggressive towards the molybdenum and Nimonic sample holders used so far, another version of this part of the high-temperature X-ray diffractometer has been constructed. In the new version the metal parts are replaced by a ceramic material (alumina). This construction is shown in the schematic drawing Fig. 2.

The scattered intensity from various vitreous materials (cf. sect. 4.1.2) containing molybdenum (Cu radiation) or wolfram (Mo radiation) has been measured using the following experimental conditions:

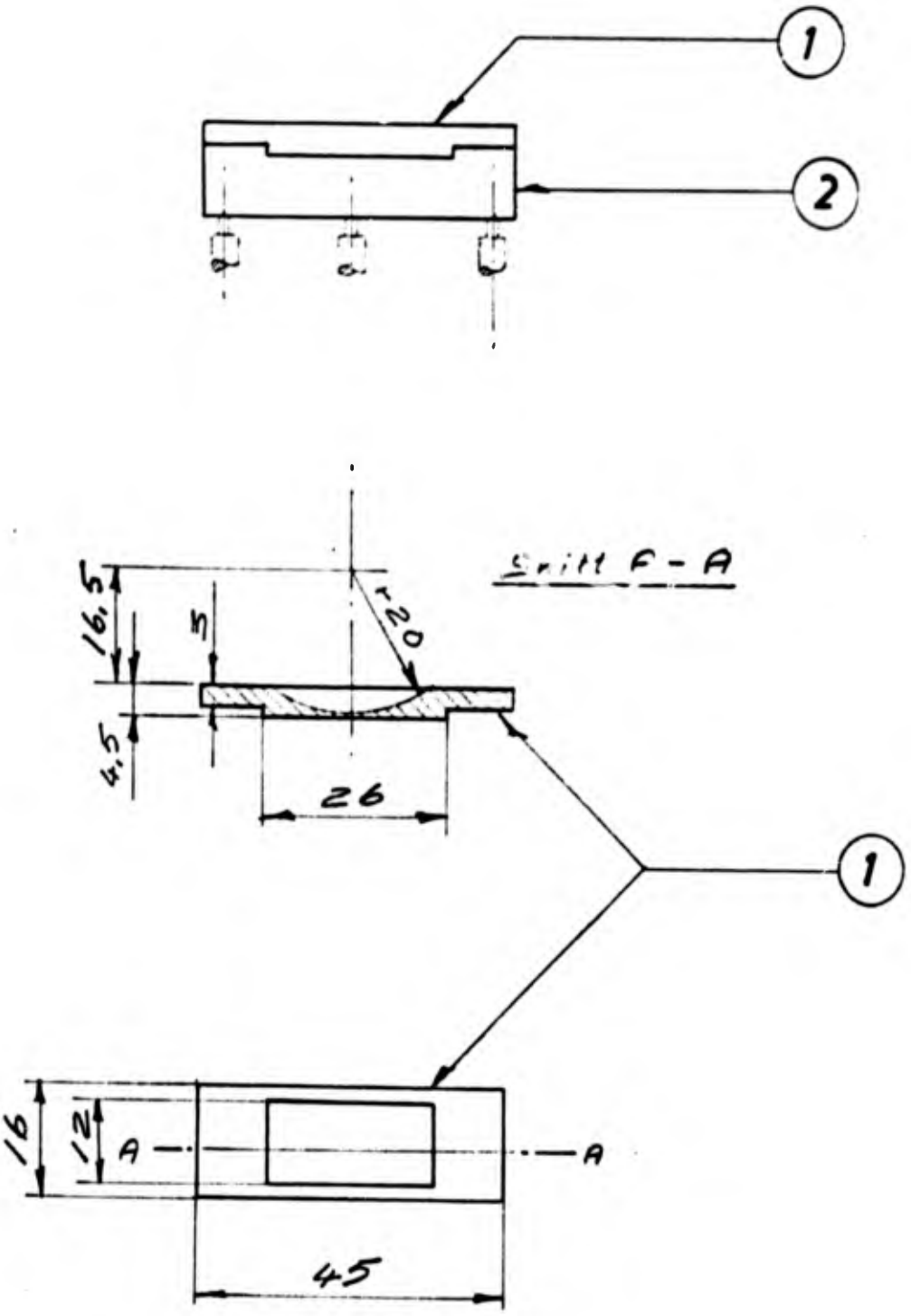


Figure 2. Drawing of the specimen holder.

1. Specimen holder made of alumina or platinum.
2. Base plate of specimen holder.

| | Cu radiation | Mo radiation |
|---|---|---|
| Voltage: | 40 kV | 50 kV |
| Current: | 16 mA | 16 mA |
| Radiation, wavelength: | 1.5418 Å | 0.7107 Å |
| Focusing monochromator crystal: | $SiO_2$ | LiF |
| Recorded range ($\theta$): | $1.75^\circ \leq \theta \leq 50^\circ$ | $1.75^\circ \leq \theta \leq 50^\circ$ |
| " " ($s$): | $0.25\ Å^{-1} \leq s \leq 6.24\ Å^{-1}$ | $0.54\ Å^{-1} \leq s \leq 13.55\ Å^{-1}$ |
| Angular steps ($\Delta\theta$): | $0.25^\circ$ | $0.25^\circ$ |
| Number of counts per step: | 10.000 | 10.000 |

The focusing slit system was adjusted to exclude scattering from the sample holder at low angles. This was accomplished by using a slit opening of $1/12^\circ$ for $\theta \leq 3^\circ$, $1/4^\circ$ for $2.75^\circ \leq \theta \leq 10^\circ$ and $1^\circ$ for $\theta \leq 9.5^\circ$. The resulting intensity curves were normalized in overlap regions.

## 2.3. MEASUREMENT OF MAGNETIC SUSCEPTIBILITY

The materials studied within this research program on structural relations in crystalline and vitreous compounds containing both hexa-coordinating and tetra-coordinating elements have comprised in the first place molybdenum and wolfram oxide phosphates. The vitreous materials contain metal atoms (molybdenum or wolfram) in an oxidation state less than six (see Refs. 1,2). In order to get more information about the electronic conditions within these materials it was found worthwhile to include measurements of magnetic susceptibility as an auxiliary technique.

### 2.3.1. Description of apparatus and measuring techniques (Lars Kihlborg)

An apparatus for the measurement of magnetic susceptibility on milligram samples according to the Faraday principle has been constructed. It has been equipped with a cryostat for measurements from liquid air temperature up to room temperature and a furnace covering the range from room temperature up to at least $600^\circ C$.

The weight of the sample as well as the force acting on it in the magnetic field is measured by means of a Cahn Gram Electrobalance, Mod. 1570, enclosed in the accessory glass bottle No. 1507. Sample amounts of 4-9 mg and the balance sensitivity range 0-10 mg are normally used. Absolute calibration of the balance is unnecessary since the mass susceptibility is a function of the ratio of the force of the magnetic field and the sample weight. The sample holder used is a platinum micro stirrup-pan (No. 1884) hanging on a quartz fibre. The weight of the empty pan is approximately compensated by counterweights.

The electromagnet is a Varian V-4004 four-inch Laboratory Electromagnet with a V-2300A Power Supply and V-2301A Current Regulator. The pole caps used are V-4084 Tapered Pole Caps the shape of which is indicated in Fig. 3. The pole gap currently used is 43 mm. A field of approximately 8500 gauss of the position of the sample is produced by the maximum magnet current, 4 A.

While the magnet is stationary the balance can be raised to about 35 cm above the normal measuring position in order to facilitate change of sample. This is accomplished by means of a pneumatic elevator with a smooth movement. The measuring level can be adjusted with a stop screw (Fig. 3 ). The position of the balance (and the sample hanging down from it) in the horizontal plane can also be adjusted relative to the magnet by means of screws.

The cryostat consists principally of three cylindrical shells separated by metal walls surrounding the test tube connected to the balance bottle (Fig. 4 ). The space between the two outer shells can be evacuated and acts as a metal Dewar. The middle compartment contains the liquid air (or nitrogen), and the innermost one provides possibility to vary the heat flow from the sample. A fine, isolated, copper wire which acts as a heating element is wound around the inner wall, which is also made of copper. When used in the upper temperature range (approximately above 200°K) the space between the two inner shells is evacuated to isolate the sample from the cooling agent as effectively as possible. In order to reach the lowest temperatures one fills it with argon which condenses at liquid air temperatures and gives a high heat transmission. The cryo-

Legend to Figure 3

1. Stop screw.
2. " "
3. " "
4. Tube with balance pan inside the cryostat.
5. Cold trap.
6. Manometer for the elevator pneumatic system.
7. Inlet for compressed gas.
8. To vacuum pump.
9. Inlet for argon gas.
10. Manometer for cryostat.
11. Liquid air level regulator.
12. Inlet for liquid air (or nitrogen).
13. Balance arm.
14. Piston of the pneumatic elevator.
15. Balance supporting arm.
16. Adjustable cryostat support.
17. To vacuum pump (also inlet for nitrogen).

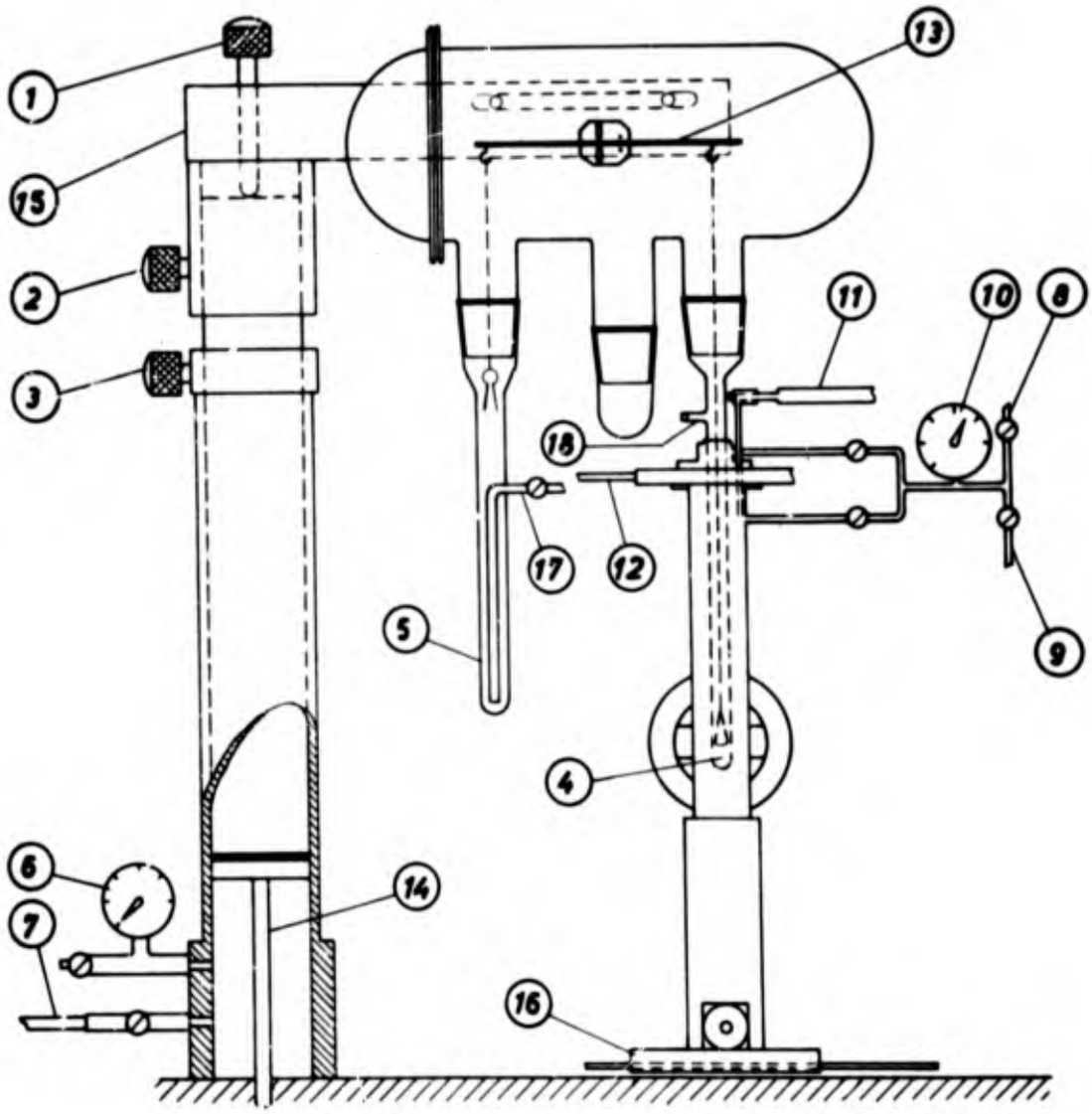


Figure 3. The magnetic susceptibility balance with elevator and the low-temperature attachment mounted on its support.

Legend to Figure 4

1. Inlet for liquid air.
2. To vacuum pump and argon tube.
3. Defrosting element.
4. To vacuum pump.
5. Evacuated space (Dewar vessel).
6. Liquid air reservoir.
7. Inner space.
8. Heating element.

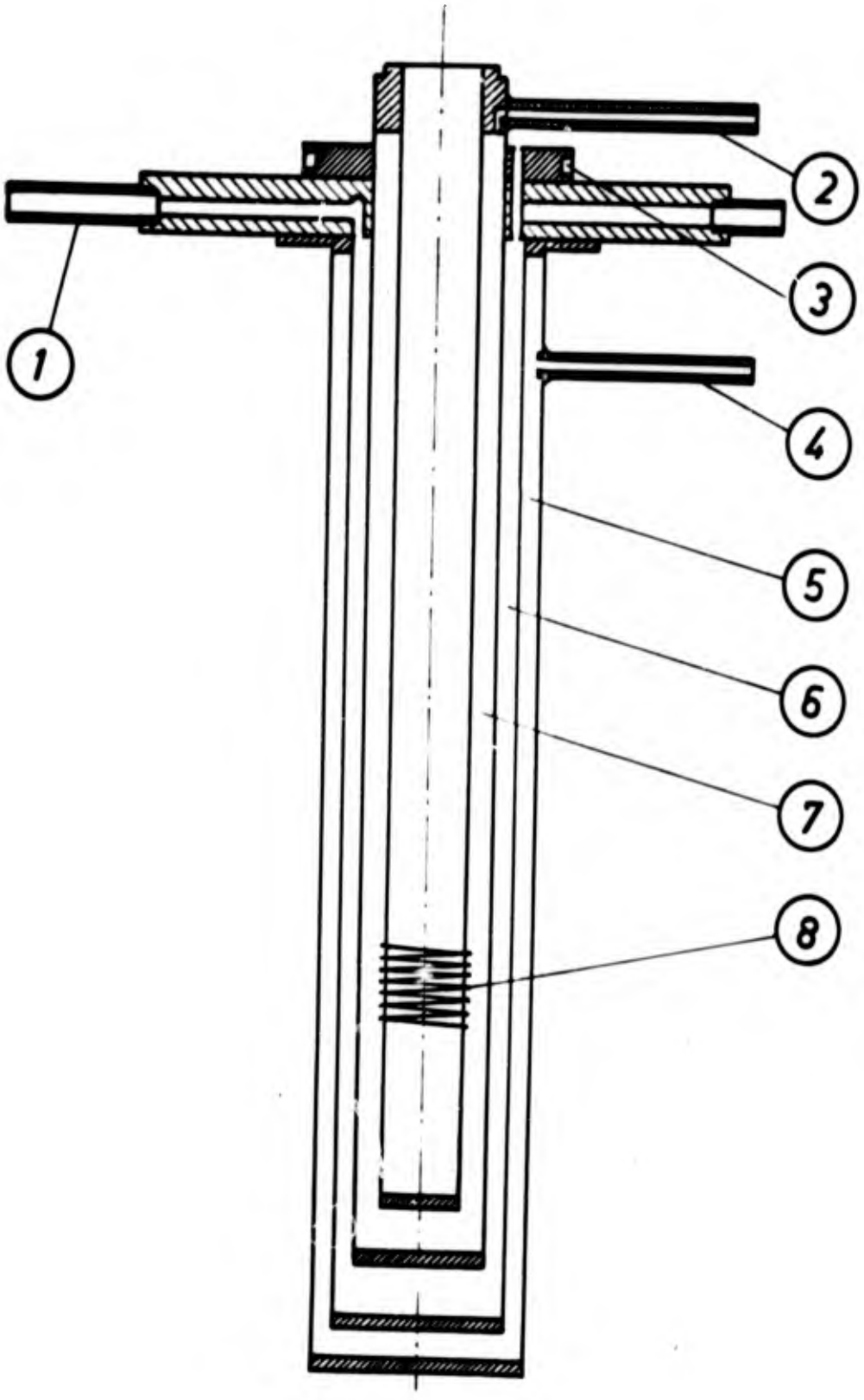


Figure 4. Low-temperature attachment to the magnetic susceptibility balance.

Legend to Figure 5

1. Adjustable slit.
2. Slit adjustment screw.
3. Sealing.
4. Inner tube.
5. Outer tube.
6. Connection to vacuum pump.
7. Radiation shield (outer platinum foil).
8. Heating element.
9. Leads to the heating element.
10. Thermocouple.
11. Inner platinum foil.
12. Pole pieces.

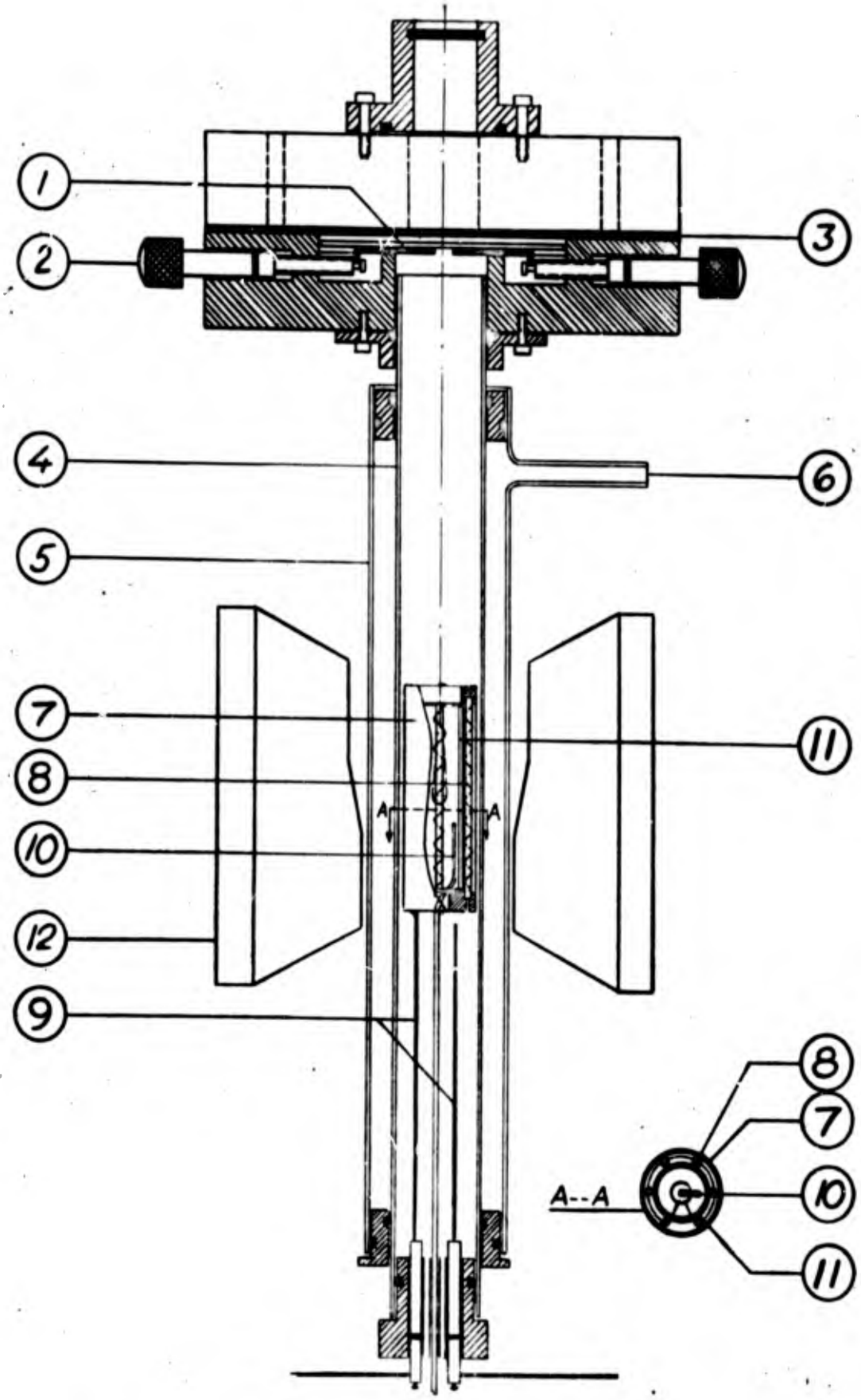


**Figure 5.** High temperature attachment to the magnetic susceptiblity balance.

stat is also equipped with a heating element at the top in order to keep the joints and vacuum sealings there at moderate temperatures. The minimum temperature reached with this cryostat using liquid air as cooling medium is 97°K (measured by means of a copper-constantan thermo-couple inside the test tube and close to the sample position) and with liquid nitrogen 93°K. By variation of the current in the heating element a higher temperature can be arbitrarily selected, which can be held sufficiently constant without the use of any regulator other than an automatic level regulator for the cooling liquid. In order to avoid deposition of ice on the sample or the fibre in the cryostat one removes all moisture from the balance compartment by means of a liquid air cold trap which is applied an hour or so before the cryostat is cooled down.

The furnace (Fig. 5) is at present connected directly to the balance bottle with the test tube removed. The heating element is a platinum wire wound around five vertical ceramic rods, placed outside a cylindrical platinum foil which serves to distribute the temperature evenly over the sample region. It is also surrounded by a cylindrical platinum foil which acts as a radiation shield. Two adjustable slits at the top of the furnace tube are used to reduce the convection streams up into the balance bottle in cases when the system is not evacuated.

All measurements are normally made with several different magnet currents corresponding to values of $H_y \frac{dH_y}{dx}$ within the range $15\text{-}50 \cdot 10^5$ $\text{gauss}^2\text{cm}^{-1}$. The apparatus has been tested and calibrated with $CoHg(SCN)_4$ and $(NH_4)_2Fe(SO_4)_2 \cdot 6H_2O$.

## 2.4. THERMAL ANALYSIS

In order to obtain a qualitative view of the phase relations at elevated temperatures, melting points, devitrification temperatures etc. differential thermal analyses have been performed. The specimen contained in a platinum crucible was heated in a temperature-controlled electric furnace at a uniform rate (10°/min.) and the differential temperature with respect to the standard substance (calcined kaolin) was recorded directly on an xy recorder. The curves thus obtained are given and discussed in the sect. 4.1.1.

## 3. COMPUTATIONAL METHODS EMPLOYED IN X-RAY DIFFRACTION STUDIES

Extensive use of electronic computers has been one of the most important conditions for the research reported in this document. Some information about the computers and programs used are given below.

### 3.1. COMPUTER PROGRAMS FOR CRYSTAL STRUCTURE STUDIES

Several programs written or modified by staff members of this Institute (S) and of the Institute of Chemistry, University of Uppsala (U) for the computers mentioned in the list given below, have been employed in these investigations. Some of the programs are included in the second edition of the World List of Crystallographic Computer Programs ( 3 ). General descriptions of the programs are available, on request, from the authors.

The following abbreviations are used to indicate:

| | |
|---|---|
| 1800 | IBM 1800 |
| 3200 | Control Data 3200 |
| 3600 | Control Data 3600 |

| Program (name) | Function | Machine | Author | Ref. |
|---|---|---|---|---|
| KUSK | Calculates scale factors by comparison of equivalent reflections from different layers | 1800 | S. Westman (S) | (4) |
| STYRE | Performs Fourier summations with expanded data stored on tape | 1800 | R. Karlsson (S) | (4) |
| SFEXP | Calculates structure factors, expands and stores reflections on tape | 1800 | R. Karlsson (S) | (4) |
| TRICLIN | Calculates, for unit cells of general shape, the direct and reciprocal cell parameters | 1800 | L. Kihlborg (S) | (4) |
| SFLS | Least-squares, diagonal matrix, refinement of structural parameters | 1800 | C.-I. Brändén (U) and S. Åsbrink (S) | (3) |
| | | | and modified for IBM 1800 by B. Brandt (S) and S. Åsbrink (S) | (4) |

| Program (name) | Function | Machine | Author | Ref. |
|---|---|---|---|---|
| STORK<br>STORA<br>STORB<br>STORC<br>DATRE<br>SORTE | This program system stores crystallographic data on disk and/or tape, restores data from disk on tape, corrects cell or reflection data, transforms and reduces indices and reflections, sorts reflection data. The programs are used in combination with subsequent calculations by means of STYRE, SFLS etc. | 1800 | L.-O. Larsson and L.-O. Hagman (S) | (4) |
| LAZY | Calculates $\sin^2\theta$- and d-values with standard deviations from l(obs) and l(KCl) in a Hägg-Guinier camera powder photograph | 1800 | A. Nord (S) | (4) |
| ABSW<br>LP<br>EXT | Calculates Lorentz-, polarization, extinction and absorption corrections | 1800 | P.-E. Werner and M. Leijonmarck (S) | (4) |
| PIRUM | Program for indexing and determination of accurate cell parameters from powder data by the method of least squares | 1800<br>3600 | P.-E. Werner (S) | (4) |
| DISTAN | Distance and angle calculations with standard deviations | 3600 | A. Zalkin (Berkeley, Calif.) | (3) |
| DIST | Distance calculations with standard deviations | 1800 | A. Zalkin (Berkeley, Calif.) modified by R. Norrestam (S) | (3)<br>(4) |
| DRF | Data reduction and Fourier programs | 3600 | A. Zalkin (Berkeley, Calif.) modified by R. Liminga and J.-O. Lundgren (U) | (3) |
| LALS | Crystallographic least-squares program | 3600 | A. Zalkin (Berkeley, Calif.) modified by R. Liminga, J.-O. Lundgren and C.-I. Brändén (U) | (3) |

| Program (name) | Function | Machine | Author | Ref. |
|---|---|---|---|---|
| DATACORR | Correction and transformation of crystallographic data stored on magnetic tape | 3600 | R. Liminga (U) | |
| DATAP2 EXTDATA | Absorption, Lorentz and polarization and extinction correction of crystallographic data | 3600 | P. Coppens, L. Leiserowitz and D. Rabinovich (Rehovoth, Israel) modified by O. Olofsson and M. Elfström (U) and by E. Brandt and S. Åsbrink (S) | (3) |
| GIP | Calculates the setting angles for manual and automatic 4-circle diffractometers | 3600 3200 | R. Norrestam (S) | (3) |
| PLANE | Fits a plane to a set of points using the method of least squares | 3600 | C.-I. Brändén (U) | |
| ORFLS | Performs least-squares refinement (full matrix) of crystal structure parameters | 3600 | W.R. Busing, K.O. Martin and H.A. Levy (Oak Ridge, Tenn.) modified by B. Sellberg (U) | (3) |
| ORFFE | Crystallographic function and error program | 3600 | W.R. Busing and H.A. Levy (Oak Ridge, Tenn.) | (3) |
| ORTEP | Program for drawing crystal structure illustrations with a plotter | 3600 | C.K. Johnson (Oak Ridge, Tenn.) | (3) |
| SMIN HOMIN | Symmetry and high order minimum function programs | 3600 | P.G. Simpson, R.D. Dobrott and W.N. Lipscomb (Harvard Univ., Mass.) modified by R. Liminga (U) | (3) |

## 3.2. TREATMENT OF X-RAY DIFFRACTION DATA FROM VITREOUS MATERIALS

In order to obtain radial distribution functions from the experimental intensities of non-crystalline materials (glasses, melts or solutions) registered by means of the special diffractometer (1) the data require extensive computational treatment. These are performed by means of a special program which is described in the following sections.

### 3.2.1. Mathematical background of the computer program (Stig Axrup)

The data consist of diffracted X-ray intensity measured as a function of diffraction angle. The intensity is a sum of a coherent and an incoherent part, of which the coherent part contains information about the structure of the glass (melt or solution). The intensity function cannot be interpreted in terms of structure by direct inspection, since every measured intensity value contains contributions from all interatomic distances in the glass. In order to make use of the measurements, one has to transform the data so that the number of contributing interatomic distances will be finite and preferably rather small. This end is accomplished by Fourier inversion of the intensity function after the incoherent part has been subtracted. The result is a radial distribution function containing contributions exclusively from the short interatomic distances - up to a chosen maximum distance. The function displays directly the magnitudes of the contributing distances. It also yields an estimate of the number of distances of each magnitude present in the glass structure. Thus, one is furnished with data concerning the coordination around different kinds of atoms in the glass. The coherently diffracted intensity, I(s) from a glass is given by the function:

$$I(s) = \sum_{mn}\sum f_m f_n \frac{\sin(s \cdot R_{mn})}{s \cdot R_{mn}} \qquad 1$$

The proof of this equation has been given by several authors (5-7).

The reciprocal vector, $\bar{s}$, is related to the diffraction angle, $\theta$. Its magnitude is: $s = \frac{4\pi}{\lambda} \cdot \sin\theta$. The atomic scattering factors (which are functions of s) are denoted $f_m$ and $f_n$ for atoms m and n respectively and the distance between those atoms will be called $R_{mn}$.

For a glass containing several different atoms, I(s) is conveniently expressed in the following manner:

$$I(s) = N \cdot \sum_i f_i^2 + \sum_m \sum_n f_m f_n \frac{\sin(s \cdot R_{mn})}{s \cdot R_{mn}} \qquad 2$$

where a certain formula unit has been selected as a constituent element, and the irradiated sample contains N such elements. The first sum is taken over one formula unit, whereas the second term - the double sum - runs over all different pairs of separate atoms in the entire sample.

A "weighted atomic density function" $\rho_m(r)$, which expresses the average concentration of scattering power at distance r from atom m will be defined in the following manner;

$$4\pi r^2 \rho_m(r) dr = \sum_j f_j \qquad 3$$

where the sum is taken over all atomic centers situated between two concentric spherical shells of radii r and r+dr around atom m. Clearly, the contribution to the diffracted intensity from all interatomic distances of magnitudes r to r+dr between atom m and after atom s is

$$f_m \sum_j f_j \cdot \frac{\sin(s \cdot r)}{s \cdot r} = f_m \cdot 4\pi r^2 \rho_m(r) \cdot \frac{\sin(s \cdot r)}{s \cdot r} \, dr \qquad 4$$

and expression 2 will take the following appearance:

$$I(s) = N \cdot \left[ \sum_i f_i^2 + \sum_m f_m \cdot \int_0^\infty 4\pi r^2 \rho_m(r) \frac{\sin(s \cdot r)}{s \cdot r} \, dr \right] \qquad 5$$

where both sums, over i and m are taken over the formula unit.

Fourier inversion of I(s) yields the radial atomic distribution function

$$D(r) = 4\pi r^2 \rho_o + \frac{2r}{\pi} \cdot \int_0^\infty s \cdot i(s) \cdot \sin(sr) \, ds \qquad 6$$

where $i(s) = (I(s) - N\Sigma_i f_i^2)/N$ and $\rho_o$ = average atomic density.

In order to use the experimentally determined intensities in expression 6 one must correct them for polarization, absorption and Compton scattering. The relative intensities must then be converted to an absolute scale.

Division of the raw intensities by

$$(1 \cos^2 2\alpha \cdot \cos^2 2\theta)/(1 + \cos^2 2\alpha) \qquad 7$$

yields polarization corrected intensities, assuming the monochromator, placed in the diffracted beam, to be an "ideally mosaic crystal", which, in turn diffracts the radiation through an angle of $2\alpha$ (8).

The absorption correction factor A for strongly absorbing samples with a plane surface is (8):

$$A = \frac{1}{\mu} \cdot \frac{\sin(2\theta-\Delta)}{\sin\Delta + \sin(2\theta-\Delta)} \qquad 8$$

where $\Delta$ is the angle between sample surface and incident beam direction. For a Bragg-Brentano focusing arrangement ($\Delta = \theta$), expression 8 reduces to:

$$A = \frac{1}{2\mu} \qquad 9$$

since, in this case, A is a constant for all $\theta$ it may be included in the scale factor which transforms relative intensities to absolute.

In the following expression:

$$I_{coherent} = k.I_{corrected} - I_{incoherent} \qquad 10$$

$I_{coherent}$ is the I(s) to be used in expression 6, i is a scale factor (including absorption), and $I_{corrected}$ is the experimental intensity corrected for polarization according to 7. $I_{incoherent}$ is calculated theoretically and multiplied by a semiempirical factor which takes into account the spectral distribution of the X-rays, losses at the monochromator crystal etc.

The coherent intensity consists of a dominating part deriving from an average atomic density, and, superposed on this, a part con-

taining the structural information. The dominating part of I(s) on the scale of the formula unit is equal to $\Sigma n_j f_j^2$ over the different kinds of atoms in the structure, $n_j$ being the number (not necessarily integral) of atoms with structure factor $f_j$ in the formula unit. The superposed intensity, $\frac{I(s)}{N} - \Sigma n_j f_j^2$, will henceforth be called i(s) (cf. expression 6).

The spurious peaks which are of necessity introduced into the radial distribution function D(r) by the numerical computation of the Fourier integral between finite limits are attenuated and the intensity contributions from different ranges of s are weighted by the introduction of a modification function, M(s), into D(r) which then assumes the following appearance:

$$D(r) = 4\pi r^2 \rho_o + \frac{2r}{\pi} \int_{s_{min}}^{s_{max}} s \cdot i(s) \cdot M(s) \cdot \sin(sr) ds \qquad 10$$

The modification function:

$$M(s) = \exp(-bs^2) \cdot sf(s) \qquad 11$$

where sf(s) is usually one of the following: 1, $(z_j/f_j(s)^2$ for a particular atom; or $\Sigma n_j z_j^2 / \Sigma n_j f_j^2$ over the different kinds of atoms in the structure.

3.2.2. Functioning of the program (Stig Axrup)

A program written in FORTRAN and intended to be used mainly on an IBM 1800 computer installed at this Institute (cf. 4) has been developed, partly on the basis of an ALGOL program written by Johansson (9).

The input data are:

1) A table of θ (degrees) and corresponding $I_{obs}$ values corrected for background

2) Atomic scattering factor tables, each entry for any one kind of atom consisting of sin θ/λ, $f_o$, $\Delta f'$, $\Delta f''$ and the theoretically calculated value of the atomic contribution to $I_{incoherent}$

3) A table of the semi-empirically found multiplier for $I_{incoherent}$ as a function of sin θ/λ

For each measured pair of θ and $I_{obs}$, the program calculates $s = \frac{4\pi}{\lambda} \cdot \sin\theta$ and corrects $I_{obs}$ for polarization.

The total incoherent intensity and the contribution to the coherent intensity from an appropriate average atomic density are calculated for the sin $\theta/\lambda$ values listed in the scattering factor tables. The values of these functions at the sin $\theta/\lambda$ values of the intensity measurements are found by interpolation according to Newton's method.

If desired, the result can be pointed out as a table of: $\theta$, $I_{obs}$ (corrected for background), the polarization factor, s, $I_{obs}$ (corrected for polarization), the average atomic density contribution to $I_{coherent}$, $I_{incoherent}$ x multiplier and, finally, the sum of the last two quantities.

Scaling of $I_{obs}$ can be effected in two different ways by the program.

The first method is based on the fact that, for large values of s, the total scattered intensity is very nearly equal to the part derived from the average atomic density. Consequently, the $I_{obs}$ values at high $\theta$ angles are scaled to match, as nearly as possible the entries on the last column of the table described above. The scale factor thus derived is applied to all $I_{obs}$ values.

The second method for obtaining a scale factor has been originated and described by Norman and Krogh-Moe (9a-9c). The two methods yield very nearly the same result if the intensity has been measured correctly over the whole investigated $\theta$ range.

The printed output consists of

1) Scale factor
2) A table containing: s, $I(s)_{obs}$ (corrected and scaled), $I(s)_{coherent}$, i(s) and s·i(s).

If desired, graphs of $I(s)_{obs}$ (corrected and scaled), and I(s) coherent can be printed. Furthermore, one has the option of calculating and printing the sum of negative i(s) values and the sum of positive i(s) values. These two sums must have approximately identical absolute magnitudes, which provides a check of the correctness of the calculations.

The Fourier inversion. In the radial distribution function D(r) (expression 10) the integral is approximated by a sum

$$\sum_{n}^{i} \tfrac{1}{2}[s_n \cdot i(s_n) \cdot M(s_n) \cdot \sin(s_n \cdot r) + s_{n+1} \cdot i(s_{n+1}) \cdot M(s_{n+1} \cdot \sin(s_{n+1} \cdot r)] \cdot (s_{n+1} - s_n) \qquad (12)$$

over the experimental $s_n$ values. There is no facility on the program for calculating a smoothed intensity function. The limits of integration can be chosen arbitrarily by the user of the program.

The printed output consists of a table of r, D(r), $4\pi r^2 \rho_o$, and $D(r) - 4\pi r^2 \rho_o$. Graphs of the three functions are printed simultaneously with the tables.

## 3.3. RADIAL DISTRIBUTION FUNCTIONS FOR CRYSTALLINE MATERIALS

A direct comparison between the radial distribution functions of vitreous materials and the crystal structure of substances of the same or approximately the same compositions implies some obvious difficulties. The assembly of discrete interatomic distances corresponding to the atomic arrangement of the crystal is not easily compared with the continuous curve of the radial distribution function. An alternative way of comparison is by deriving for the crystalline material a radial distribution function based on the structure factor values corresponding to the crystal structure.

Appendix II presents a procedure for deriving the radial distribution function from X-ray powder data which has been found useful for studies of materials with unknown crystal structures. In the present work a somewhat modified procedure has been applied. The structure factor values corresponding to the known crystal structures are converted to intensities and the radial distribution function is obtained from the expression

$$r[\rho(r) - \rho_o(r)] = K \sum_{i=1}^{u} \sin\theta_i \quad I(\theta_i) \cdot \sin\frac{4\pi \sin\theta_i}{\lambda} \cdot r \cdot e^{-\left(\frac{\beta \sin^2\theta_i}{\lambda^2}\right)}$$

# 4. RESULTS AND INTERPRETATIONS OF MATERIALS STUDIES

## 4.1. STUDIES ON VITREOUS AND CRYSTALLINE MATERIALS OF COMPOSITIONS $Na_2O \cdot n\underline{M}O_3$ ($\underline{M}$ = Mo or W)

In the previous annual report on this research project (2) some preliminary results of X-ray diffraction studies on potassium polywolframate glasses after different thermal treatments were described. It was observed that the radial distribution functions derived from the X-ray recordings of such materials showed considerable differences. It was emphasized that any attempt to interpret the findings would require more extensive experimental data.

Part of the work during the present period of research has been conducted with the aim to contribute to the understanding of the observations thus described. In order to simplify as far as possible the interpretation of the radial distribution functions it was found suitable to concentrate the work on studies of sodium polywolframate glasses instead of the potassium compounds. The influence of the relatively heavy potassium atom on the appearance of the distribution function was thus removed. The X-ray scattering power of sodium is practically identical with that of oxygen and the wolfram atoms of the vitreous materials should thus in an admittedly very rough picture be considered as distributed in a "matrix" of light atoms, all having about the same weight.

### 4.1.1. Preparative Work Including Studies on Glass Formation and Devitrification (Kaija Eistrat)

Investigations of the formation of glasses in the systems $\underline{A}_2O \cdot n\underline{W}O_3$ ($\underline{A}$ = Li, Na, K, Rb and Cs) have been described by Gelsing *et al.* (10). They report the glass-forming tendency for all the systems mentioned to be highest at compositions around $\underline{A}_2W_2O_7$. For the $Na_2O \cdot n\underline{W}O_3$ system, glasses were obtained within the compositional region $Na_2O \cdot 1.5WO_3$-$Na_2O \cdot 3WO_3$.

The starting materials for the present preparations were $Na_2WO_4 \cdot 2H_2O$ ("zur Analyse", Merck), $Na_2MoO_4 \cdot 2H_2O$ (analytical reagent, Mallinckrodt), $MoO_3$ (analytical reagent, Mallinckrodt) and $WO_3$ (puriss, KEBO). $Na_2WO_4$ and $Na_2MoO_4$ were prepared from the hydrates by melting in a platinum crucible.

Crystalline samples of $Na_2W_2O_7$ and $Na_2Mo_2O_7$ were prepared by the method applied by Seleborg (11), *i.e.* by melting of stoichiometric mixtures of $Na_2\underline{M}O_4$ and $\underline{M}O_3$ in a platinum crucible and subsequent heating of the product for about a week at 600°C. Batches of about 20 g of the diwolframate and dimolybdate were thus prepared to serve as starting materials for the preparation of glasses. The X-ray powder patterns registered with $Cu\underline{K}\alpha_1$ radiation in a Guinier-Hägg type focusing camera were found to be identical with those obtained by Seleborg (11).

Vitreous $Na_2W_2O_7$ was then prepared by melting of the crystalline phase either at 850°C (series I) or 1100°C (series II). The material, which was kept in a platinum crucible, was introduced in furnaces of the above temperatures for one or two minutes, whereupon the melts were rapidly quenched in an ice-water mixture. The vitreous character of the products was checked by visual inspection and by examination with a polarizing microscope and also by the appearance of their Guinier photographs. The weight of the samples did not change appreciably during the treatments. The chemical composition of crystals and glasses should thus be the same.

Using these techniques it was found possible to obtain sodium diwolframate in a vitreous state with batches not exceeding about 0.5 g.

The glasses of series I and II were found to differ slightly in colour. The former, *i.e.* those obtained by melting at 800°C, are colourless while the latter (heating temperature 1100°C) are faintly yellowish.

Portions of the series I and II samples were subjected to further heat-treatment for the subsequent X-ray diffraction work.

This included annealing at 200°C and 300°C for extended periods of time. For these experiments samples of 1.5 g were sealed in evacuated silica capsules. After heating periods of 1, 10 and 30 days respectively, the capsules were rapidly quenched in ice-water mixtures. The products were again studied by visual inspection, with the polarizing microscope and by Guinier photographs. As far as these techniques are concerned the results for the series I and II materials were the same. Thus, the heat-treatment at 200°C did not change the vitreous character or the colour of the material. The samples heated at 300°C were all found to be crystalline. The Guinier photographs differed in intensity with the duration of the heat-treatment, which was interpreted as reflecting the progress of the recrystallization process.

The results thus obtained showed that the vitreous-to-crystal transition of $Na_2W_2O_7$ proceeds fairly rapidly at a temperature between 200°C and 300°C. In order to shed further light on this transition differential thermal analyses were performed for crystalline and vitreous (series I and II) sodium diwolframate. The results thus obtained are represented in Fig. 6. The heating rate was 10°C/min. Both series of vitreous materials show a sharp "exothermic" peak at about 360°C corresponding to a rapid crystallization process. The two thermograms as well as the one yielded by crystalline $Na_2W_2O_7$ show sharp "endothermic" peaks at about 740°C, *i.e.* the melting temperature. This figure is close to the value 735°C reported by Gelsing *et al.* (10).

The glass-to-crystal transition temperature of 365°C observed in the DTA studies with a heating rate of 10°C/min. may be compared with the "stability" of $Na_2W_2O_7$ when heated for about a month at 200°C and the transformation of the material within periods of days at 300°C. Preliminary experiments have shown that with much higher rates of heating the transition temperature may be increased to at least 450°C.

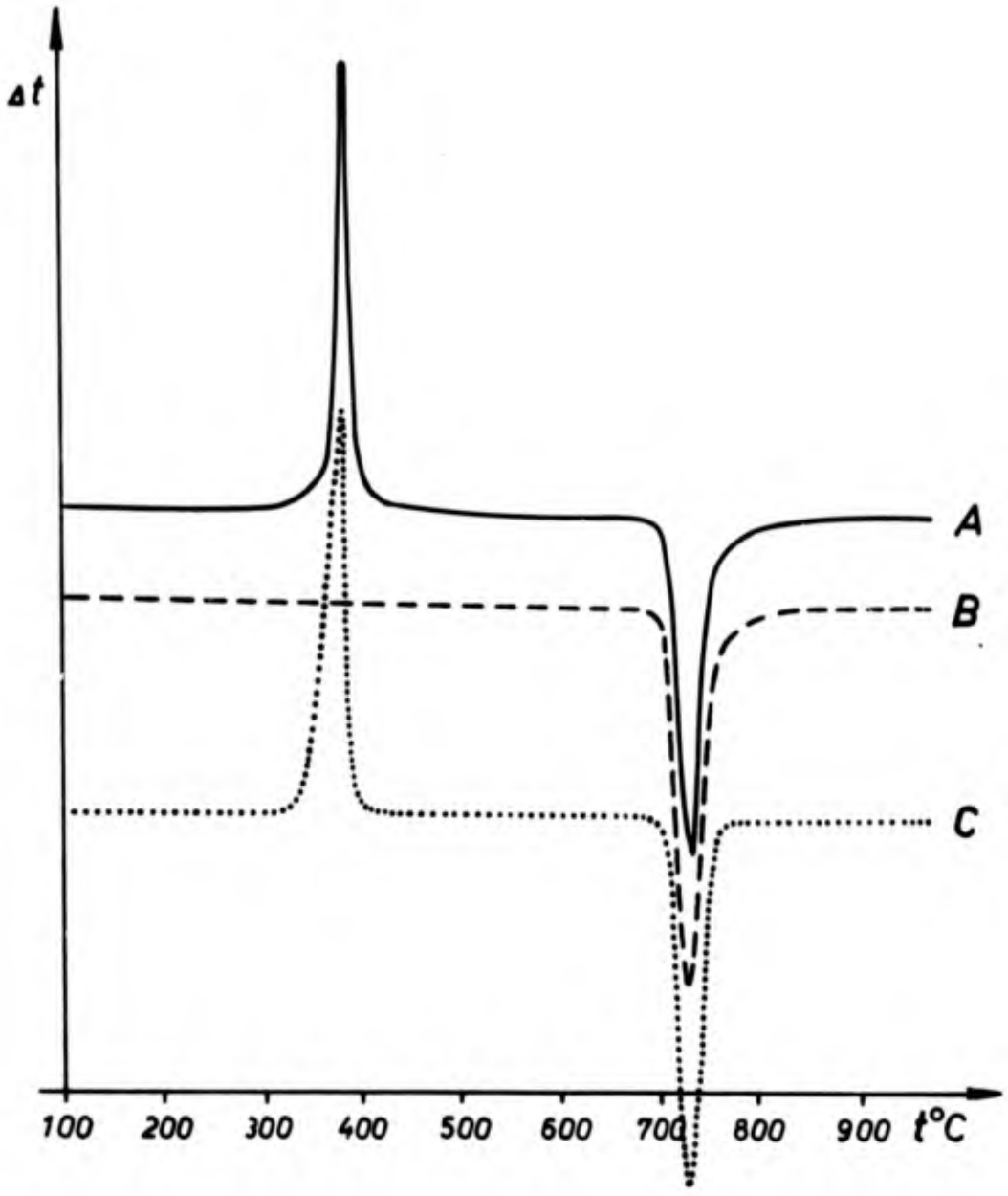


Figure 6. Differential thermal analyses.
Schematic drawing of the curves obtained for $Na_2W_2O_7$.
Glass (I) curve A; crystals curve B and glass II curve C.

The tendency to glass formation was found to be less with sodium polywolframates higher in $WO_3$ than was observed with the diwolframate. Thus, applying the techniques described above $Na_2O \cdot 1.5WO_3$ could only be obtained as a glass with batches weighing less than 0.1 g. This amount of $Na_2O \cdot 2.3WO_3$ also resulted in a glassy product. With larger amounts of starting material crystalline products were invariably obtained, obviously due to lower cooling rates. Both of the latter samples have compositions within the "glass-forming" range reported by Gelsing et al. (10). The observation made by these authors that $Na_2O \cdot WO_3$ does not form a glass was also confirmed by the present study.

Experiments analogous to those described above with $Na_2W_2O_7$ were also performed for $Na_2Mo_2O_7$. The melting temperature used was 800°C. With the experimental conditions applied, the amount of the sample could not exceed 75 mg without at least partial formation of crystalline material. The colour of $Na_2Mo_2O_7$ thus prepared was a faintly brownish or yellow one, clearly different from the colourless appearance of the crystalline material.

The synthesis experiments indicated that the glass-to-crystal transition occurs more rapidly with $Na_2Mo_2O_7$ than with $Na_2W_2O_7$. Further studies on this process for $Na_2Mo_2O_7$ were made by DTA analyses. The results thus obtained when heating crystalline and vitreous sodium dimolybdate at a heating rate of 10°C/min are represented in Fig. 7 . The "endothermic" peak corresponding to the devitrification process between 200° and 300°C is not a very sharp one. The melting temperature at 625°C is close to the value (612°C) reported by Hoermann (12).

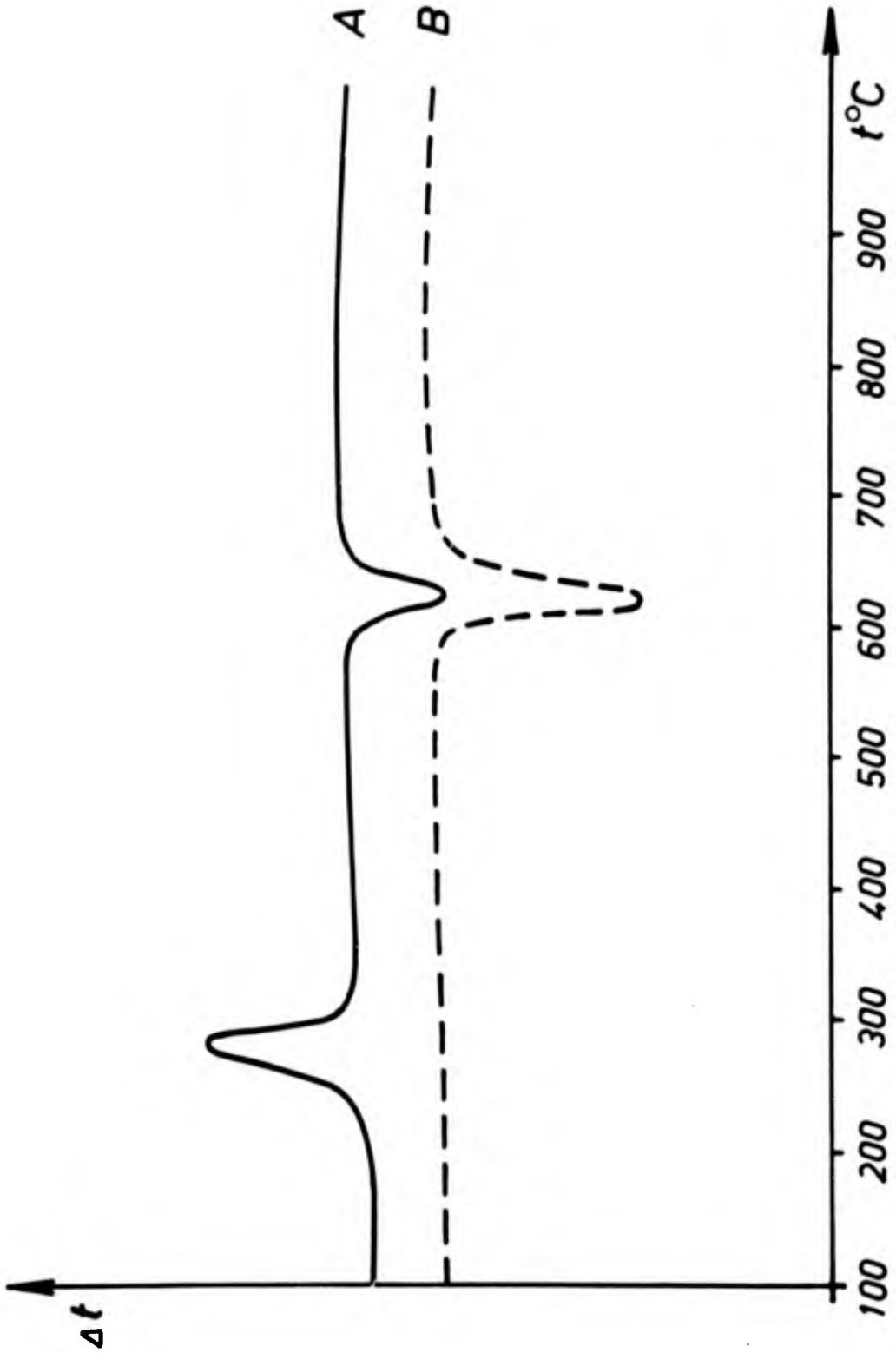


Figure 7. Differential thermal analyses.
Schematic drawing of the curves obtained for vitreous (A) and crystalline (B) $Na_2Mo_2O_7$.

4.1.2. X-Ray Diffraction Studies (Barbro Linnros)

The radial distribution function corresponding to the crystal structure of disodium dimolybdate (11,13) and calculated by the procedure described above (sect. 3.3) is illustrated in Fig. 8. This structure contains infinite chains formed by $MoO_6$ octahedra sharing corners. $MoO_4$ tetrahedra bridge adjacent $MoO_6$ octahedra by corner sharing. The shortest Mo-Mo distances of the structure, viz. those corresponding to linking between two octahedra or a tetrahedron and an octahedron are very nearly the same (3.6 Å). The distances between the Mo atoms of octahedra of parallel chains are 5.1 and 7.15 Å. The closest approach between Mo atoms of tetrahedra in a chain is 6.5 Å. Further important interatomic distances of the structure occur around 3.7 Å (Mo-Na distances), 2.8 Å (O-O) and 1.75 Å (Mo-O). (The interatomic distances of $Na_2Mo_2O_7$ are close to those of $Na_2W_2O_7$ which are listed below.) The appearance of the radial distribution function (Fig. 8 ) is in agreement with the interatomic distances required by the structure. In particular the maxima around 1.9, 2.7, 3.6 and 5.0 Å stand out as corresponding to characteristic groups of interatomic distances of the structure.

Fig. 10 shows the appearance of the radial distribution function for vitreous disodium dimolybdate prepared in the manner described above by quenching from 800°C. The dashed and full curves, which do not differ appreciably, correspond to normalization by the Norman method and by fitting of the intensities at high values of s to a background function based on theoretically calculated scattering amplitudes (cf. Ref. 1, p. 62). The curve of the $Na_2Mo_2O_7$ glass shows considerably less detail than the one given by the crystals. The heavy peak at 3.7 Å, however, stands out very clearly, suggesting that the Mo-Mo distances in the glass are nearly the same as in the crystalline state. The rather flat character of the curve at lower r-values might be due to a less distinct character of the oxygen coordination around molybdenum in the vitreous state. To conclude, however, it may be said that the glass curve shows no indications of other structural elements

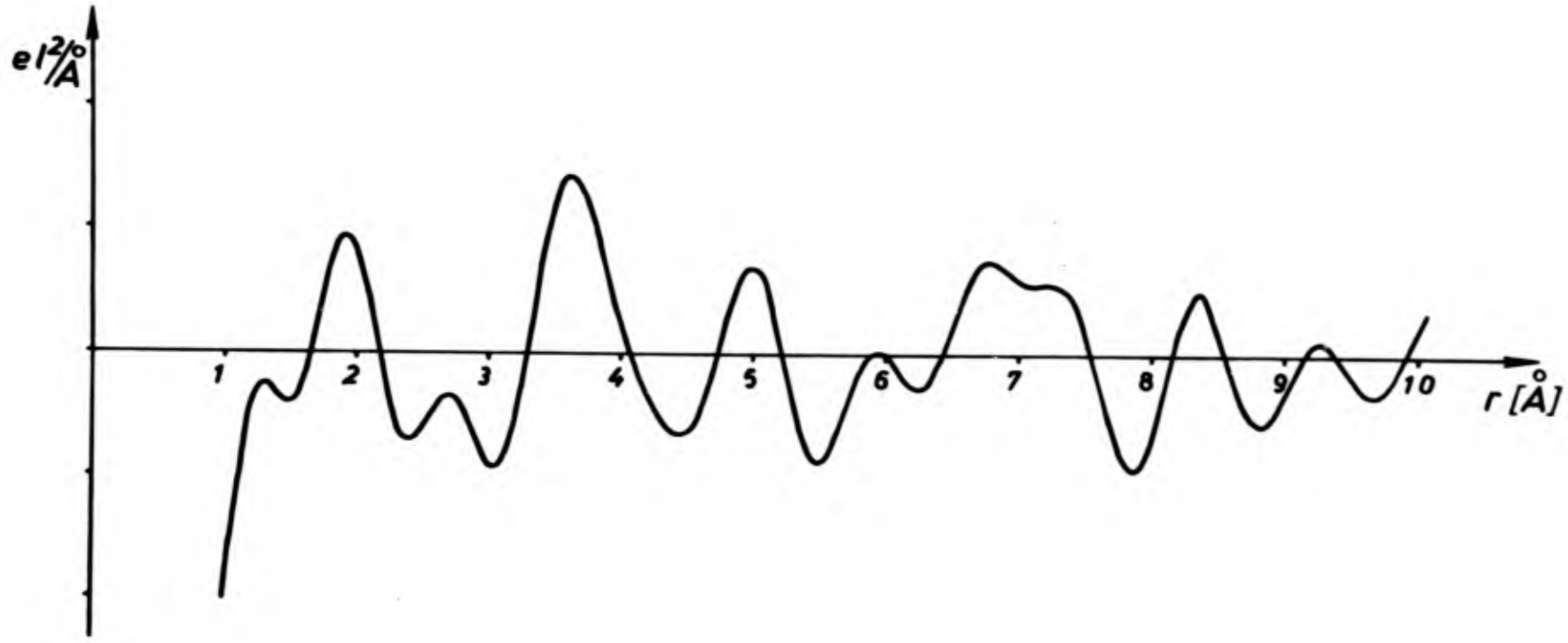


Figure 8. Radial distribution curve for the crystalline compound $Na_2Mo_2O_7$.

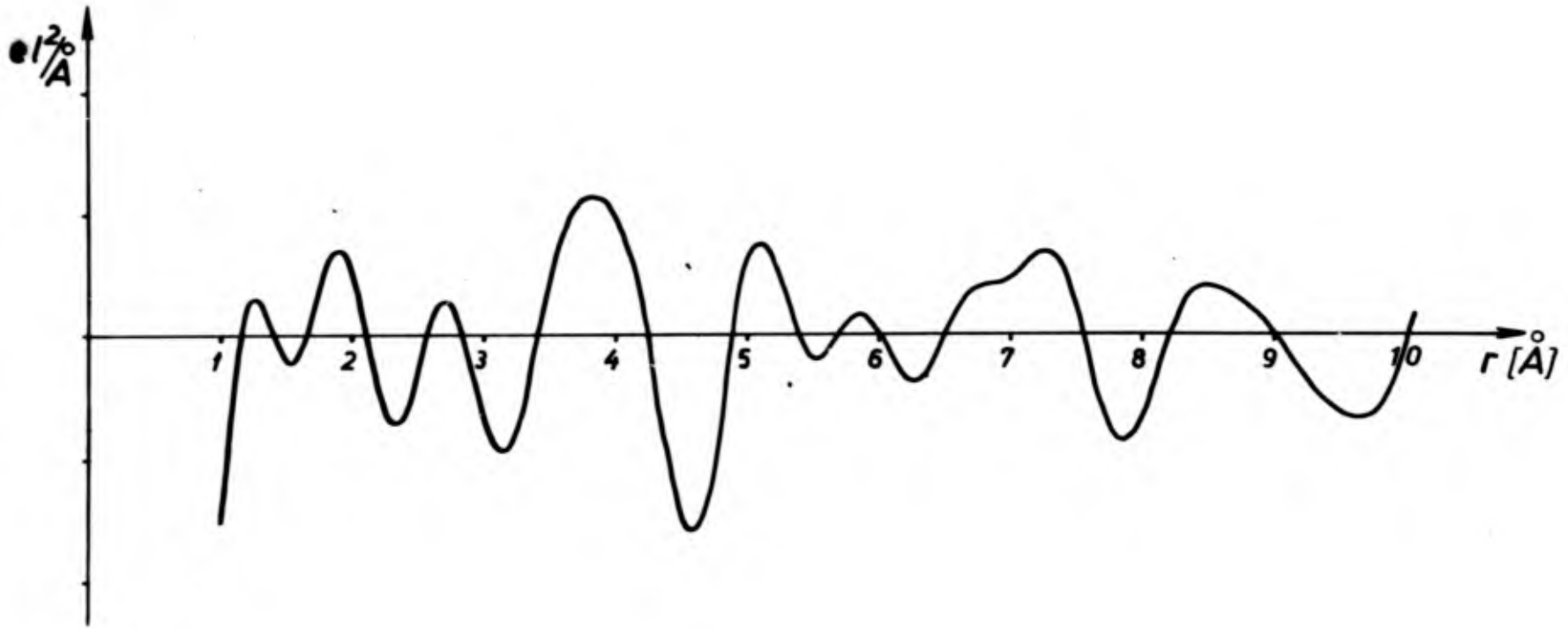


Figure 9. Radial distribution curve for the crystalline compound $Na_2W_2O_7$.

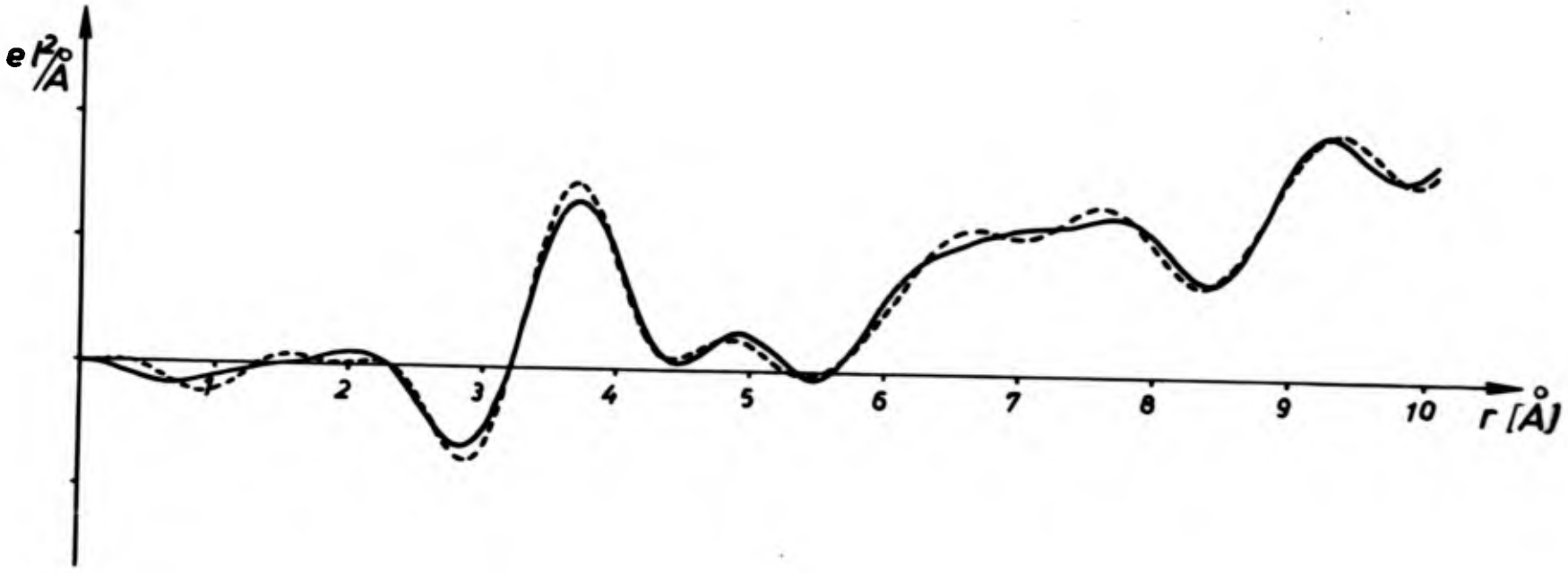




Figure 10. Radial distribution curve for $Na_2Mo_2O_7$ glass. The experimental intensity has been normalized by means of the Norman method (dotted curve) or by fitting of intensity values recorded at high values of s to a background function based on theoretically calculated scattering amplitudes (continuous line).

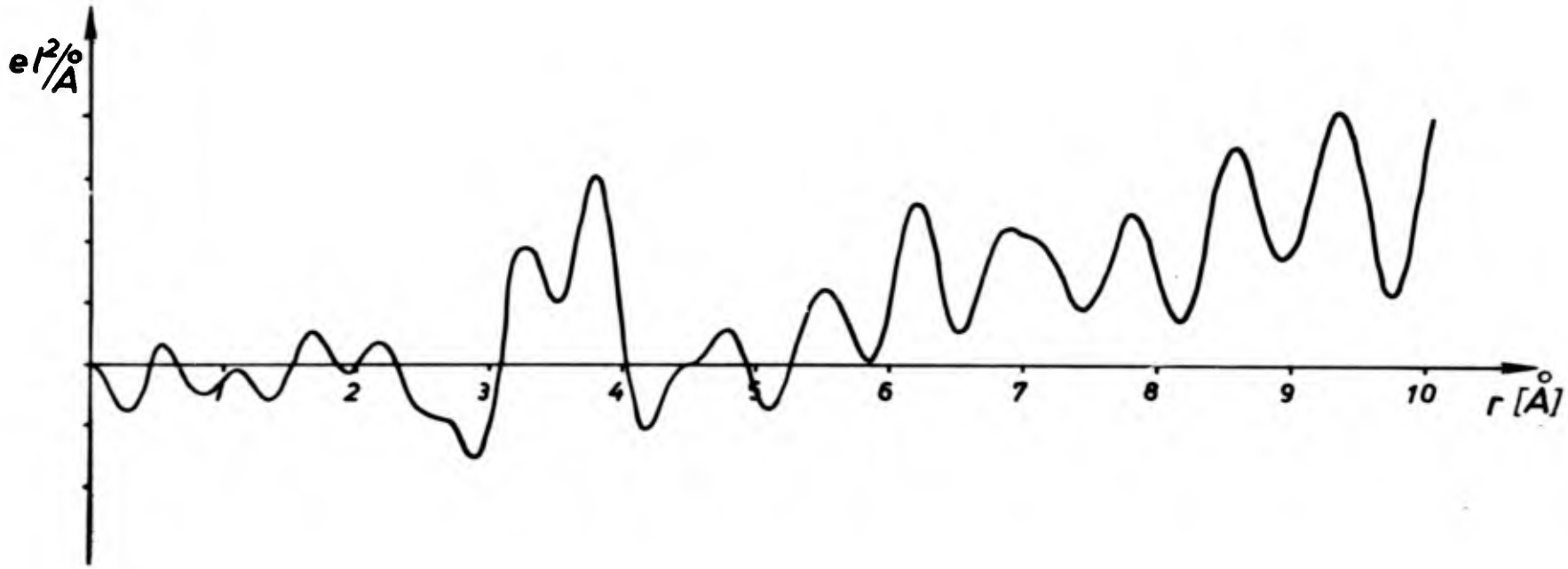


Figure 11. Radial distribution curve for $Na_2W_2O_7$-glass.
(Quenched after melting at 800°C.)

being present in the vitreous state than in the crystals.

A radial distribution function for crystalline disodium diwolframate is reproduced in Fig. 9. The curve is in satisfactory agreement with the interatomic distances required by the crystal structure (cf. Table 1). The minor differences between the present curve and the one given by crystalline $Na_2Mo_2O_7$ may be attributed to the different scattering powers of molybdenum and wolfram.

Radial distribution functions of vitreous $Na_2W_2O_7$ have been derived on the basis of X-ray diffraction data collected for several samples of different thermal prehistory. Figs. 11-13 reproduce the appearance of some of these curves, viz. those given by the following samples:

$Na_2W_2O_7$ glass, quenched after melting at 800°C (Fig. 11)

$Na_2W_2O_7$ glass, same as preceding one with additional heat-treatment at 200°C for 10 days (Fig. 12)

$Na_2W_2O_7$ glass, quenched after melting at 1100°C and additional heat-treatment at 200°C for 30 days (Fig. 13)

It may be stated that the general chatacter of the three curves is the same. It thus seems rather likely that the three glasses do not show considerable structural differences among themselves. The curve representing the radial distribution function of crystalline $Na_2W_2O_7$ is, on the other hand, rather different in character (Fig. 9). If the comparison is restricted to the r-range 1.5-4 Å, the peaks present in the crystal curve at 1.9 and 2.7 Å may be identified with minor displacements as peaks also appearing in the glass curves. Most striking, however, is the presence of two dominating maxima at 3.25 and 3.75 Å in the latter curves as compared to the single peak at 3.9 Å in the crystal curve. The latter is rather composite in character corresponding not only to W-W but also to W-Na and W-O distances.

The two very sharp maxima present in all the glass curves are most likely to reflect W-W distances. If so, they indicate a marked structural difference to exist in crystalline and vitreous $Na_2W_2O_7$.

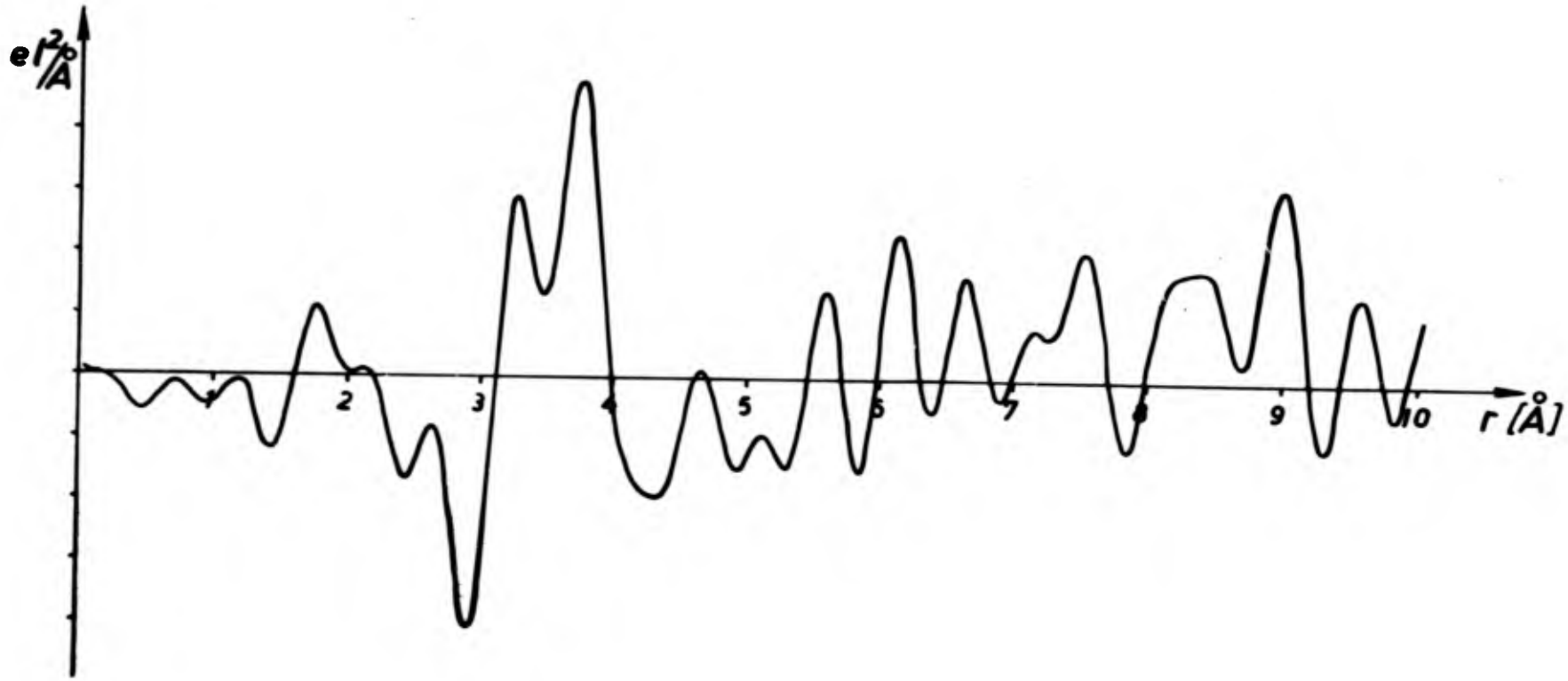


Figure 12. Radial distribution curve for $Na_2W_2O_7$-glass. (Quenched after melting at 800°C and heat-treated at 200°C for 10 days.)

The infinite $W_2O_7$ chains which are the structural elements of the former state can thus hardly be preserved in the glasses. If $W_2O_7$ chains, Fig.14 are to be dismembered into minor species the atomic ratio of oxygen to wolfram of 3.5 requires that the coordination number of oxygen around the metal atom is reduced and/or the number of oxygen atoms common to polyhedra increases over one. In this connection the studies on polywolframate glasses performed by Gelsing et al. (10) by means of infrared measurements are of considerable interest. These authors concluded that the coordination number of wolfram is four in the vitreous state. If this were the case in the diwolframate glasses these would in the simplest case contain $W_2O_7^{2-}$ groups. Assuming normal W-O distances and a W-O-W angle of 130° the W-W distance would be about 3.25 Å, in good agreement with the position of one of the heavy peaks in the radial distribution function. With this model or with more complicated ones implying the presence of aggregates of different sizes, formed by $WO_4$ tetrahedra linked by corners it seems rather difficult to account for the very sharp maximum at 3.75 Å. The latter is the normal distance for $WO_6$ octahedra joined by corners and also close to the value for octahedra and tetrahedra linked in this way.

The presence of the two sharp heavy maxima at 3.25 and 3.75 Å might be accounted for by assuming a model consisting exclusively of $WO_6$ octahedra joined by edges and corners to compact groups of low oxygen to wolfram ratii similar to atomic arrangements found by Lindqvist to be present in e.g. the paramolybdate ion $Mo_7O_{24}^{6-}$ (12b).

It may be said, however, that relatively small groups, be they composed of small numbers of tetrahedra or octahedra, are not very likely to favour the formation of a glass. A vitreous state is often thought to be more easily adopted by substances containing structural units of considerable extensions and likely to be readily distorted. From this point of view it would seem rather likely that $Na_2W_2O_7$ glass does not contain just wolfram-oxygen aggregates of one kind but rather a mixture of groups showing structural characteristics of the various kinds outlined above.

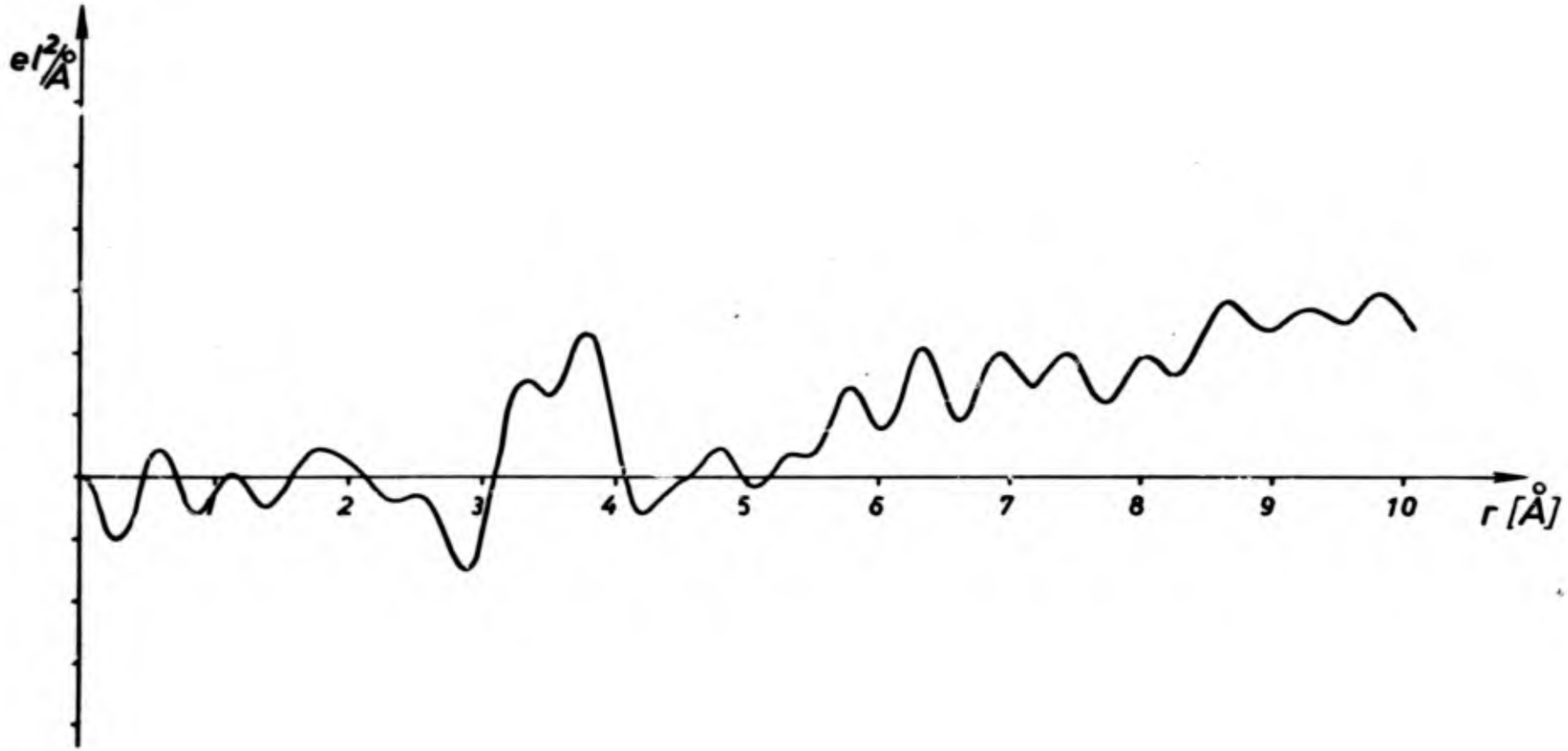


Figure 13. Radial distribution curve for $Na_2W_2O_7$-glass. (Quenched after melting at 1100°C and heat-treated at 200°C for 30 days.)

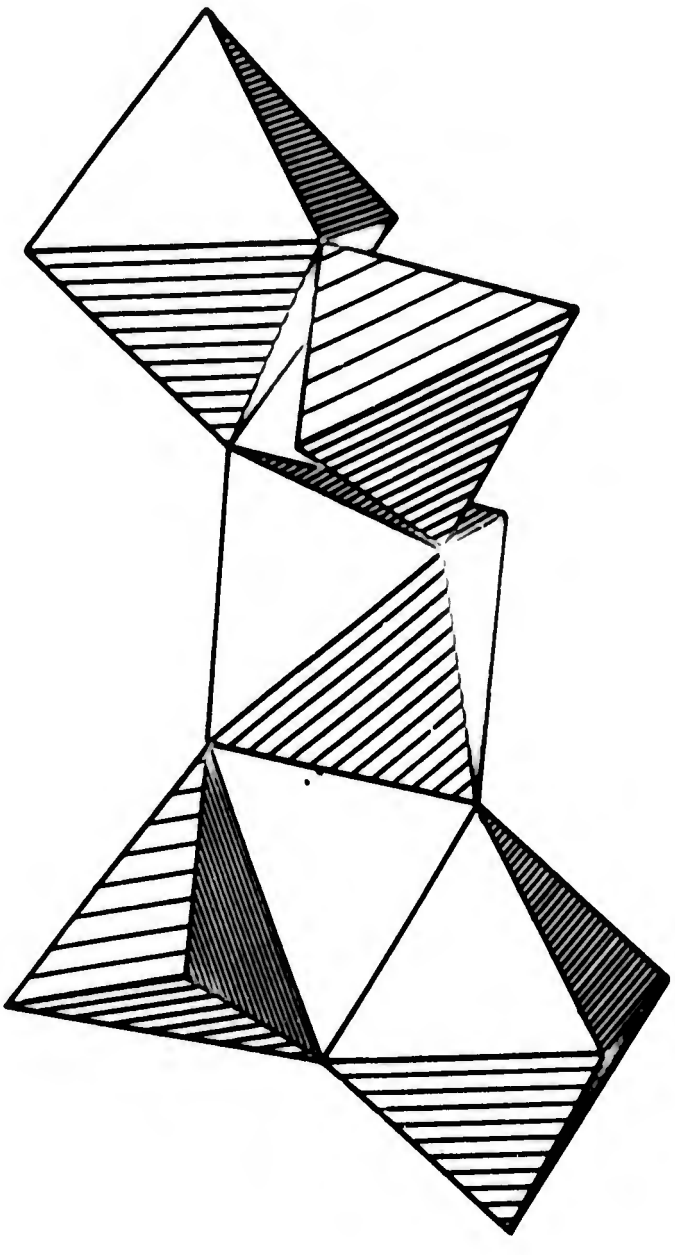

Figure 14. Part of the infinite chain ion $\underline{L}_2O_7^{2-}$ ($\underline{L}$ = Mo or W) of the sodium dimolybdate (diwolframate). Idealized with regular polyhedra. (The figure from Ref. 12b.)

The ideas put forward on the structure of vitreous $Na_2W_2O_7$ are not applicable to the data found for $Na_2Mo_2O_7$ in the glassy state. It has been suggested above that the atomic arrangement of the latter preserves considerable similarities with the one present in crystalline $Na_2Mo_2O_7$. If one considers that the dimolybdate and diwolframate of sodium are isomorphous the marked difference between the structural arrangements in the vitreous state is a rather surprising and interesting result of the research.

Table 1. The most important distances (average values) in the crystal structure of $Na_2W_2O_7$ and their weight factors.

| Type of distance | Number of distances | Length in Å |
|---|---|---|
| W - W | 5 | 3.58 |
| | 3 | 4.99 |
| | 3 | 5.62 |
| | 5 | 6.09 |
| | 4 | 6.50 |
| | 9 | 7.19 |
| | 7 | 7.60 |
| W - Na | 20 | 3.71 |
| | 6 | 5.21 |
| | 16 | 6.27 |
| W - O | 10 | 1.72 |
| | 4 | 2.26 |
| | 9 | 3.46 |
| | 12 | 4.00 |
| | 21 | 4.43 |
| | 17 | 4.84 |
| | 16 | 5.16 |
| | 7 | 5.43 |
| Na - Na | 6 | 3.60 |
| Na - O | 19 | 2.45 |
| O - O | 32 | 2.76 |
| | 11 | 3.24 |

## 4.2. STUDIES ON AMORPHOUS MOLYBDENUM TRIOXIDE (Lars Kihlborg)

The device described above (sect. 2.1) for deposition of metal oxide vapours on a cool surface has been found very useful for the preparation of $MoO_3$ in an amorphous state. During the course of this work the preparation of amorphous $MoO_3$ by a different method has been reported by Sarjent and Roy (14). The samples thus obtained, however, also contained crystalline material.

### 4.2.1. Preparative work

In the present study samples of 10-50 mg of $MoO_3$ were placed on the platinum strip. The system was evacuated whereupon the element was heated to temperatures roughly in the region 600-900°C for periods of time ranging from 2 to 15 min. The cooling agent was either liquid air or a dry ice-alcohol mixture. The deposit thus obtained on the cool surface could easily be removed after the experiment. Considerable amounts of a very slightly greenish material were thus collected.

### 4.2.2. Properties and recrystallization of the amorphous material

The character of the deposit was studied by the taking of X-ray photographs and by infrared spectroscopy. The appearance of the X-ray pictures was clearly that of an amorphous material. The IR spectra obtained are represented in Fig. 15, which also gives the corresponding curve for crystalline $MoO_3$.

The two curves show very striking differences. Thus, the transmission minimum at 990 $cm^{-1}$ ascribed to a Mo=O stretching band and the less sharp minima at lower frequencies characteristic of the crystalline material are absent in the curve of the amorphous substance which shows far less detail within this range of frequency. At higher frequencies, however, amorphous $MoO_3$ shows transmission minima not given by the crystals, viz. at 1400 and 1600 $cm^{-1}$ and in the 3000-3500 $cm^{-1}$ region. Such minima are encountered in materials containing hydroxide groups and it seems rather likely that in the

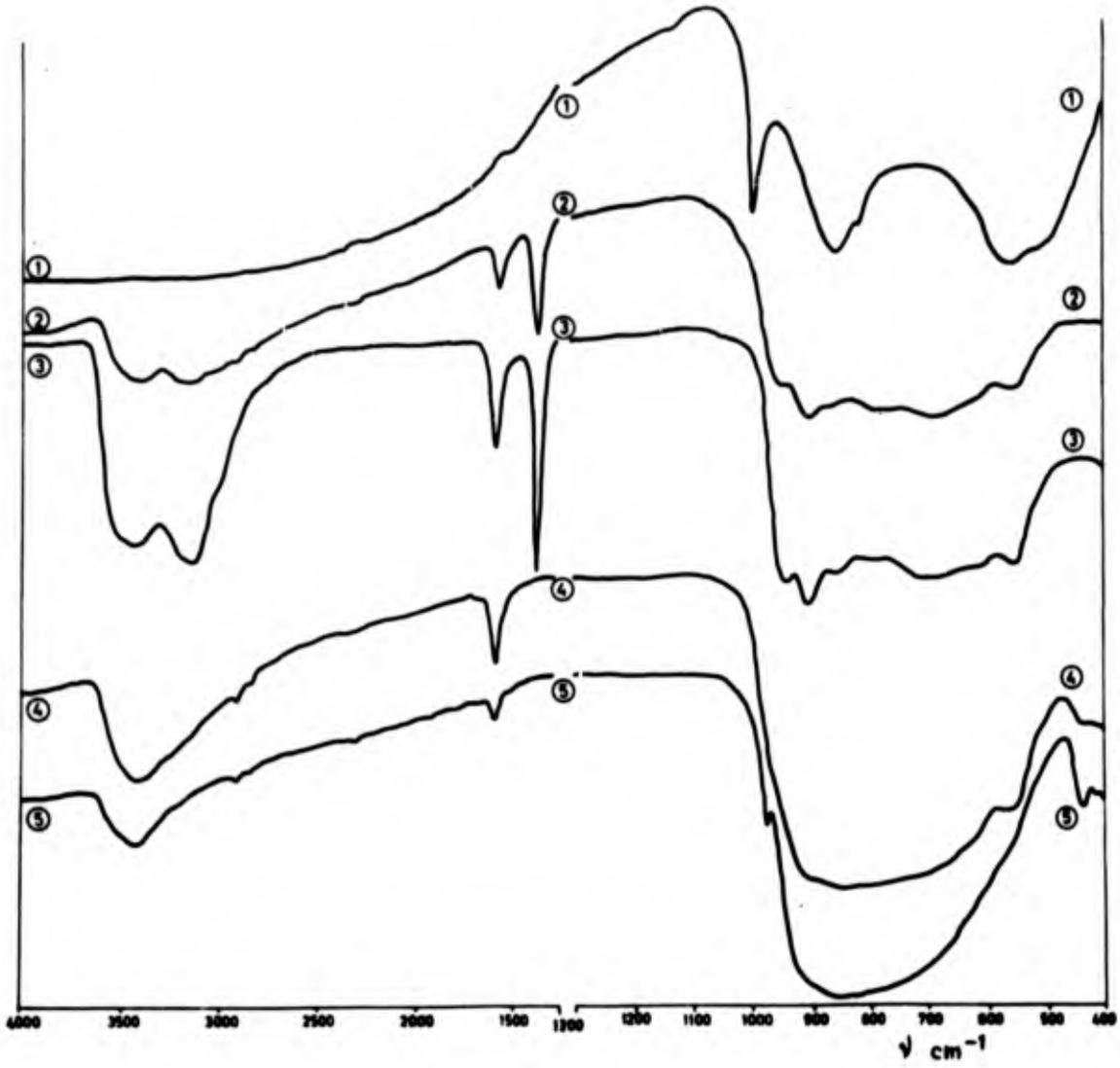


Figure 15. IR spectra of molybdenum trioxide treated in various ways.

1. Original crystalline sample (resublimed).
2. Sample A, obtained by vapour deposition on a surface cooled by liquid air.
3. Sample A after being kept for one day in air.
4. Sample A heated a few seconds in air. Dark blue-green sample.
5. Sample A heated a few minutes in air. Yellow greenish sample.

present case they indicate a hygroscopic character of amorphous $MoO_3$ not exhibited in the normal crystalline state. This is also supported by the marked increase of the absorption at those frequences when the sample is exposed to the laboratory atmosphere over night. (Fig. 15, curve 3). Experiments to test this hypothesis are now being made using dry-box techniques in order to prevent any exposure of the amorphous material to moisture. The general idea so far arrived at is that if the interpretation of the observations advanced above holds true the water absorption power of amorphous $MoO_3$ is a very strong one.

Some preliminary experiments on the recrystallization of amorphous $MoO_3$ may also be mentioned here. Gradual heating of the samples in air was found to change the colour from almost white to deep blue-green. Upon further heating a gradual change into the normal yellowish white of crystalline $MoO_3$ was found to take place. The latter product was characterized as crystalline $MoO_3$ by its X-ray powder pattern. The IR curve of the intermediary materials showed a gradual transition towards the spectrum of the crystalline material. The features in the high frequency range was thus successively disappearing while the 990 $cm^{-1}$ peak which is characteristic for the crystals appeared (Fig. 15 curve 4 and 5).

## 4.3. STUDIES ON THE SYSTEMS $\underline{A}_2WO_4$-$WO_3$ ($\underline{A}$ = K or Rb)

### 4.3.1. Studies on the system $K_2WO_4$-$WO_3$

Attempts have previously been made to synthesize $K_2W_3O_{10}$ which, when heated above the melting point (718°C) decomposes into $K_2W_4O_{13}$ and $K_2O$. By use of a very slow cooling rate it has been possible to obtain the triwolframate.

To the stoichiometric composition $K_2WO_4$ + 2 $WO_3$ an excess of $K_2WO_4$ was added to increase the probability of obtaining a product of the desired composition. Mixtures with 0, 1, 5 and 10 (weight) per cent excess $K_2WO_4$ kept in unsealed silica tubes were heated to 750°C and allowed to cool to 600°C at a rate of 2°C an hour. Guinier powder photographs were taken which showed the pattern of $K_2W_3O_{10}$ as given

by Gelsing et al. (15). The mixture with 10 per cent excess $K_2WO_4$ gives a phase consisting of yellow needle-shaped crystals contrary to the three other compositions which gave colourless crystals. This phase produced a powder pattern which differs slightly from the others but is in accordance with the powder photograph of $Rb_2W_3O_{10}$ and mixed products such as $K_2Mo_{1.5}W_{1.5}O_{10}$ and $K_2MoW_2O_{10}$.

A preliminary single crystal investigation of the yllow triwolframate has been made. The symmetry is hexagonal as is also the case with $K_2W_4O_{13}$, the structure of which is given in this report. From the Weissenberg photographs it seems probable that there are mirror planes perpendicular to and also parallel to the c axis. The c axis, 3.86 Å, is of the same length as in $K_2W_4O_{13}$ (3.85 Å). It is also interesting to compare the length of the a axes of $K_2W_3O_{10}$ which are about 7.7 Å to the length of the a axes in $K_2W_4O_{13}$ i.e. 15.53 Å. These values make the volume of the unit cell of $K_2W_3O_{10}$ one quarter of the volume of the tetrawolframate cell which contains three formula units. Accordingly, the cell content of the triwolframate would be one formula unit.

Listed d-values calculated from powder photographs have been given by Gelsing (15) and Caillet (16) for the di-, tri-, and tetrawolframates. The two authors give different sets of d values for $K_2W_2O_7$. Furthermore, our values do not agree with either listing. The d values of $K_2W_3O_{10}$, as determined by both authors, are in accordance with our data. In the case of $K_2W_4O_{13}$ the two authors' sets of d-values differ. Our values show agreement with those of Gelsing et al. (15).

### 4.3.2. The crystal structure of dipotassium tetrawolframate (Madeleine Seleborg)

Investigations of the structures of some alkali isopolymolybdates have previously been carried out at this Institute (11, 17). As the corresponding alkali isopolywolframates should be expected to display analogous crystallographic features it was thought worthwhile to extend the investigations to include some of the phases in

the system $WO_3$-$\underline{A}_2WO_4$ where $\underline{A}$ stands for alkali metal. The system $WO_3$-$K_2WO_4$ was first studies extensively by Hoermann (12) who established the presence of intermediary phases of the composition $K_2W_3O_{10}$ and $K_2W_4O_{13}$. More recently, this system has been investigated by Gelsing et al. (15) who observed a range of glass formation. Crystal studies of the intermediary phases should therefore prove valuable to elucidate the structural conditions of wolfram in the vitreous state as well.

a. Experimental

Dipotassium tetrawolframate was formed when an intimate mixture of potassium wolframate (British Drug Houses Ltd) and wolfram trioxide ("Baker's Analyzed", J.T. Baker Chemical Co., USA) was heated at 750°C in a platinum crucible. The Guinier powder photograph of the product obtained agrees well with the list of $\underline{d}$-values given for $K_2W_4O_{13}$ by Gelsing et al. The crystals were of a faintly green colour and had the shape of very long thin needles adhering very strongly to each other, which condition made it difficult to locate a single crystal. The one finally found was of an awkward shape being very long and thin but was, however, mounted in the needle direction for recording of Weissenberg data of the layer lines $\underline{hk}0$-$\underline{hk}2$. $\underline{CuK}$ radiation and multiple film technique were used. The intensities of the 434 independent reflections were measured visually by comparison with an intensity scale obtained by photographing a reflection from this crystal with different periods of exposure.

All calculations were performed on a CD 3600 computer. The atomic scattering factors used were those of unionized W, K and O with the real part of the dispersion correction applied to the scattering factors of W and K.

b. Derivation of the structure

The Weissenberg photographs showed hexagonal symmetry. The unit cell dimensions were determined by the method of least squares from a powder pattern recorded in a Guinier focusing camera using $CuK_{\alpha_1}$ radiation and with potassium chloride as an internal standard. The cell parameters thus obtained were $\underline{a}$ = 15.530 ± 0.003 Å and $\underline{c}$ = 3.8502 ± ± 0.0007 Å, $\underline{z}$ = 3.

On account of the strong resemblance in intensity distribution between the hk0, hk1 and hk2 layer lines it was assumed that the heavy atoms were all situated in one plane perpendicular to the c-axis (or nearly so). No systematic absences were observed. As the only element of symmetry which could be postulated would then be a mirror plane perpendicular to the c axis, the space group initially tried was P6/m. The location of the wolfram atoms could be treated as a two-dimensional problem. Approximate positions were obtained from a Patterson projection along [001]. The twelve wolfram atoms were found to be situated in two six-fold positions with the z parameter $\approx 0$. A least squares refinement of the heavy atom parameters alone resulted in a value of 0.243 of the discrepancy index:

$$R = \frac{\Sigma \left| |F_o(hkl)| - |F_c(hkl)| \right|}{\Sigma |F_o(hkl)|}$$

Although this was not quite as good an agreement as one might expect with heavy atoms, a difference Fourier synthesis was calculated on the basis of the structure factor signs thus obtained. The difference synthesis clearly showed that the two sets of wolfram atoms should be separated in the c direction. Accordingly, the non-centrosymmetric space group P6 was settled upon. A subsequent least squares refinement yielded an R-factor value of 0.146, a significantly lower value than gave the previous calculation.

Another three-dimensional difference Fourier synthesis was computed at points spaced 0.30 Å apart along the a axes and 0.38 Å apart along the c axis. This synthesis showed potassium to be located in a six-fold position at z approximately 0.50.

The positions of those oxygen atoms which were situated around wolfram in roughly the same plane ($z \sim 0$) were easily located. Three sixfold positions and one three-fold position were displayed on the Fourier maps. Mainly on spatial grounds the remaining oxygens were assuemd to reside in three six-fold positions. The electron density in these regions was about half the value of the average height of the other oxygen peaks.

Table 2. Comparison between calculated and observed structure factors for $K_2W_4O_{13}$.

| h | k | l | $F_{obs}$ | $F_{calc}$ | h | k | l | $F_{obs}$ | $F_{calc}$ |
|---|---|---|---|---|---|---|---|---|---|
| 1 | 1 | 0 | 177 | 203 | 10 | 4 | 0 | 192 | 163 |
| 2 | 1 | 0 | 202 | 214 | 12 | 4 | 0 | 76 | 78 |
| 3 | 1 | 0 | 303 | 286 | 13 | 4 | 0 | 60 | 55 |
| 4 | 1 | 0 | 248 | 227 | 0 | 5 | 0 | 118 | 128 |
| 5 | 1 | 0 | 33 | 38 | 1 | 5 | 0 | 98 | 116 |
| 6 | 1 | 0 | 161 | 142 | 3 | 5 | 0 | 145 | 151 |
| 7 | 1 | 0 | 222 | 228 | 4 | 5 | 0 | 163 | 153 |
| 8 | 1 | 0 | 102 | 102 | 5 | 5 | 0 | 62 | 66 |
| 9 | 1 | 0 | 157 | 147 | 6 | 5 | 0 | 138 | 124 |
| 11 | 1 | 0 | 65 | 63 | 7 | 5 | 0 | 108 | 95 |
| 12 | 1 | 0 | 67 | 59 | 8 | 5 | 0 | 43 | 54 |
| 13 | 1 | 0 | 153 | 147 | 9 | 5 | 0 | 277 | 264 |
| 14 | 1 | 0 | 120 | 107 | 10 | 5 | 0 | 183 | 174 |
| 15 | 1 | 0 | 144 | 128 | 11 | 5 | 0 | 53 | 47 |
| 1 | 2 | 0 | 67 | 56 | 12 | 5 | 0 | 47 | 43 |
| 3 | 2 | 0 | 647 | 635 | 13 | 5 | 0 | 52 | 49 |
| 5 | 2 | 0 | 175 | 188 | 0 | 6 | 0 | 70 | 69 |
| 6 | 2 | 0 | 112 | 121 | 1 | 6 | 0 | 136 | 115 |
| 8 | 2 | 0 | 142 | 141 | 2 | 6 | 0 | 443 | 461 |
| 10 | 2 | 0 | 105 | 94 | 3 | 6 | 0 | 50 | 52 |
| 14 | 2 | 0 | 265 | 265 | 4 | 6 | 0 | 147 | 150 |
| 15 | 2 | 0 | 51 | 42 | 5 | 6 | 0 | 146 | 137 |
| 0 | 3 | 0 | 79 | 119 | 7 | 6 | 0 | 109 | 111 |
| 1 | 3 | 0 | 222 | 234 | 8 | 6 | 0 | 112 | 111 |
| 2 | 3 | 0 | 87 | 101 | 11 | 6 | 0 | 106 | 107 |
| 3 | 3 | 0 | 107 | 118 | 12 | 6 | 0 | 40 | 32 |
| 4 | 3 | 0 | 63 | 67 | 13 | 6 | 0 | 168 | 205 |
| 5 | 3 | 0 | 139 | 128 | 0 | 7 | 0 | 137 | 155 |
| 6 | 3 | 0 | 386 | 395 | 1 | 7 | 0 | 376 | 378 |
| 7 | 3 | 0 | 312 | 311 | 2 | 7 | 0 | 116 | 115 |
| 8 | 3 | 0 | 48 | 46 | 3 | 7 | 0 | 189 | 198 |
| 9 | 3 | 0 | 63 | 48 | 4 | 7 | 0 | 134 | 146 |
| 10 | 3 | 0 | 167 | 167 | 5 | 7 | 0 | 106 | 104 |
| 12 | 3 | 0 | 134 | 120 | 9 | 7 | 0 | 98 | 84 |
| 13 | 3 | 0 | 72 | 63 | 10 | 7 | 0 | 74 | 70 |
| 14 | 3 | 0 | 43 | 45 | 11 | 7 | 0 | 85 | 79 |
| 0 | 4 | 0 | 125 | 137 | 12 | 7 | 0 | 105 | 111 |
| 1 | 4 | 0 | 144 | 141 | 0 | 8 | 0 | 72 | 73 |
| 2 | 4 | 0 | 100 | 114 | 1 | 8 | 0 | 117 | 127 |
| 3 | 4 | 0 | 60 | 53 | 2 | 8 | 0 | 57 | 43 |
| 5 | 4 | 0 | 84 | 87 | 3 | 8 | 0 | 69 | 66 |
| 6 | 4 | 0 | 245 | 252 | 4 | 8 | 0 | 167 | 160 |
| 8 | 4 | 0 | 120 | 113 | 5 | 8 | 0 | 345 | 356 |

| h | k | l | $F_{obs}$ | $F_{calc}$ |
|---|---|---|---|---|
| 8 | 8 | 0 | 97 | 101 |
| 9 | 8 | 0 | 45 | 38 |
| 10 | 8 | 0 | 89 | 85 |
| 11 | 8 | 0 | 52 | 41 |
| 0 | 9 | 0 | 59 | 35 |
| 1 | 9 | 0 | 148 | 145 |
| 3 | 9 | 0 | 139 | 137 |
| 4 | 9 | 0 | 58 | 45 |
| 6 | 9 | 0 | 97 | 99 |
| 7 | 9 | 0 | 99 | 100 |
| 8 | 9 | 0 | 214 | 206 |
| 9 | 9 | 0 | 60 | 42 |
| 10 | 9 | 0 | 42 | 41 |
| 2 | 10 | 0 | 70 | 64 |
| 3 | 10 | 0 | 52 | 40 |
| 4 | 10 | 0 | 111 | 116 |
| 5 | 10 | 0 | 76 | 76 |
| 6 | 10 | 0 | 42 | 38 |
| 7 | 10 | 0 | 110 | 101 |
| 8 | 10 | 0 | 203 | 205 |
| 9 | 10 | 0 | 42 | 50 |
| 0 | 11 | 0 | 398 | 416 |
| 1 | 11 | 0 | 54 | 38 |
| 2 | 11 | 0 | 54 | 38 |
| 3 | 11 | 0 | 62 | 69 |
| 4 | 11 | 0 | 80 | 85 |
| 5 | 11 | 0 | 79 | 86 |
| 6 | 11 | 0 | 103 | 97 |
| 0 | 12 | 0 | 113 | 97 |
| 1 | 12 | 0 | 78 | 80 |
| 2 | 12 | 0 | 143 | 141 |
| 3 | 12 | 0 | 106 | 92 |
| 4 | 12 | 0 | 111 | 108 |
| 5 | 12 | 0 | 47 | 38 |
| 6 | 12 | 0 | 69 | 65 |
| 7 | 12 | 0 | 100 | 105 |
| 1 | 13 | 0 | 64 | 52 |
| 3 | 13 | 0 | 264 | 264 |
| 6 | 13 | 0 | 62 | 73 |
| 1 | 14 | 0 | 120 | 115 |
| 0 | 15 | 0 | 103 | 89 |
| 1 | 15 | 0 | 43 | 58 |
| 2 | 15 | 0 | 53 | 47 |
| 0 | 1 | 1 | 92 | 95 |
| 1 | 1 | 1 | 188 | 184 |
| 2 | 1 | 1 | 232 | 254 |
| 3 | 1 | 1 | 264 | 297 |
| 4 | 1 | 1 | 188 | 210 |
| 5 | 1 | 1 | 29 | 20 |
| 6 | 1 | 1 | 126 | 161 |
| 7 | 1 | 1 | 209 | 190 |
| 8 | 1 | 1 | 77 | 74 |
| 9 | 1 | 1 | 100 | 100 |
| 10 | 1 | 1 | 52 | 26 |
| 11 | 1 | 1 | 56 | 51 |
| 12 | 1 | 1 | 75 | 71 |
| 13 | 1 | 1 | 131 | 129 |
| 14 | 1 | 1 | 88 | 84 |
| 15 | 1 | 1 | 134 | 134 |
| 0 | 2 | 1 | 98 | 81 |
| 1 | 2 | 1 | 135 | 133 |
| 3 | 2 | 1 | 334 | 358 |
| 4 | 2 | 1 | 74 | 76 |
| 5 | 2 | 1 | 171 | 148 |
| 6 | 2 | 1 | 106 | 76 |
| 8 | 2 | 1 | 118 | 99 |
| 9 | 2 | 1 | 72 | 43 |
| 10 | 2 | 1 | 102 | 90 |
| 11 | 2 | 1 | 54 | 40 |
| 12 | 2 | 1 | 75 | 73 |
| 13 | 2 | 1 | 49 | 47 |
| 14 | 2 | 1 | 246 | 245 |
| 15 | 2 | 1 | 47 | 48 |
| 0 | 3 | 1 | 107 | 72 |
| 1 | 3 | 1 | 244 | 239 |
| 2 | 3 | 1 | 76 | 55 |
| 3 | 3 | 1 | 106 | 75 |
| 4 | 3 | 1 | 51 | 65 |
| 5 | 3 | 1 | 180 | 191 |
| 6 | 3 | 1 | 364 | 384 |
| 7 | 3 | 1 | 258 | 267 |
| 8 | 3 | 1 | 68 | 17 |
| 9 | 3 | 1 | 74 | 73 |
| 10 | 3 | 1 | 153 | 131 |
| 11 | 3 | 1 | 60 | 46 |
| 12 | 3 | 1 | 98 | 100 |
| 13 | 3 | 1 | 68 | 55 |
| 14 | 3 | 1 | 45 | 46 |
| 0 | 4 | 1 | 132 | 134 |
| 1 | 4 | 1 | 95 | 127 |
| 2 | 4 | 1 | 97 | 84 |
| 3 | 4 | 1 | 52 | 49 |

| h | k | l | $F_{obs}$ | $F_{calc}$ |
|---|---|---|---|---|
| 4 | 4 | 1 | 70 | 76 |
| 5 | 4 | 1 | 93 | 48 |
| 6 | 4 | 1 | 180 | 168 |
| 7 | 4 | 1 | 89 | 87 |
| 8 | 4 | 1 | 81 | 92 |
| 10 | 4 | 1 | 170 | 166 |
| 11 | 4 | 1 | 44 | 29 |
| 12 | 4 | 1 | 66 | 85 |
| 13 | 4 | 1 | 82 | 70 |
| 0 | 5 | 1 | 129 | 80 |
| 1 | 5 | 1 | 82 | 56 |
| 2 | 5 | 1 | 139 | 127 |
| 3 | 5 | 1 | 117 | 104 |
| 4 | 5 | 1 | 166 | 157 |
| 5 | 5 | 1 | 72 | 47 |
| 6 | 5 | 1 | 109 | 96 |
| 7 | 5 | 1 | 139 | 138 |
| 8 | 5 | 1 | 96 | 89 |
| 9 | 5 | 1 | 238 | 244 |
| 10 | 5 | 1 | 163 | 159 |
| 11 | 5 | 1 | 64 | 39 |
| 12 | 5 | 1 | 46 | 46 |
| 13 | 5 | 1 | 60 | 37 |
| 0 | 6 | 1 | 149 | 148 |
| 1 | 6 | 1 | 141 | 151 |
| 2 | 6 | 1 | 387 | 431 |
| 3 | 6 | 1 | 45 | 42 |
| 4 | 6 | 1 | 98 | 128 |
| 5 | 6 | 1 | 145 | 96 |
| 6 | 6 | 1 | 67 | 73 |
| 7 | 6 | 1 | 84 | 84 |
| 8 | 6 | 1 | 98 | 85 |
| 9 | 6 | 1 | 43 | 36 |
| 10 | 6 | 1 | 37 | 25 |
| 11 | 6 | 1 | 96 | 87 |
| 12 | 6 | 1 | 36 | 28 |
| 13 | 6 | 1 | 155 | 201 |
| 0 | 7 | 1 | 114 | 108 |
| 1 | 7 | 1 | 222 | 245 |
| 2 | 7 | 1 | 57 | 74 |
| 3 | 7 | 1 | 150 | 138 |
| 4 | 7 | 1 | 93 | 103 |
| 5 | 7 | 1 | 83 | 93 |
| 6 | 7 | 1 | 60 | 49 |
| 8 | 7 | 1 | 47 | 46 |
| 9 | 7 | 1 | 65 | 59 |
| 10 | 7 | 1 | 96 | 100 |
| 11 | 7 | 1 | 87 | 81 |
| 12 | 7 | 1 | 81 | 95 |
| 0 | 8 | 1 | 86 | 33 |
| 1 | 8 | 1 | 119 | 120 |
| 2 | 8 | 1 | 85 | 89 |
| 3 | 8 | 1 | 125 | 110 |
| 4 | 8 | 1 | 144 | 155 |
| 5 | 8 | 1 | 314 | 337 |
| 6 | 8 | 1 | 60 | 30 |
| 8 | 8 | 1 | 109 | 80 |
| 9 | 8 | 1 | 50 | 64 |
| 10 | 8 | 1 | 82 | 77 |
| 11 | 8 | 1 | 47 | 31 |
| 0 | 9 | 1 | 68 | 63 |
| 1 | 9 | 1 | 136 | 143 |
| 2 | 9 | 1 | 72 | 61 |
| 3 | 9 | 1 | 130 | 117 |
| 6 | 9 | 1 | 75 | 70 |
| 7 | 9 | 1 | 91 | 87 |
| 8 | 9 | 1 | 198 | 197 |
| 9 | 9 | 1 | 48 | 49 |
| 10 | 9 | 1 | 48 | 49 |
| 0 | 10 | 1 | 79 | 63 |
| 1 | 10 | 1 | 43 | 35 |
| 2 | 10 | 1 | 52 | 54 |
| 3 | 10 | 1 | 55 | 58 |
| 4 | 10 | 1 | 99 | 99 |
| 5 | 10 | 1 | 93 | 113 |
| 6 | 10 | 1 | 64 | 56 |
| 7 | 10 | 1 | 73 | 83 |
| 8 | 10 | 1 | 191 | 195 |
| 9 | 10 | 1 | 50 | 48 |
| 0 | 11 | 1 | 369 | 390 |
| 1 | 11 | 1 | 57 | 71 |
| 2 | 11 | 1 | 60 | 31 |
| 3 | 11 | 1 | 82 | 52 |
| 4 | 11 | 1 | 87 | 91 |
| 5 | 11 | 1 | 87 | 71 |
| 6 | 11 | 1 | 92 | 84 |
| 8 | 11 | 1 | 29 | 21 |
| 0 | 12 | 1 | 68 | 75 |
| 1 | 12 | 1 | 59 | 56 |
| 2 | 12 | 1 | 103 | 113 |
| 3 | 12 | 1 | 77 | 86 |
| 4 | 12 | 1 | 91 | 90 |

| h | k | l | $F_{obs}$ | $F_{calc}$ | h | k | l | $F_{obs}$ | $F_{calc}$ |
|---|---|---|---|---|---|---|---|---|---|
| 5 | 12 | 1 | 33 | 24 | 10 | 2 | 2 | 66 | 65 |
| 6 | 12 | 1 | 62 | 75 | 11 | 2 | 2 | 74 | 61 |
| 7 | 12 | 1 | 76 | 89 | 12 | 2 | 2 | 115 | 98 |
| 0 | 13 | 1 | 49 | 35 | 13 | 2 | 2 | 39 | 39 |
| 1 | 13 | 1 | 60 | 62 | 14 | 2 | 2 | 162 | 191 |
| 3 | 13 | 1 | 243 | 254 | 0 | 3 | 2 | 140 | 90 |
| 4 | 13 | 1 | 39 | 44 | 1 | 3 | 2 | 153 | 147 |
| 5 | 13 | 1 | 60 | 50 | 2 | 3 | 2 | 112 | 105 |
| 6 | 13 | 1 | 57 | 65 | 3 | 3 | 2 | 136 | 93 |
| 0 | 14 | 1 | 50 | 37 | 4 | 3 | 2 | 81 | 93 |
| 1 | 14 | 1 | 130 | 113 | 5 | 3 | 2 | 153 | 85 |
| 3 | 14 | 1 | 45 | 43 | 6 | 3 | 2 | 247 | 281 |
| 0 | 15 | 1 | 80 | 68 | 7 | 3 | 2 | 203 | 217 |
| 1 | 15 | 1 | 64 | 79 | 8 | 3 | 2 | 104 | 34 |
| 2 | 15 | 1 | 53 | 43 | 9 | 3 | 2 | 109 | 117 |
| 0 | 16 | 1 | 69 | 56 | 10 | 3 | 2 | 168 | 119 |
| 1 | 16 | 1 | 41 | 32 | 11 | 3 | 2 | 87 | 24 |
| 0 | 1 | 2 | 125 | 118 | 12 | 3 | 2 | 91 | 91 |
| 1 | 1 | 2 | 129 | 137 | 13 | 3 | 2 | 71 | 60 |
| 2 | 1 | 2 | 150 | 122 | 14 | 3 | 2 | 61 | 60 |
| 3 | 1 | 2 | 164 | 192 | 0 | 4 | 2 | 101 | 97 |
| 4 | 1 | 2 | 177 | 187 | 1 | 4 | 2 | 149 | 201 |
| 5 | 1 | 2 | 56 | 34 | 2 | 4 | 2 | 116 | 102 |
| 6 | 1 | 2 | 154 | 205 | 3 | 4 | 2 | 103 | 100 |
| 7 | 1 | 2 | 173 | 148 | 4 | 4 | 2 | 102 | 105 |
| 8 | 1 | 2 | 137 | 152 | 5 | 4 | 2 | 119 | 89 |
| 9 | 1 | 2 | 96 | 100 | 6 | 4 | 2 | 178 | 177 |
| 10 | 1 | 2 | 69 | 56 | 7 | 4 | 2 | 64 | 76 |
| 11 | 1 | 2 | 73 | 71 | 8 | 4 | 2 | 76 | 99 |
| 12 | 1 | 2 | 55 | 47 | 9 | 4 | 2 | 28 | 47 |
| 13 | 1 | 2 | 134 | 105 | 10 | 4 | 2 | 108 | 126 |
| 14 | 1 | 2 | 76 | 78 | 11 | 4 | 2 | 74 | 50 |
| 15 | 1 | 2 | 81 | 105 | 12 | 4 | 2 | 90 | 109 |
| 0 | 2 | 2 | 161 | 118 | 13 | 4 | 2 | 60 | 51 |
| 1 | 2 | 2 | 160 | 156 | 0 | 5 | 2 | 193 | 113 |
| 3 | 2 | 2 | 346 | 422 | 1 | 5 | 2 | 97 | 92 |
| 4 | 2 | 2 | 126 | 112 | 2 | 5 | 2 | 141 | 102 |
| 5 | 2 | 2 | 150 | 114 | 3 | 5 | 2 | 147 | 107 |
| 6 | 2 | 2 | 112 | 83 | 4 | 5 | 2 | 111 | 100 |
| 7 | 2 | 2 | 58 | 72 | 5 | 5 | 2 | 79 | 49 |
| 8 | 2 | 2 | 151 | 107 | 6 | 5 | 2 | 120 | 105 |
| 9 | 2 | 2 | 96 | 70 | 7 | 5 | 2 | 154 | 135 |

| h | k | l | $F_{obs}$ | $F_{calc}$ | h | k | l | $F_{obs}$ | $F_{calc}$ |
|---|---|---|---|---|---|---|---|---|---|
| 8 | 5 | 2 | 88 | 45 | 4 | 9 | 2 | 40 | 76 |
| 9 | 5 | 2 | 173 | 197 | 5 | 9 | 2 | 37 | 54 |
| 10 | 5 | 2 | 128 | 139 | 6 | 9 | 2 | 67 | 67 |
| 11 | 5 | 2 | 93 | 42 | 7 | 9 | 2 | 98 | 84 |
| 12 | 5 | 2 | 51 | 42 | 8 | 9 | 2 | 132 | 147 |
| 0 | 6 | 2 | 134 | 79 | 9 | 9 | 2 | 47 | 63 |
| 1 | 6 | 2 | 99 | 109 | 0 | 10 | 2 | 90 | 40 |
| 2 | 6 | 2 | 281 | 315 | 1 | 10 | 2 | 65 | 52 |
| 3 | 6 | 2 | 43 | 72 | 2 | 10 | 0 | 57 | 62 |
| 4 | 6 | 2 | 138 | 199 | 3 | 10 | 2 | 78 | 75 |
| 5 | 6 | 2 | 168 | 95 | 4 | 10 | 2 | 68 | 85 |
| 7 | 6 | 2 | 88 | 81 | 5 | 10 | 2 | 109 | 128 |
| 8 | 6 | 2 | 124 | 86 | 6 | 10 | 2 | 62 | 46 |
| 9 | 6 | 2 | 68 | 64 | 7 | 10 | 2 | 65 | 75 |
| 11 | 6 | 2 | 100 | 75 | 8 | 10 | 2 | 104 | 148 |
| 0 | 7 | 2 | 98 | 118 | 0 | 11 | 2 | 255 | 294 |
| 1 | 7 | 2 | 212 | 248 | 1 | 11 | 2 | 44 | 80 |
| 2 | 7 | 2 | 75 | 105 | 2 | 11 | 2 | 93 | 68 |
| 3 | 7 | 2 | 151 | 126 | 3 | 11 | 2 | 123 | 60 |
| 4 | 7 | 2 | 86 | 102 | 4 | 11 | 2 | 84 | 64 |
| 5 | 7 | 2 | 91 | 79 | 5 | 11 | 2 | 110 | 61 |
| 6 | 7 | 2 | 96 | 73 | 6 | 11 | 2 | 92 | 71 |
| 7 | 7 | 2 | 36 | 59 | 7 | 11 | 2 | 28 | 42 |
| 8 | 7 | 2 | 71 | 82 | 0 | 12 | 2 | 91 | 98 |
| 9 | 7 | 2 | 69 | 58 | 1 | 12 | 2 | 79 | 73 |
| 10 | 7 | 2 | 101 | 114 | 2 | 12 | 2 | 111 | 105 |
| 11 | 7 | 2 | 47 | 59 | 3 | 12 | 2 | 68 | 73 |
| 0 | 8 | 2 | 121 | 40 | 4 | 12 | 2 | 98 | 92 |
| 1 | 8 | 2 | 122 | 97 | 5 | 12 | 2 | 33 | 24 |
| 2 | 8 | 2 | 109 | 89 | 0 | 13 | 2 | 82 | 46 |
| 3 | 8 | 2 | 110 | 61 | 1 | 13 | 2 | 103 | 105 |
| 4 | 8 | 2 | 113 | 118 | 3 | 13 | 2 | 160 | 199 |
| 5 | 8 | 2 | 251 | 265 | 4 | 13 | 2 | 50 | 59 |
| 6 | 8 | 2 | 96 | 61 | 0 | 14 | 2 | 91 | 40 |
| 7 | 8 | 2 | 143 | 77 | 1 | 14 | 2 | 76 | 82 |
| 10 | 8 | 2 | 70 | 65 | 2 | 14 | 2 | 35 | 45 |
| 0 | 9 | 2 | 125 | 96 | 3 | 14 | 2 | 46 | 48 |
| 1 | 9 | 2 | 99 | 99 | 0 | 15 | 2 | 81 | 70 |
| 2 | 9 | 2 | 114 | 91 | 1 | 15 | 2 | 53 | 95 |
| 3 | 9 | 2 | 121 | 110 | | | | | |

The final least squares refinement with a full matrix program and individual isotropic temperature factors gave an R-factor of 0.134. Hughes' weighting function $w = 1/h^2|F_o \text{ min}|^2$ for $|F_o| \leq h|F_o \text{ min}|$ and $w = 1/|F_o|^2$ for $|F_o| \geq |F_o \text{ min}|$ was used with the parameter $h$ given the value 4. A comparison between calculated and observed F values is given in Table 2.

In addition to small spurious maxima in the electron density maps - easily dismissed as they lead to abnormal interatomic distances - there were two lower ones situated on the six-fold axis. The interpretation of either one of these as being a potassium site with the remaining five potassium atoms statistically distributed over the six-fold position could not be conclusively ruled out.

c. Description and discussion of the structure

A list of the structural parameters is given in Table 3. The temperature factors of the oxygens are somewhat anomalous which may be due to the difficulty in getting first class data from a crystal of unsuitable shape. No real physical significance can be attached to the temperature factors as the data have not been corrected for absorption.

Table 3. The crystal structure of $K_2W_4O_{13}$.

Space group P6 (No. 168 of the International Tables)

Cell content $3K_2W_4O_{13}$

12 W, 6 K and 36 O in 6(d): $x,y,z$; $\bar{y},x-y,z$; $y-x,\bar{x},z$; $\bar{x},\bar{y},z$; $y,y-x,z$; $x-y,x,z$.

3 O in 3(c): $\frac{1}{2},0,z$; $0,\frac{1}{2},z$; $\frac{1}{2},\frac{1}{2},z$

| Atom | $x \pm \sigma(x)$ | $y \pm \sigma(y)$ | $z \pm \sigma(z)$ | B |
|---|---|---|---|---|
| W(1) | .1780±.0003 | .2665±.0003 | .088±.003 | 1.04±.10 |
| W(2) | .0899±.0003 | .4523±.0003 | 0 | .90 ±.10 |
| O(1) | .352 ±.004 | .036 ±.004 | .97 ±.03 | |
| O(2) | .029 ±.006 | .186 ±.006 | .19 ±.03 | |
| O(3) | .156 ±.004 | .378 ±.004 | .05 ±.03 | |
| O(4) | .636 ±.008 | .196 ±.008 | .18 ±.04 | Average value 3.0 |
| O(5) | .066 ±.010 | .433 ±.010 | .56 ±.07 | |
| O(6) | 0 | 1/2 | .02 ±.06 | |
| O(7) | .161 ±.013 | .257 ±.013 | .57 ±.099 | |
| K | .497 ±.002 | .182 ±.002 | .51 ±.02 | 3.4 ±0.6 |

The structure is built of $WO_6$ octahedra which are connected by shared corners to form six-membered rings in the xy plane. As a consequence of the short c axis, all octahedra also share corners in the z direction. A projection along 001 is given in Fig. 16 since the z parameter values of the top oxygens of the $WO_6$ octahedra obtained in different least squares refinements varied, the positions of these atoms were difficult to settle accurately. This effect may be the result if the wolfram atoms are in fact subject to "rattling" within the octahedra especially along the z direction.

Through the centres of the six-membered rings of octahedra are formed tunnels of infinite extension running in the direction of the short axis. This is a structural feature which several wolfram compounds have in common. The hexagonal wolfram bronzes (18) which are represented by a potassium bronze and also by rubidium and caesium bronzes have tunnel structures. In these compounds, the tunnels enclose the statistically distributed alkali ions. The pseudo-hexagonal wolfram trioxide (19), which has a superlattice due to the substitution of one molybdenum for every twelfth wolfram, contains six-edged empty channels running parallel to the c-axis which in this case has a length of 3.834 Å. Empty tunnels of infinite extension are also found in the wolfram oxide $W_{18}O_{49}$ (20).

In the tetrawolframate, the six potassium ions are probably located in a six-fold position, thus occupying interstices of a somewhat complicated shape. The one-fold position 00z would also be a plausible site in analogy with the conditions in wolfram bronzes. That this may in fact be the case is indicated by the difference Fourier syntheses and consequently by least-squares refinements based on that assumption. The potassium atoms may, thus, be distributed over a six-fold and one or two one-fold positions. That the two types of tunnel interstices arise in the tetrawolframate, only one of which is present in the structurally similar wolfram bronzes is due to the different manner of coupling of the $WO_6$ octahedra in the two structures. Whereas, in the latter structure the six-membered rings are

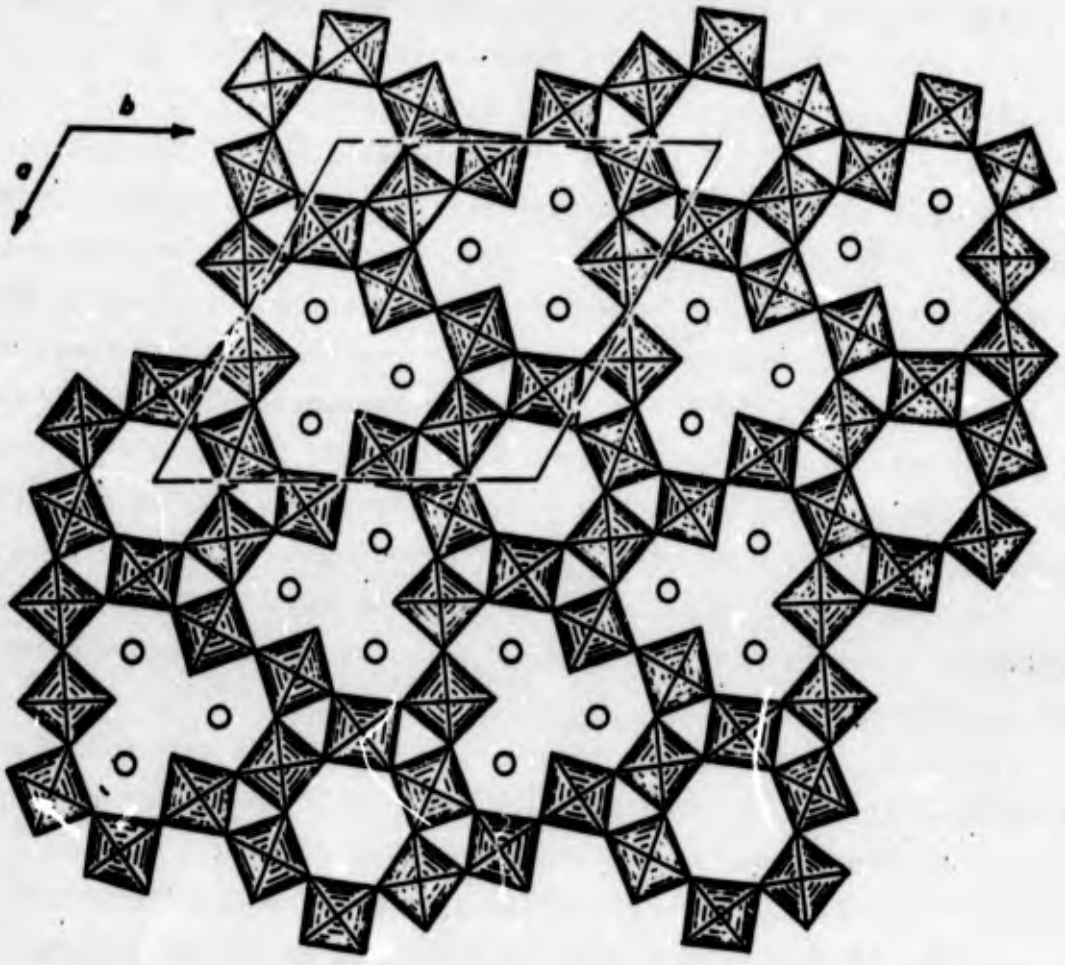


Figure 16. The structure of $K_2W_4O_{13}$ projected along the c-axis. The extent of one unit cell is indicated. The six-fold position of potassium is symbolized by circles.

sharing octahedra with adjacent rings, in the tetrawolframate the rings have no octahedra in common. They are more loosely connected sideways via a link of two corner-sharing octahedra. Additional tunnels of a more irregular shape are thus also formed in the structure (cf. Fig. 16).

4.3.3. Studies of the system $Rb_2WO_4$-$WO_3$

A thermal analysis of the system $Rb_2WO_4$-$WO_3$ has been made by Spitsyn and Kuleshov (21). The existence of di-, tri-, and hexawolframates was demonstrated. These phases melt incongruently at approximately 681°, 858° and 1045°C.

As the complexity of the isopolymolybdate and isopolywolframate anions studied so far seems to depend to a large extent on the nature of the alkali cation present, a comparison of the crystal structures of rubidium polywolframates to those of the potassium or sodium compounds may prove to be of interest. The presence of rubidum, which is one of the largest and least "polarizing" of the cations, would probably be conductive to the build-up of complex wolframate chains or a net-work with a high oxygen coordination number around wolfram. An analogous investigation of caesium polywolframates has not as yet been considered since one might anticipate that the presence of a heavy cation together with wolfram would tend to render the positions of the oxygen atoms as determined from X-ray investigations rather inaccurate.

Prepatations have been made using $Rb_2CO_3$ and $WO_3$ as starting materials and heating appropriate mixtures of the components in platinum crucibles at temperatures slightly below the melting points of the desired products.

$Rb_2W_2O_7$ was prepared at 660°C. A lightly salmon-coloured crystalline product was obtained. The crystals are, however, poorly developed. The Guinier powder photograph does not indicate structural similarity with $Na_2W_2O_7$, the only diwolframate the structure of which has as yet been determined. Efforts are now being made to obtain larger crystals of $Rb_2W_2O_7$.

$Rb_2W_3O_{10}$ was prepared by heating of the reaction mixture to 840°C. A two phase system was obtained: a salmon-coloured phase identical with the one mentioned above which was interspersed with green prismatic crystals. The Guinier powder photograph of the latter was almost identical with a diffraction pattern of one of the preparations of $K_2W_3O_{10}$ (mentioned below) as well as with that of mixed compounds like e.g. $K_2MoW_2O_{10}$. This implies that the green crystals are in fact of the composition $Rb_2W_3O_{10}$. As the green prisms are easily separated from the mixture, attempts will be made to select a single crystal for data recording and subsequent structure determination.

Stoichiometric $Rb_2W_6O_{19}$ was heated to 1040°C and gave a dark green substance which under the microscope revealed the presence of prismatic crystals. The Guinier powder photograph consisted mainly of diffraction lines identical with those obtained from pure $WO_3$ previously heated to 800°C. A few extra lines appeared, however, and noticeable among these were two diffraction lines at low $\theta$ angles. Additional lines of similar character were also present on the powder photograph obtained from a $Li_2O$ + 4 $WO_3$ mixture heated to 800°C. The product was suspected to contain what Hoermann (12) calls an octowolframate, a strongly acidic compound like $Rb_2W_6O_{19}$.

## 4.4. GLASSES AND CRYSTALLINE MATERIALS ON ARSENATE MOLYBDATE (WOLFRAMATE) BASIS

As described in previous reports (1,2) investigations have been performed within this research project on glasses prepared from the crystalline phases $\underline{A}MoO_2PO_4$ ($\underline{A}$ = Na, Ag) (22,23) and $NaWO_2PO_4$ (22). The structural analogies often displayed by phosphorus(V) and arsenic(V) made it of interest to find out whether corresponding crystalline phases and a similar tendency to glass formation exist in the systems $\underline{A}_2O$-$\underline{M}O_3$-$As_2O_5$ ($\underline{A}$ = Li, Na, K, Rb, Cs or Ag; $\underline{M}$ = Mo or W). The results so far obtained are somewhat preliminary in character.

4.4.1. Preparative work (Kaija Eistrat)

Preparations of the general composition $\underline{A}_2O \cdot 2\underline{M}O_3 \cdot As_2O_5$ were prepared by melting of alkali or silver carbonate (Baker Analyzed), arsenic pentoxide (Matheson, Coleman and Bell, Reagent) and molybdenum trioxide or wolfram trioxide (Mallinckrodt, analytical reagent) in a platinum crucible for two or three minutes at a temperature of about 1050°C. After rapid quenching, the character of the products was tested by visual inspection and microscopically, and also by means of X-ray powder techniques. The compositions were checked by weighing of the samples before and after the heat-treatment. Vitreous products were thus obtained for all the samples except $Li_2O \cdot 2WO_3 \cdot As_2O_5$. Additional heat-treatment of the vitreous materials at 500°C for periods up to 7 days resulted in devitrification of all the samples containing molybdenum and also of the preparations $\underline{A}_2O \cdot 2WO_3 \cdot As_2O_5$ ($\underline{A}$ = Na, K and Ag). Further data concerning the results of the preparative studies are summarized in Table 4.

Table 4. Data for preparations of general composition $A_2O \cdot 2\underline{M}O_3 \cdot As_2O_5$ ($\underline{A}$ = Li, Na, K, Rb, Cs or Ag; $\underline{M}$ = Mo or W).

| Atom $\underline{A}$ | Character * and colour ** of the product after: quenching a melt from 1050°C | | heat-treatm. 500°C 7 days | |
|---|---|---|---|---|
| | $\underline{M}$ = Mo | $\underline{M}$ = W | $\underline{M}$ = Mo | $\underline{M}$ = W |
| Li | G, green | C, white | C, white | C, white |
| Na | G, green | G, yellow | C, white | C, white |
| K | G, brown | G, yellow | C, white | C, white |
| Rb | G, brown | G, yellow | C, white | C, white |
| Cs | G, brown | G, light yellow | C, white | C, white |
| Ag | G, dark brown | G, green-yellow | C, light yellow | C, white |

* G = glasses or C = crystalline material.

** Given for the materials as powders.

The structural study undertaken for the phase $Li_2O \cdot 2MoO_3 \cdot As_2O_5$ (cf. below) made it of interest to investigate the range of glass formation and also the phase conditions of the lithium molybdate arsenate system in some more detail. By varying of the proportions of the constituents and treating of the mixtures in the way described above it was found that glasses of rather different compositions could be easily obtained in this system. The colour of these materials, the vitreous character of which was verified by X-ray techniques, varied from brownish to greenish. Upon further heat-treatment at 500°C for a week, crystallisation was found to have taken place in all the samples investigated with the exception of a green preparation of the approximate composition $Li_2O \cdot 2MoO_3 \cdot 2As_2O_5$ which still retained its vitreous character. The powder patterns of the devitrified samples, which represented $MoO_3 : As_2O_5$ ratios ranging from 1:4 to 2:1 and also different contents of $Li_2O$, showed the presence of a considerable number of ternary phases. Further studies on this matter are in progress.

A structural study is now being performed on the crystalline phase obtained by devitrification of the glass of composition $Li_2O \cdot 2MoO_3 \cdot As_2O_5$. The composition of the colourless crystals is likely to be the same as that of the glass, i.e. $LiMoO_2AsO_4$. The symmetry is orthorhombic or pseudoorthorhombic. Further work is in progress.

## 4.5. STUDIES ON PHOSPHATES OF ZIRCONIUM AND URANIUM

One of the aims of the present research has been to study the linking of $\underline{M}O_6$ octahedra and $\underline{M}'O_4$ tetrahedra and their role as structural units in glasses and crystals. Most of this work has, as far as the $\underline{M}$ atoms are concerned, dealt with Mo and W compounds while in addition to P and As, as $\underline{M}'$ atoms have also been included, transition elements such as Mo, W and V. A group of substances of interest from the point of view of further varying the character of the $\underline{M}$ atom includes the so-called Peyronel phases, i.e. $\underline{M}P_2O_7$ ($\underline{M}$ = tetravalent atoms ranging from Si to U and Th). Recent studies

on this interesting family of compounds have shown that the structure originally reported by Peyronel and coworkers (24,25) does not cover all the details of the atomic arrangement but represents a substructure. The $ZrP_2O_7$ phase, which is now being investigated at this Institute, actually has a unit cell 27 times larger than the one previously reported. The symmetry is lower than cubic. It is probably orthorhombic.

The very complicated superstructures thus found for the Peyronel phases has made it seem desirable to undertake studies on some related phases with less complex structures. The work in this area has so far comprised $NaZr_2(PO_4)_3$ and $U(PO_3)_4$.

4.5.1. The structure of $NaZr_2(PO_4)_3$ (Lars-Ove Hagman)

Within the present study the compounds $NaZr_2(PO_4)_3$, $NaTi_2(PO_4)_3$ and $NaGe_2(PO_4)_3$ have been synthesized and found to be isomorphous. According to data reported by Sljukić et al. (26) further compounds of this stoichiometry, viz. zirconium and hafnium phosphates of all the alkali metals, should also belong in this structural family. The sodium zirconium phosphate was chosen for a single-crystal X-ray study of this extensive isomorphous series. $MO_6$ octahedra and $PO_4$ tetrahedra, linked by corners to form a threedimensional network were thus found to represent the structural principle of these compounds. A detailed account of the investigation have been submitted as a Special Technical and Scientific Report, which is also enclosed as Appendix IV of this report.

4.5.2. The structure of $U(PO_3)_4$ (Ann Kopwillem)

a. Experimental

$U(PO_3)_4$ was prepared by heating $U_3O_8$ with excess $(NH_4)_2HPO_4$ to 1000°C. The crystalline powder thus obtained which was somewhat heterogeneous was further heated with conc. orthophosphoric acid at 600°C. In this way green single crystals of $U(PO_3)_4$ were obtained which could be easily separated from the residue. Analyses, density measurements and other methods of preparation are described by Colani (27), Burdese and Borlera (28), Douglas (29) and Baskin (30).

The powder pattern was easily interpreted assuming an orthorhombic unit cell. Values for the cell dimensions were calculated from a photograph taken with strictly monochromatized $CuK_1$ radiation in a Guinier-Hägg type focusing camera. Potassium chloride was used as an internal standard (see Table 5). The unit cell dimensions are (25°C):

$$\underline{a} = 6.9106 \pm 0.0009 \text{ (Å)}$$
$$\underline{b} = 14.9399 \pm 0.0003 \text{ (Å)}$$
$$\underline{c} = 8.9868 \pm 0.0007 \text{ (Å)}$$
$$\underline{V} = 927.8 \text{ (Å}^3\text{)}$$

From rotation and Weissenberg photographs (hk0-hk5, 0kl-4kl) of a single crystal with the dimensions 0.032 mm (in the direction of the a axis) x 0.018 mm (b) x 0.021 mm (c) - taken with CuK radiation, it was concluded that the crystals have the Laue symmetry mmm. The reflections systematically absent are 0kl with k = odd, h0l with l = odd and hk0 with h+k = odd, which is characteristic of the space group Pbcn.

The reflections were recorded photographically with multiple film technique. The relative intensities were estimated visually by comparison with an intensity scale obtained by photographing a reflection with different exposure times. A total of 321 independent reflections were assigned an intensity.

Practically all the computational work involved in this study, including refinement of the lattice constants (Program No. 6018), absorption correction (No. 6019), Lorentz polarization correction (No. 6024), Fourier summations (No. 6015), least-squares refinement (No. 6023) and calculation of interstomic distances (No. 6016) were performed on the electronic computers FACIT EDB and TRASK. The numbers refer to the list of crystallographic computer programs (3).

When determining the $F^2$ values, the linear absorption coefficient, $\mu = 670.8$ cm$^{-1}$, was derived from atomic absorption coefficients given by Victoreen (31).

Table 5. X-ray powder data observed for $U(PO_3)_4$. $CuK\alpha_1$ radiation. $\lambda_{CuK\alpha_1}$ = 1.54050 Å.

| h k l | $10^5 \sin^2\vartheta$ obs | $10^5 \sin^2\vartheta$ calc | I |
|---|---|---|---|
| 1 1 0 | 1511 | 1511 | s |
| 1 2 1 | 1799 | 1801 | s |
| 1 1 1 | 2247 | 2247 | s |
| 0 0 2 | 2949 | 2943 | vw |
| 1 2 1 | 3047 | 3045 | vw |
| 1 3 0 | 3640 | 3641 | vs |
| 0 2 2 | 4005 | 4009 | m |
| 1 0 2 | 4189 | 4188 | m |
| 1 3 1 | 4374 | 4377 | m |
| 1 1 2 | 4453 | 4454 | vs |
| 1 3 2 | 6585 | 6584 | m |
| 2 2 1 | 6772 | 6779 | s |
| 0 4 2 | 7197 | 7204 | vs |
| 0 2 3 | 7690 | 7688 | s |
| 2 0 2 | 7921 | 7921 | m |
| 1 1 3 | 8129 | 8133 | m |
| 1 5 1 | 8628 | 8637 | m |
| 2 4 0 | 9239 | 9238 | m |
| 2 3 2 | 10298 | 10317 | vvw |
| 0 6 1 | | 10321 | |
| 1 5 2 | 10867 | 10844 | vvw |
| 0 4 2 | | 10883 | |
| 2 4 2 | 12186 | 12181 | m |
| 3 1 1 | | 12202 | |
| 2 2 3 | 12661 | 12665 | w |
| 1 1 4 | 13288 | 13284 | w |
| 1 5 3 | 14531 | 14523 | s |
| 2 6 1 | 15289 | 15299 | w |
| 1 3 4 | 15411 | 15414 | s |
| 3 4 1 | 16201 | 16196 | w |
| 0 6 3 | | 16208 | |
| 3 3 2 | 16534 | 16540 | w |
| 2 0 4 | 16739 | 16751 | w |
| 1 7 2 | 17233 | 17234 | s |
| 2 6 2 | 17503 | 17506 | vw |
| 3 5 1 | 18591 | 18592 | w |
| 0 2 5 | 19451 | 19461 | w |
| 1 1 5 | 19919 | 19907 | m |
| 4 0 0 | | 19911 | |
| 4 2 0 | 21004 | 20976 | w |
| 2 4 4 | | 21011 | |
| 1 9 1 | 23546 | 23547 | w |
| 2 2 5 | 24449 | 24439 | vw |
| 2 8 2 | 24940 | 24962 | vw |
| 3 3 4 | 25353 | 25370 | vw |
| 1 7 4 | 26075 | 26064 | vw |
| 1 5 5 | 26306 | 26097 | vw |
| 4 4 2 | 27132 | 27114 | vw |
| 0 6 5 | 27999 | 27981 | vw |
| 1 1 6 | | 28001 | |

b. Investigation of the structure

The structural analysis performed on the basis of the data mentioned above included investigations of the Patterson and electron density functions and least-squares refinement of the atomic arrangement thus obtained. In this way result given in Table 6 was arrived at, corresponding to an R-value of 13 %.

Table 6. The substructure of $U(PO_3)_4$.

Space group: No. 60 Pbcn.

Unit cell dimensions: $a = 6.9106 \pm 0.0009$ Å

$b = 14.9399 \pm 0.0003$ Å

$c = 8.9868 \pm 0.0007$ Å

Cell content: 4 $U(PO_3)_4$

4 U and 4 $O_6$ in 4(c): $\pm(0,y,\frac{1}{4})$; $(\frac{1}{2},\frac{1}{2}+y,\frac{1}{4})$

8 $P_1$, 8 $P_2$, 8 $O_1$, 8 $O_2$, 8 $O_3$, 8 $O_4$, 8 $O_5$ and 4 $O_7$ in 8(d):

$\pm(x,y,z)$; $\pm(\frac{1}{2}-x,\frac{1}{2}-y,\frac{1}{2}+z)$; $\pm(\frac{1}{2}+x,\frac{1}{2}-y,\bar{z})$; $\pm(\bar{x},y,\frac{1}{2}-z)$

| Atom | $x \pm \sigma(x)$ | $y \pm \sigma(y)$ | $z \pm \sigma(z)$ | $B \pm \sigma(B)$ Å$^2$ |
|---|---|---|---|---|
| U | 0 | 0.1379± 0.0002 | 1/4 | 1.17 ± 0.05 |
| $P_1$ | 0.346 ± 0.003 | 0.314 ± 0.001 | 0.139 ± 0.005 | 1.53 ± 0.38 |
| $P_2$ | 0.287 ± 0.003 | 0.017 ± 0.001 | 0.520 ± 0.004 | 1.54 ± 0.46 |
| $O_1$ | 0.231 ± 0.008 | 0.246 ± 0.003 | 0.195 ± 0.007 | |
| $O_2$ | 0.915 ± 0.009 | 0.264 ± 0.004 | 0.998 ± 0.009 | |
| $O_3$ | 0.211 ± 0.011 | 0.399 ± 0.005 | 0.157 ± 0.014 | |
| $O_4$ | 0.737 ± 0.011 | 0.056 ± 0.004 | 0.139 ± 0.013 | Average 2.19 |
| $O_5$ | 0.338 ± 0.014 | 0.549 ± 0.005 | 0.071 ± 0.015 | |
| $O_6$ | 0 | 0.855 ± 0.004 | 1/4 | |
| $O_7$ | 0.014 ± 0.022 | 0.519 ± 0.005 | 0.027 ± 0.017 | |

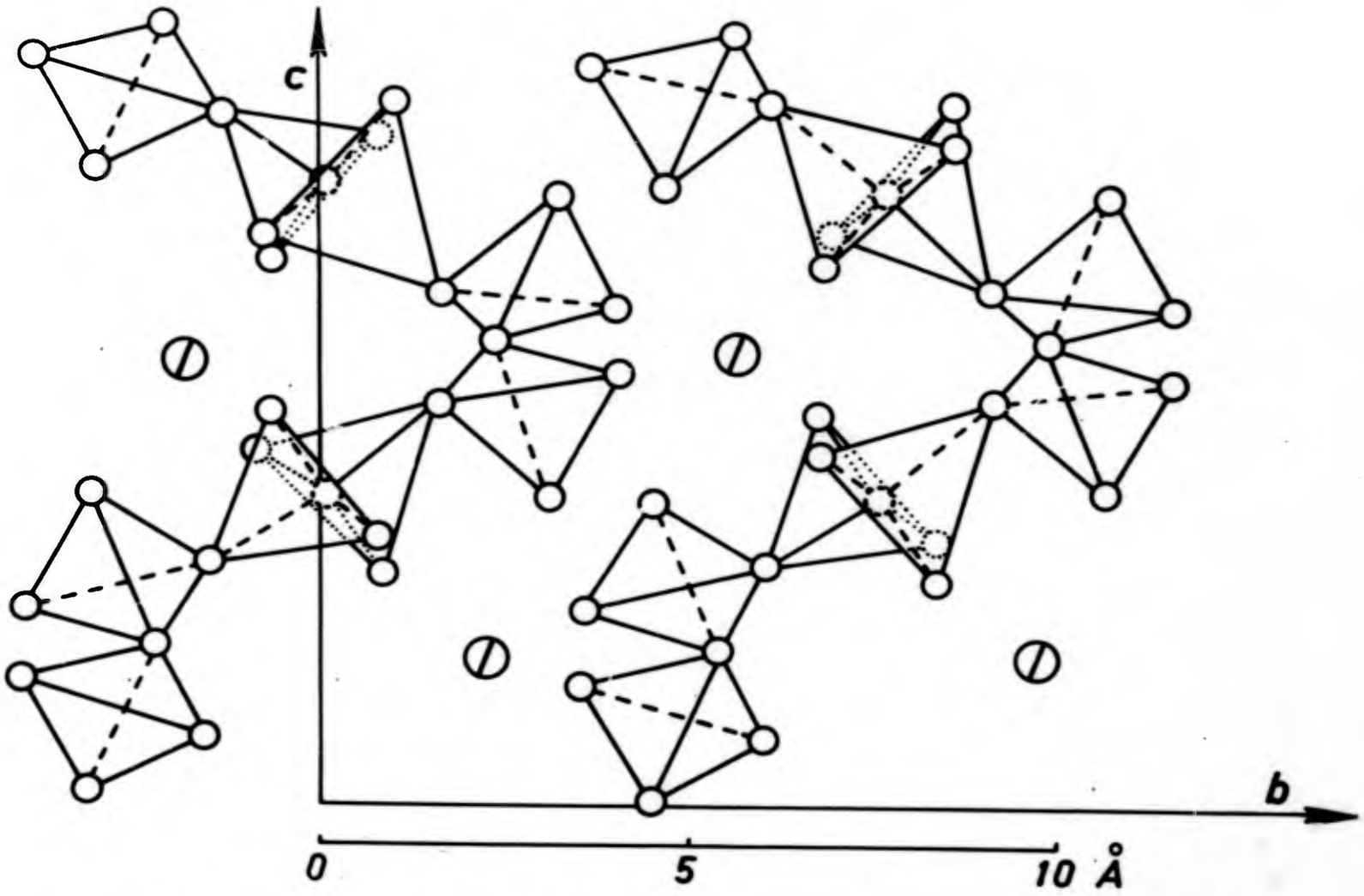


Figure 17. Schematic drawing of the crystal structure of $U(PO_3)_4$. Small circles denote oxygen atoms and big, lined circles uranium atoms. The phosphorus atoms in the $PO_3^-$-chains have not been indicated.

An inspection of the positional and "thermal" parameters as obtained in the course of the refinement suggests that the structure is essentially correct but casts some doubt on the arrangement of the $O_7$ atoms. The high "thermal" parameter value of this atom indicated the presence of either a disorder or a superstructure. The former alternative was considered less probable as it was likely to effect some disorder in the arrangement of neighbouring O atoms. The possibility of a superstructure was thus carefully tested by close inspection of single-crystal photographs registered with very ample exposure, viz. for periods ten times the normal ones. In this way very faint reflections were disclosed which required a doubling of the a axis. This observation actually confirms the unit cell size reported by Baskin (30).

So far a refinement of the structural details of the superstructure cannot be undertaken due to the unfavourable proportion between the number of observed independent reflections and the number of atomic parameters.

However, the picture given by the analysis of the substructure provides some essentials about the structure principles of $U(PO_3)_4$ (cf. Fig. 17). Thus the oxygen arrangement around uranium is eightfold in a somewhat distorted square antiprism. Metaphosphate chains form spirals with a repeat unit of 8 $PO_4$-tetrahedra.

## 4.6. STUDIES ON TERNARY OXIDE SYSTEMS CONTAINING VANADIUM AND MOLYBDENUM OR WOLFRAM

Recent studies conducted at this Institute and elsewhere have given ample evidence that the coordination numbers in oxide compounds of vanadium, molybdenum, wolfram and also some other transition elements may differ quite a lot dependent on the structural character of the particular oxide. All of these metals may occur in $\underline{M}O_4$ tetrahedra or $\underline{M}O_6$ octahedra but such polyhedra often deviate considerably from regularity. Arrangements of atoms better described as intermediates between tetrahedra and octahedra are frequently met with. In the pohosphates of transition elements investigated within this program the P

atoms invariably occur in a tetrahedral environment. The present investigations of the ternary oxide systems with vanadium and molybdenum or wolfram have been undertaken in order to find out how variations in composition and oxidation number affect the coordination conditions of these transition elements. It is thus to be looked upon as an extension of the research described above on alkali polymolybdates and polywolframates.

4.6.1. The molybdenum vanadium oxide system (Lars Kihlborg)

The results of an extensive phase analysis investigation of the Mo-V-O system at 600°C are summarized in Fig. 18. Starting from reagent grade $MoO_3$ and $V_2O_5$, batches of $MoO_2$ and $V_2O_3$ respectively were prepared by reduction with hydrogen. Appropirate mixtures of the various oxides were heated for periods of several days in sealed evacuated silica or platinum capsules at 600°C.

Upon quenching, the ternary oxide products were investigated by X-ray powder techniques. The ternary phases thus found to exist are listed in Table 7 which also presents some crystallographic characteristics.

The binary border-line systems Mo-O and V-O have been studied in considerable detail by members of this and associated groups and were consequently not included in the present investigation.

The crystal structures of the phases $VOMoO_4$ and $V_2Mo_3$ were determined some time ago by Eick and the present author (32, 33). The structure of $(Mo_{0.3}V_{0.7})_2O_5$ which may be considered as the end member of a structurally related series of compounds, extending from the binary composition $V_2O_5$ has also been solved. The results of this study are described in Appendix III of this report and in a recent article (34). A discussion of the structural relations existing between $V_2O_5$, $(Mo_{0.3}V_{0.7})_2O_5$ and $V_2MoO_8$ is also given in this article.

The phase $(Mo_{0.93}V_{0.07})_5O_{14}$ has been found to be isostructural with $Mo_5O_{14}$ (35) but with somewhat different unit cell parameters. The binary $Mo_5O_{14}$ phase has never been obtained at temperatures ex-

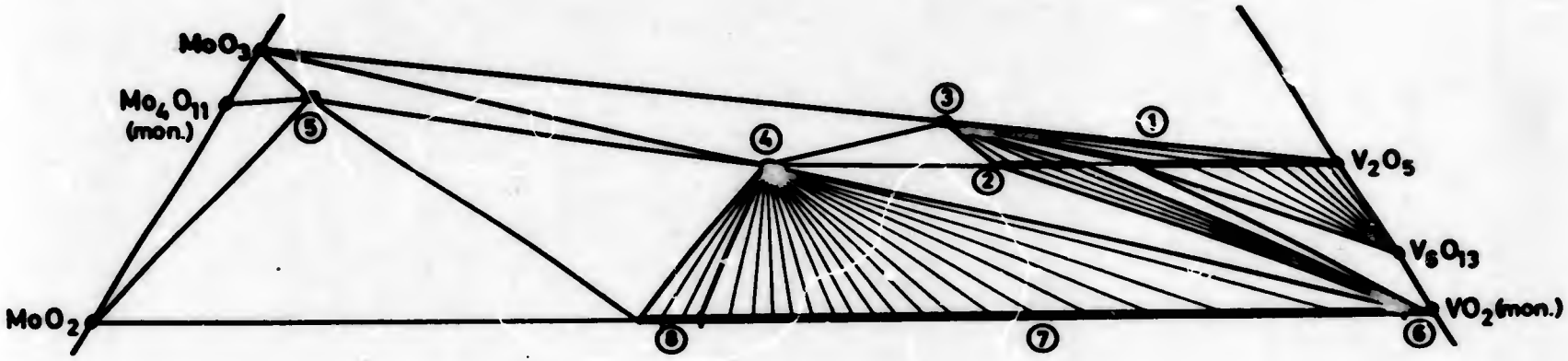


Figure 18. Part of the Mo-V-O phase diagram as obtained from X-ray powder diffraction photographs taken at room temperature after heat treatment of the samples at 600°C. The intermediate phases are designated by numbers which are explained in Table

Table 7. Intermediate phases in the Mo-V-O system forming at about 600°C.

| Designation in Fig. | Composition | Symmetry | Unit cell dimensions | Remarks |
|---|---|---|---|---|
| 1 | $(Mo_xV_{1-x})_2O_5$ $0 \leq x < \sim 0.17$ | Orthorhombic | See Fig. 19 | $V_2O_5$ structure. The upper limit of x is approximate. The powder patterns of samples around x=20 are complex and may possibly indicate the presence of a phase with a more complicated struct. |
| 2 | $(Mo_xV_{1-x})_2O_5$ $\sim 0.23 < x < 0.30$ | Monoclinic | See Fig. 19 | Structure related to that of $V_2O_5$ (34). Lower limit of x is approximate, see above. |
| 3 | $MoV_2O_8$ | Monoclinic | a = 19.40 Å<br>b = 7.258 Å<br>c = 4.117 Å<br>β = 90.34° | Structure related to those of $V_2O_5$ and $(Mo_{0.3}V_{0.7})_2O_5$ (33). May have a narrow homogeneity range. |
| 4 | $VOMoO_4$ | Tetragonal | a = 6.6078 Å<br>c = 4.2646 Å | Structure see (32). May have a narrow homogeneity range. |
| 5 | $(V_{0.07}Mo_{0.93})_5O_{14}$ | Tetragonal | a = 22.85 Å<br>c = 3.990 Å | $Mo_5O_{14}$ structure (35). |
| 6 | $(Mo_xV_{1-x})O_2$ | Monoclinic | a = 7.751 Å<br>b = 4.526 Å<br>c = 5.383 Å<br>β = 122.6° | Low-$VO_2$ structure (distorted rutile). The upper limit of x is uncertain but not greater than 0.02 |
| 7 | $(Mo_xV_{1-x})O_2$ $\sim 0.03 < x < 0.55$ | Tetragonal | See Fig. 20 | Rutile-type struct. |
| 8 | $(Mo_xV_{1-x})O_2$ $0.55 < x < 0.60$ | Orthorhombic | a = 6.69 Å<br>b = 6.62 Å<br>c = 2.84 Å | Slightly distorted rutile structure. |

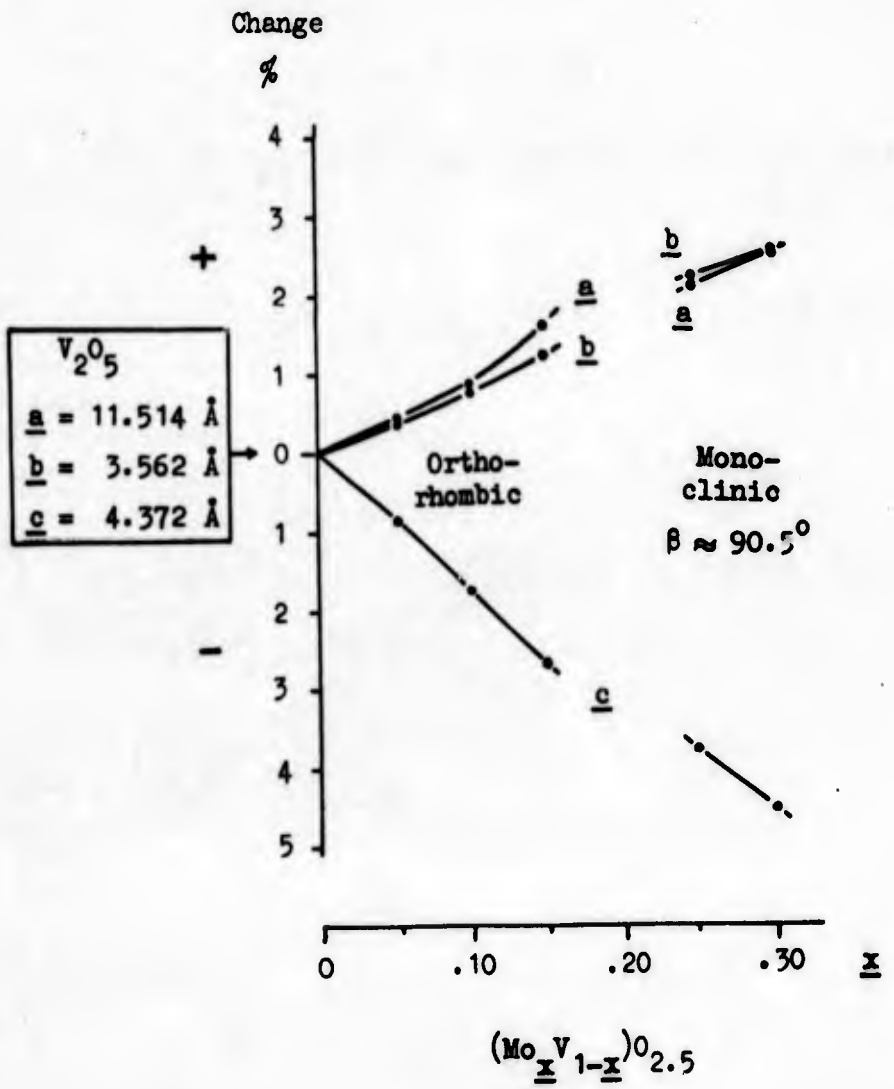


Figure 19. The change of the unit cell parameters compared to those of $V_2O_5$ plotted versus composition for phases $(Mo_xV_{1-x})_2O_5$.

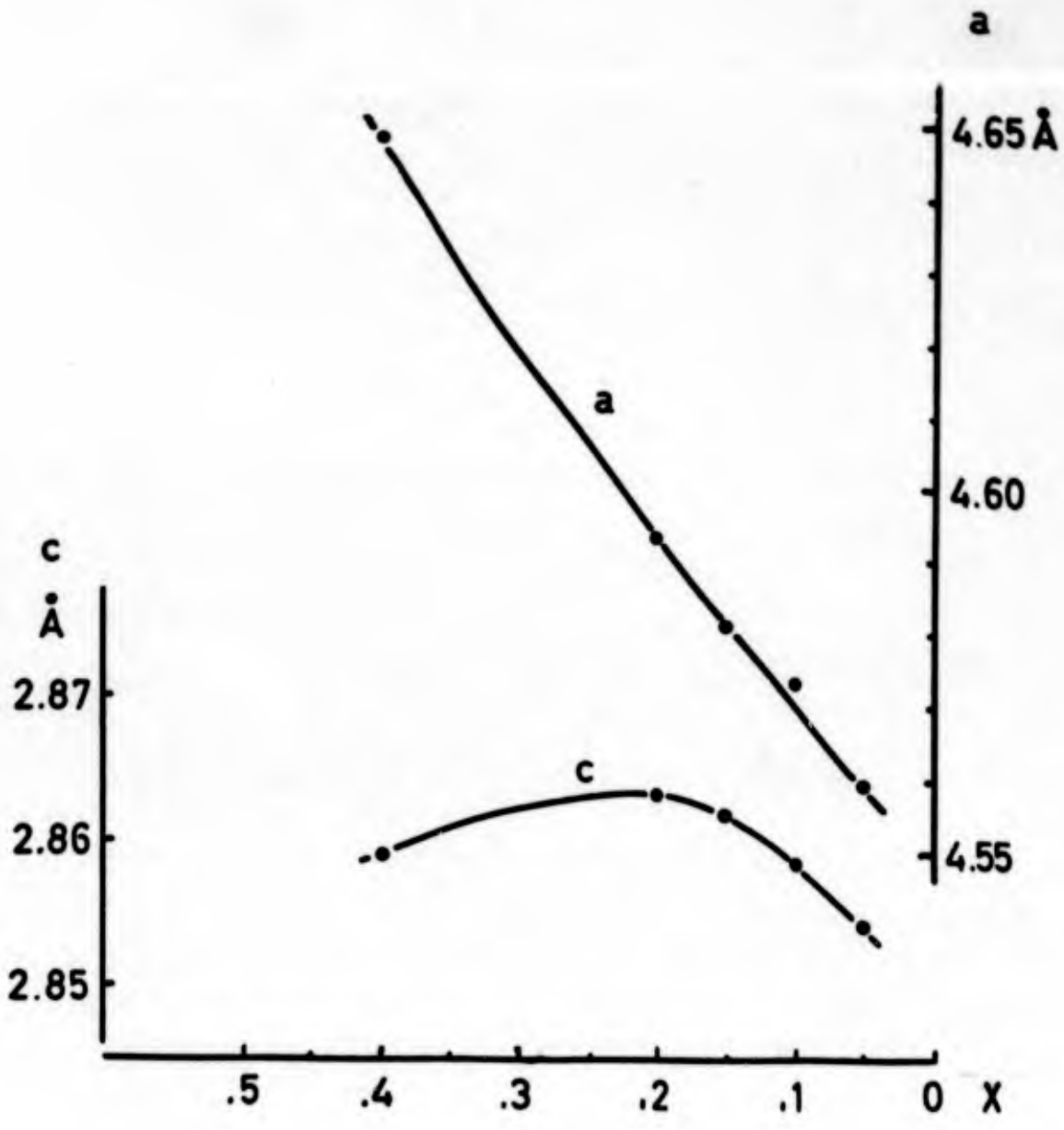


Figure 20. The variation of the unit cell parameters with composition for rutile-type phases $(Mo_{\underline{x}}V_{1-\underline{x}})O_2$.

ceeding 520°C. The ternary compound prepared at 600°C seems to have a very narrow compositional range of stability.

The present studies on the Mo-V-O system have given further evidence of the variability of the coordination numbers or vanadium and molybdenum. The structural elements present in the family comprising $V_2O_5$, $(Mo_{0.3}V_{0.7})_2O_5$ and $V_2MoO_8$ and which also includes R-$Nb_2O_5$ (36) and $Nb_3O_7F$ (37), may be described as $\underline{M}O_6$ octahedra showing a more or less marked distortion. The ternary oxide of $Mo_5O_{14}$ type likewise contains distorted $\underline{M}O_6$ octahedra and also $\underline{M}O_7$ pentagonal bipyramids. The structure of $VOMoO_4$ is of a particular interest, being isomorphous with the molybdenum oxide phosphate $MoOPO_4$. Thus, the former contains distorted $VO_6$ octahedra and fairly regular $MoO_4$ tetrahedra.

4.6.2. The wolfram vanadium oxide system (Mats Israelsson and Lars Kihlborg)

The present study of the phase relations in the W-V-O system have essentially been restricted to the regions which according to studies by Freundlich et al. (38) contain ternary phases. The preparative work was made in a way analogous to the one described above for the Mo-V-O system. Temperatures within the range 700-1100°C were used when preparing the samples.

The existence of two ternary phases has been demonstrated within the present work. The compositions found are fairly close to $W_{0.375}V_{0.625}O_{2.5}$ (temperature of formation 800-1000°C) and $V_{0.35}V_{0.65}O_{2.5}$ ( 800°C). These compositions deviate only slightly from those reported by Freundlich et al. (38). The crystal structures of the two phases have been determined from three-dimensional X-ray data.

The structure of $W_{0.375}V_{0.625}O_{2.5}$, which has so far been refined to an R-value of 0.07, may be described as belonging in the $V_2O_5$-type family (cf. Fig. 21). Thus, the structural elements are distorted

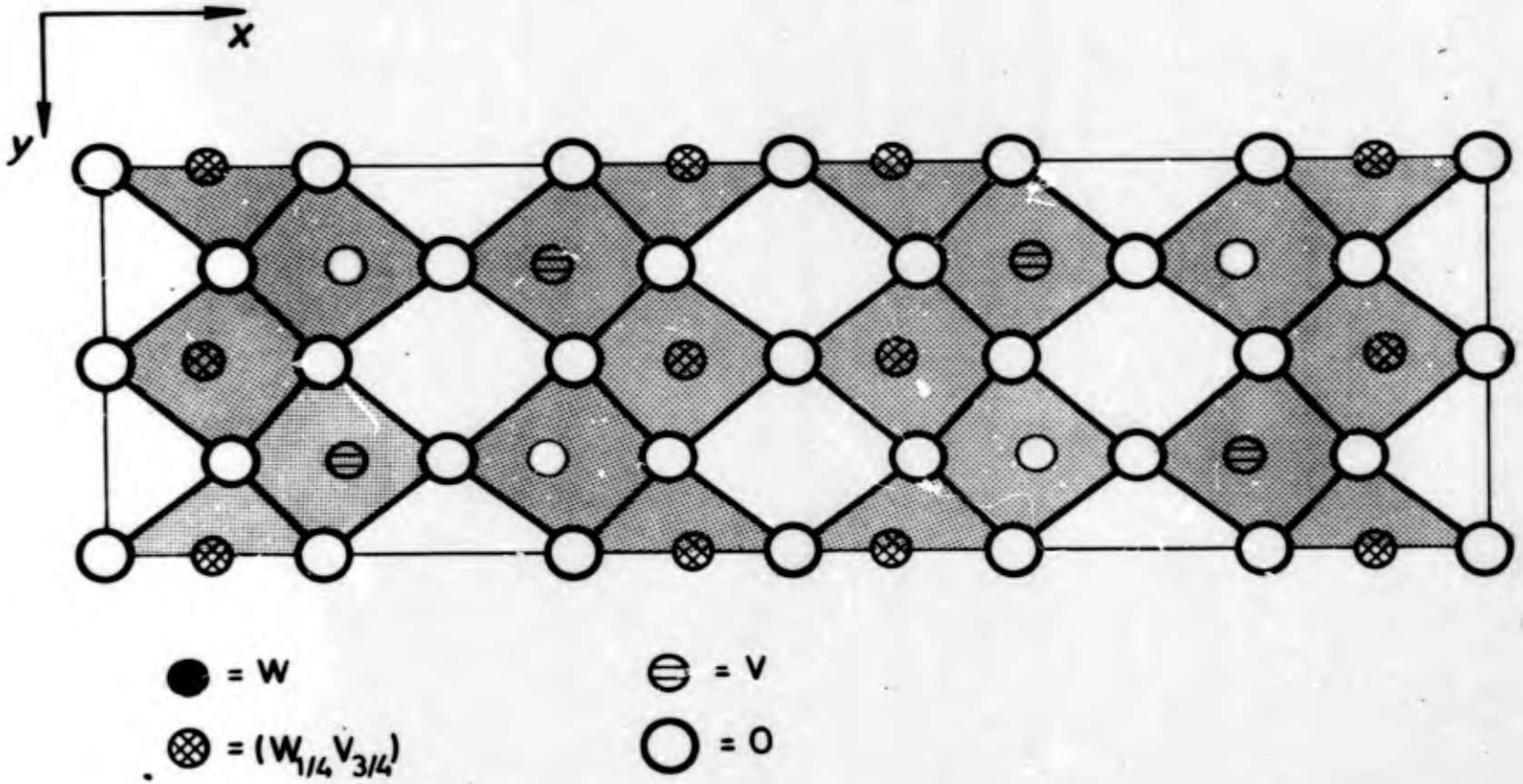


Figure 21. The crystal structure of the monoclinic wolfram vanadium oxide, $W_{0.375}V_{0.625}O_{2.5}$, viewed along the short c-axis. The oxygen atoms approximately above and below each metal atom along the line of sight have been omitted.

$\underline{M}O_6$ octahedra joined by edges and corners to form layers, the latter being linked together by additional sharing of corners. The atomic positional parameters are fairly close to those found in $(Mo_{0.3}V_{0.7})_2O_5$ (cf. Appendix III) but a partially ordered distribution of the W and V atoms gives rise to a superstructure which manifests itself in a doubling of both the $\underline{a}$ and $\underline{b}$ axes.

The tetragonal structure of $W_{0.35}V_{0.65}O_{2.5}$ is illustrated in Fig. 22. The structure contains $\underline{M}O_6$ octahedra, some of which, however, are considerably distorted in such a way that the shape approaches that of a $\underline{M}O_4$ tetrahedral polyhedron. The $\underline{M}O_6$ octahedra are joined by corners to form blocks of infinite extension along the tetragonal axis and having a cross section of 4x4 polyhedra. The blocks are mutually linked by octahedra sharing edges. The structure has been refined to an $\underline{R}$-value of 0.062. This has been achieved under the assumption of different W/V ratios on the three crystallographically different metal atom positions. The atomic distribution thus arrived at corresponds to the least divergence of the $\underline{B}$ values ("thermal parameters") of the various metal atom positions.

## 4.7. STUDIES ON COPPER WOLFRAM OXIDES (Lars Kihlborg)

The studies on copper wolfram oxides described below have been conducted in parallel with the present research project but essentially as part of other research, performed by the present author in cooperation with E. Gebert. As the results obtained, however, have been found to be of considerable interest and to give further illustrations of the structural behaviour of wolfram in oxide compounds it has been thought worth-while to report briefly on this work here.

Considerable effort has been devoted to phase analysis studies on the Cu-W-O system. Experimental difficulties, however, not yet overcome have so far prevented the attaining of a complete picture of the phase conditions of this system. The work has instead been concentrated on structural studies on the two ternary phases observed, viz. $CuWO_{4-\underline{x}}$

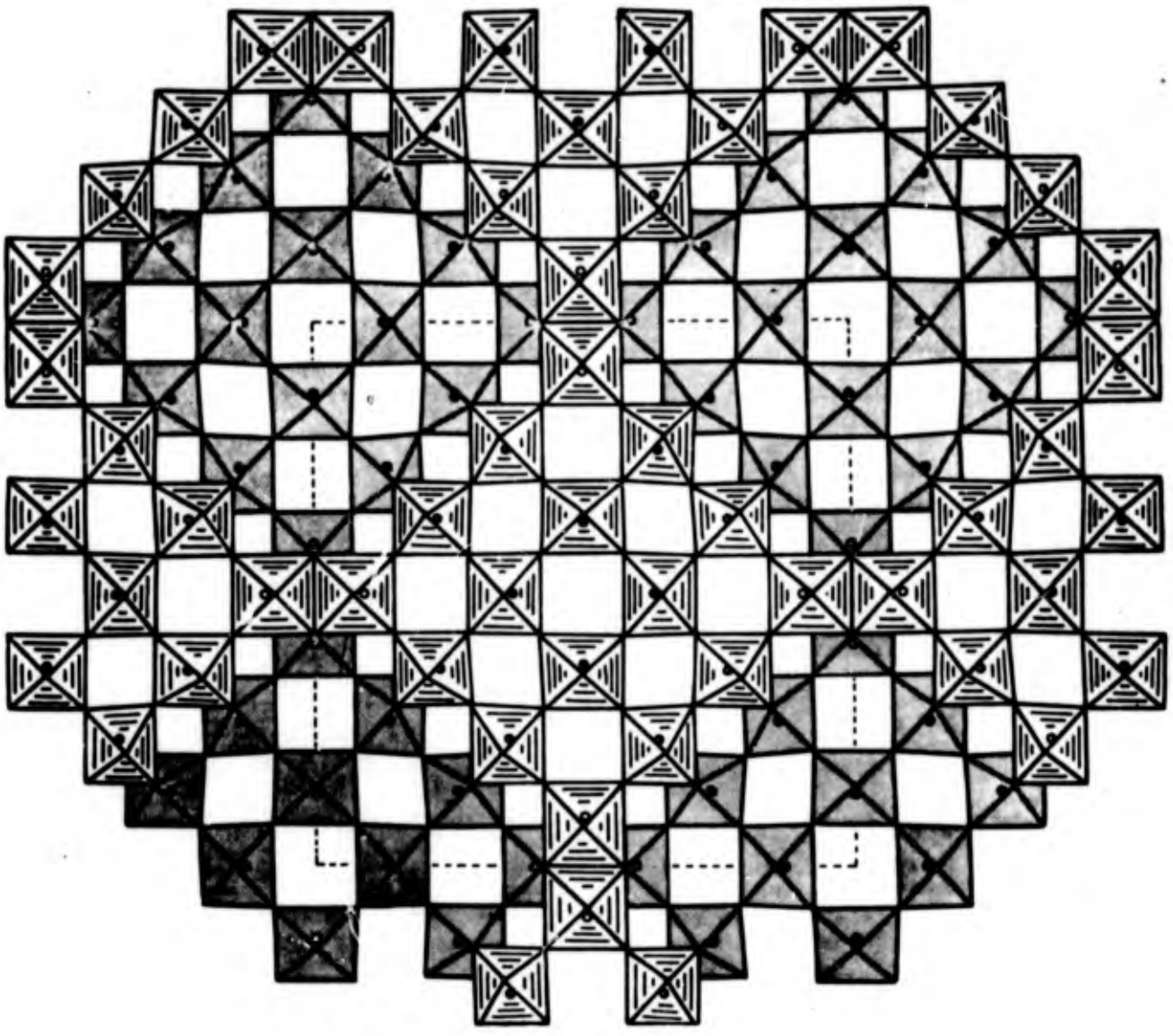

**Figure 22.** The crystal structure of the tetragonal wolfram vanadium oxide, $W_{0.35}V_{0.65}O_{2.5}$, viewed along the tetragonal axis. The structure is regarded as built up of $\underline{M}O_6$ octahedra as two levels (light and dark, respectively), joined by corners to identical octahedra above and below. The extension of the unit cell is indicated by broken lines.

and $Cu_3WO_6$. The structures have been solved and refined on the basis of accurate three-dimensional single-crystal data registered by means of a diffractometer. The final R-values are 0.038 for $CuWO_{4-x}$ and 0.065 for $CuWO_6$.

$CuWO_{4-x}$ has been found to be of a distorted wolframite type of structure. The triclinic unit cell dimensions are

$$a = 4.703 \text{ Å}, \quad b = 5.839 \text{ Å}, \quad c = 4.878 \text{ Å}$$
$$\alpha = 91.68^\circ, \quad \beta = 92.47^\circ, \quad \gamma = 82.81^\circ$$

The divergence from the normal monoclinic wolframite-type of structure lies mainly in the deviation of the angle $\gamma$ from $90^\circ$. The $WO_6$ octahedra are distorted in an irregular way, which is reflected in the W-O distance of 1.76, 1.81, 1.84, 1.98, 2.03 and 2.20 Å. The environment of copper is also an octahedral one but of a marked 4+2 character, the former distances ranging from 1.96 to 2.00 Å and the two latter being about 2.4 Å. The B-values of the oxygens all have similar but rather high values ($2.5 \pm 0.1$ Å$^2$) which may indicate some connection with the deficiency in oxygen of this compound as compared with the stoichiometry required by an ideal structure of this type.

The structure of $Cu_3WO_6$ is of a new type. The cubic unit cell ($a = 9.799$ Å) contains eight formula units. The arrangement of oxygens around wolfram represents a 3+3 type distortion of an octahedron. There is no mutual linking between the $WO_6$ groups. The coordination around copper is of a rather rare type, viz. a triangular bipyramid. Further details on this structure are given in Appendix V of this report.

## 4.8. MAGNETIC PROPERTIES OF MOLYBDENUM AND WOLFRAM OXIDE PHOSPHATES

(Gunilla Barvling and Lars Kihlborg)

The apparatus for magnetic measurements described above (sect. 2.3) has recently been taken into use for investigations of the magnetic properties of various substances studied within this program. So far this work has been mainly concerned with vitreous and crystalline oxide phosphates of molybdenum and wolfram. Measurements have, however, also been performed on samples of disodium diwolframate. The very plausible diamagnetic character of this compound has been confirmed for the crystalline material as well as for glasses of different thermal treatment. The $\chi_g$ values obtained are in the region $-0.8 \cdot 10^{-6}$ to $-1.2 \cdot 10^{-6}$ cgs units.

The data obtained for some molybdenum and wolfram oxide phosphates are summarized in Table 8.

Table 8. Magnetic data for molybdenum and wolfram oxide phosphates $\underline{M}O_{3-\underline{x}} \cdot y P_2O_5$ ($\underline{M}$ = Mo or W)

| Compound | Composition $\underline{x}$ | Composition $\underline{y}$ | Magnetic character | $\chi_g$ cgs units |
|---|---|---|---|---|
| $MoOPO_4$, cryst. | 1/2 | 1/2 | Paramagnetic | $2 \cdot 10^{-6}$ (298°K); $8 \cdot 10^{-6}$ (100°K) |
| - " - , glass | 0.23 | 0.44 | Diamagnetic | $-0.5 \cdot 10^{-6}$ |
| $W_2O_3(PO_4)_2$, cryst. | 0 | 1/2 | - " - | $-0.8 \cdot 10^{-6}$ |
| - " - , glass | 0.01 | 0.49 | - " - | $-1.2 \cdot 10^{-6}$ |

The diamagnetic character of the crystalline and vitreous wolfram oxide phosphates is in concordance with the fully or very nearly fully oxidized state of wolfram in these substances.

The values given above for crystalline $MoOPO_4$ are not very accurate as the amount of substance available was an extremely small one.

The paramagnetic character of this material is, however, secured by the measurements. This is in full accordance with the evidence given by the structural investigation previously reported (39). The arrangement of the molybdenum atoms in the structure are all crystallographically equivalent and corresponds to the description of the compound as a molybdenum(V) oxide phosphate. From this point of view the diamagnetism observed for a molybdenum oxide phosphate glass, obtained by heat-treatment of crystalline $MoOPO_4$ at 950°C is quite interesting. The oxidation state of molybdenum in the glass is higher than in the crystalline starting material, but still considerably below the maximum oxidation state of the metal. An interpretation of this observation in terms of structure seems premature. Further work is contemplated in order to shed light on this problem.

## 5. SOME GENERAL ASPECTS AND PLANS FOR FURTHER RESEARCH

The studies on structural relations in crystalline and vitreous compounds which have been conducted at this Institute for a three-year period and are described above and also in two previous annual reports, have turned out to hit on a very interesting and profitable field of research. It is felt that the results arrived at have contributed to the understanding of the structural relations which have formed the goal of the research. The work has also raised un interest in several new problems relevant to this field of research. In some cases supplementary experimental and theoretical work will be required to make it possible to extract full information from the material and results now available. This would also provide an improved basis for a general comprehensive discussion of the complex of problems included within the wide range of the present research.

The present research program has comprised studies on the structural relations in the crystalline and vitreous states for various groups of compounds. An extension of this research, which now presents itself as an urgent one is to include also the molten state. Comparative investigations, using X-ray diffraction techniques and also other methods, of the atomic arrangements present in crystals, melts and glasses of suitable compounds are likely to be a very profitable field of research. Such studies should include investigations of melts and glasses over series of temperatures. Due consideration should also be given to the premelting region of the crystalline materials. The materials to be studied should be selected very carefully to meet the requirements to suit the experimental techniques and also to possess such a moderate structural complexity as to allow atomic rearrangements in the various states of aggregation.

Research along the lines described above are now being contemplated at this Institute.

ACKNOWLEDGEMENTS

The authors wish to thank Professor Arne Magnéli, Head of this Institute, for his kindness in allowing them to perform this investigation at the Laboratory and for many stimulating discussions and invaluable advice in connection with this work.

Skilful and efficient cooperation has been rendered in the experimental work by Mr. Ove Alderbäck, Mr. Karl-Erik Johansson, Mr. Georg Kruuse, Mr. Herbert Larsson and Mrs. Stina Nord.

Thanks are due to Dr. Sven Westman for his correction of the English of this report.

The invaluable help of Mrs. Ruth Wilhelmi, who typed the manuscript, is gratefully acknowledged.

REFERENCES

(1) P. Kierkegaard, K. Eistrat, K. Gustafsson, K.-E. Johansson and A. Skancke: Structural Studies on Vitreous Compounds. Final Technical Report, April 1966 DA-91-591-EUC-3635.

(2) P. Kierkegaard, S. Axrup, B. Linnros, M. Nygren, M. Seleborg, K. Eistrat and M. Sundbäck: Studies on Structural Relations in Crystalline and Vitreous Compounds. Final Technical Report, March 1967 DA-91-591-EUC-3980.

(3) J.P. Shoemaker, editor: World List of Crystallographic Computer Programs, 2nd Ed. International Union of Crystallography Commission on Crystallographic Computing. 1966.

(3a) T.C. Furnas, Jr.: Single Crystal Orienter Instruction Manual. Direction 12130 A (1957). X-ray Department, General Electric, Milwaukee, Wisconsin.

(4) P. Kierkegaard: Contributions to the Structural Chemistry of Organic and Biochemical Molecules I. Progress report 1/7 1966 - 31/12 1967. Institute of Inorganic and Physical Chemistry, University of Stockholm, Stockholm Va.

(5) P. Debye: Dispersion of Röntgen Rays. Ann. Physik 46 (1915) 809.

(6) F. Zernike and J.A. Prins: The Bonding of X-Rays in Liquids as an effect of molecular arrangement. Z. Phys. 41 (1927) 184.

(7) C. Finbak: The Structure of Liquids. Acta Chem. Scand. 3 (1949) 1279.

(8) C.N.J. Wagner, H. Ocken, and M.L. Joshi: Interference and Radial Distribution Functions of Liquid Copper, Siver, Tin and Mercury. Z. Naturforschung 20 (1965) 325.

(9) G. Johansson: private communication.

(9a) N. Norman: Cylindrically Symmetrical Distribution Functions and their Application in the Structure Investigation of Cellulose. Acta Cryst. 7 (1954) 462.

(9b) J. Krogh-Moe: A Method for Converting Experimental X-ray Intensities to an Absolute Scale. Acta Cryst. 9 (1956) 951.

(9c) N. Norman: The Fourier Transform Method for Normalizing Intensities. Acta Cryst. 10 (1957) 370.

(10) R.J.H. Gelsing, H.N. Stein and J.M. Stevels: Vitreous Alkali Tungstates. Phys. and Chem. of Glasses 7 (1966) 185.

(11) M. Seleborg: A Refinement of the Crystal Structure of Disodium Dimolybdate. Acta Chem. Scand. 21 (1967) 499-504.

(12) F. Hoermann: Contribution to the Knowledge of Molybdates and Wolframates. Z. anorg. u. allgem. Chem. 177 (1928) 145.

(12b) I. Lindqvist: Some New Aspects of the Polymolybdates. Nova Acta Regiae Soc. Sci. Upsaliensis 4 , 15 (1950) No. 1.

(13) I. Lindqvist: Crystal Structure Studies on Anhydrous Sodium Molybdates and Tungstates. Acta Chem. Scand. 4 (1950) 1066.

(14) P.T. Sarjeant and R. Roy: New Glassy and Polymorphic Oxide Phases Using Rapid Quenching Techniques. J. Amer. Cer. Soc. 50 (1967) 500.

(15) R.J.H. Gelsing, H.N. Stein and J.M. Stevels: The Phase Diagram $K_2WO_4$-$WO_3$. Rec. des Travaux Chim. des Pays-Bas T.84, No. 9/10 (1965) 1452.

(16) P. Caillet: Polymolybdates et polytungstates de sodium on de potassium anhydres. Bull. Soc. Chim. France 12 (1967) 4750-4755.

(17) M. Seleborg: The Crystal Structure of Dipotassium Trimolybdate. Acta Chem. Scand. 20 (1966) 2195-2201.

(18) A. Magnéli: Studies on the Hexagonal Tungsten Bronzes of Potassium, Rubidum, and Caesium. Acta Chem. Scand. 7 (1953) 315-324.

(19) J. Graham and A.D. Wadsley: A Crystallographic Examination of Tungsten Trioxide Whiskers. Acta Cryst. 14 (1961) 379-383.

(20) A. Magnéli: Crystal structure studies on $\gamma$-tungsten oxide. Arkiv Kemi 1 (1949) 223-230.

(21) V.I. Spitsyn and I.M. Kuleshov: The Binary System $Rb_2WO_4$-$WO_3$. Zhur. Fiz. Khim. 24 (1950) 1197-1200.

(22) P. Kierkegaard: The Crystal Structure of $NaWO_2PO_4$ and $NaMoO_2PO_4$. Arkiv Kemi 18 (1962) 553.

(23) P. Kierkegaard and S. Holmén: The Crystal Structure of $AgMoO_2PO_4$. Arkiv Kemi 23 (1964) 213.

(24) G.R. Levi and G. Peyronel: Crystal Structure of the isomorphous group $MP_2O_7$ (M = $Si^{4+}$, $Ti^{4+}$, $Zr^{4+}$, $Sn^{4+}$, $Hf^{4+}$). Z. Krist. 92 (1935) 190.

(25) G. Peyronel: Structure of $UP_2O_7$. Z. Krist. 94 (1936) 311.

(26) M. Sljukić, B. Matković and B. Prodić: Preparation and Crystallographic Data of Phosphates with Common Formula $M^I M_2^{IV}(PO_4)_3$ ($M^I$ = Li, Na, K, Rb, Cs; $M^{IV}$ = Zr, Hf). Croat. Chem. Acta 39 (1967) 145.

(27) A. Colani: Research on Uranium Compounds. Ann. Chim. Phys. 12 (1907) 59.

(28) A. Burdese and M.L. Borlera: The System between Anhydrous Phosphoric Acid and the Dioxides of Uranium and Thorium. Ann. Chim. 53 (1963) 344.

(29) R.M. Douglas: Crystallographic Data for Orthorhombic Uranium(IV)-metaphosphate and Plutonium(IV)metaphosphate. Acta Cryst. 15 (1962) 505.

(30) Y. Baskin: Preparation and Properties of Uranium Metaphosphate, $U(PO_3)_4$. J. inorg. nucl. Chem. 29 (1967) 383.

(31) J.A. Victoreen: The Calculation of X-Ray Mass Absorption Coefficients. J. appl. Physics 20 (1949) 1141.

(32) H.A. Eick and L. Kihlborg: The Crystal Structure of $VOMoO_4$. Acta Chem. Scand. 20 (1966) 722.

(33) H.A. Eick and L. Kihlborg: The Crystal Structure of $V_2MoO_8$. Acta Chem. Scand. 20 (1966) 1658.

(34) L. Kihlborg: The Crystal Structure of $(Mo_{0.3}V_{0.7})_2O_5$ of R-$Nb_2O_5$ Type and a Comparison with the Structures of $V_2O_5$ and $V_2MoO_8$. Acta Chem. Scand. 21 (1967) 2495.

(35) L. Kihlborg: Crystal Structure Studies on $Mo_5O_{14}$, a Compound Exhibiting Two-Dimensional Disorder. Arkiv Kemi 21 (1963) 427.

(36) R. Gruehn: A New Modification of Niobiumpentoxide. J. Less-Common Metals 11 (1966) 119.

(37) S. Andersson: The Crystal Structure of $Nb_3O_7F$. Acta Chem. Scand. 18 (1964) 2339.

(38) W. Freundlich: New Ternary Phases in the System Wolfram-Vanadium-Oxygen. Compt. Rend. 260 (1965) 3077.

(39) P. Kierkegaard and M. Westerlund: The Crystal Structure of $MoOPO_4$. Acta Chem. Scand. 18 (1964) 2217.

BLANK PAGE

# Tunnel Structure of $K_2W_4O_{13}$

MADELEINE SELEBORG

Institute of Inorganic and Physical Chemistry, University of Stockholm, Stockholm, Sweden

The existence of a phase $K_2W_4O_{13}$ was pointed out by Hoermann[1] and later confirmed by Gelsing et al.[2] For the present investigation this compound was prepared by heating an intimate mixture of wolfram trioxide and a surplus of potassium wolframate at 750°C in a platimum crucible. The crystals obtained were of a faintly greenish tinge and in the shape of long, extremely thin needles adhering very strongly to each other. The Guinier powder photograph agrees well with powder data of $K_2W_4O_{13}$ as given by Gelsing et al.[2]

The present structure was derived from three-dimensional Weissenberg data using CuKα radiation. The 434 independent reflections were estimated visually. No attempt to correct for absorption effects has been made as yet. The results are as follows:

$K_2W_4O_{13}$, hexagonal, $a$ = 15.530 ± 0.003, $c$ = 3.8502 ± 0.0007 Å, $z$ = 3.

Space-group: P6 (No. 168).

The structure was derived from a Patterson synthesis and refined by least squares techniques to a present R-factor of 0.134. Only observed intensities were included in the refinement.

The structure is built up by $WO_6$ octahedra which by shared corners form six-membered rings. Through the centres of these rings are formed tunnels of infinite extension running in the direction of the short axis. This is a structural feature which several wolfram compounds have in common. The hexagonal wolfram bronzes[3], which are represented by a potassium bronze and also by rubidium and caesium bronzes have tunnel structures. In these compounds the tunnels enclose

the statistically distributed alkali ions. The pseudohexagonal wolfram trioxide[4], which has a superlattice due to the substitution of one molybdenum for every twelfth wolfram, contains six-edged empty channels running parallel to the c-axis which in this case is 3.834 Å. Empty tunnels of infinite extension are also found in the wolfram oxide $W_{18}O_{49}$[5].

In the tetrawolframate the six potassium ions are probably placed in a six-fold position, thus occupying interstices of a somewhat complicated shape. The one-fold position 00z would also be a plausible site in analogy to the conditions in the wolfram bronzes. That this in fact may be the case is indicated by the difference Fourier syntheses and consequently by least squares refinements based on that assumption. The five remaining potassium ions would then be statistically distributed over the six-fold position. That the two types of tunnel interstices arise in the tetrawolframate, only one of which is present in the structurally similar wolfram bronzes is due to the coupling of the $WO_6$ octahedra in the two structures. While in the latter structure the sixmembered rings are sharing octahedra with adjacent rings, in the tetrawolframate the rings which here may be regarded as "double", have no octahedra in common. They are more loosely connected sideways through shared corners, thus forming additional tunnels of a more irregular shape in between them.

The author wishes to thank Professor Arne Magnéli for his encouraging interest in this investigation which was started at his suggestion.

It has been sponsored in part by the Swedish Natural Science Research Council, and in part by the European Research Office, United States Army, Frankfurt am Main, Germany.

[1] F. Hoermann, Z. anorg. u. allgem. Chem., 1928, 177, 145.

[2] R.J.H. Gelsing, H.N. Stein and J.M. Stevels, Rec. des Trav. Chim. Pays-Bas, 1965, T.84, No. 9/10, 1452.

[3] A. Magnéli, Acta Chem. Scand., 1953, 7, 315.

[4] J. Graham and A.D. Wadsley, Acta Cryst., 1961, 14, 379.

[5] A. Magnéli, Arkiv Kemi, 1949, 1, 223.

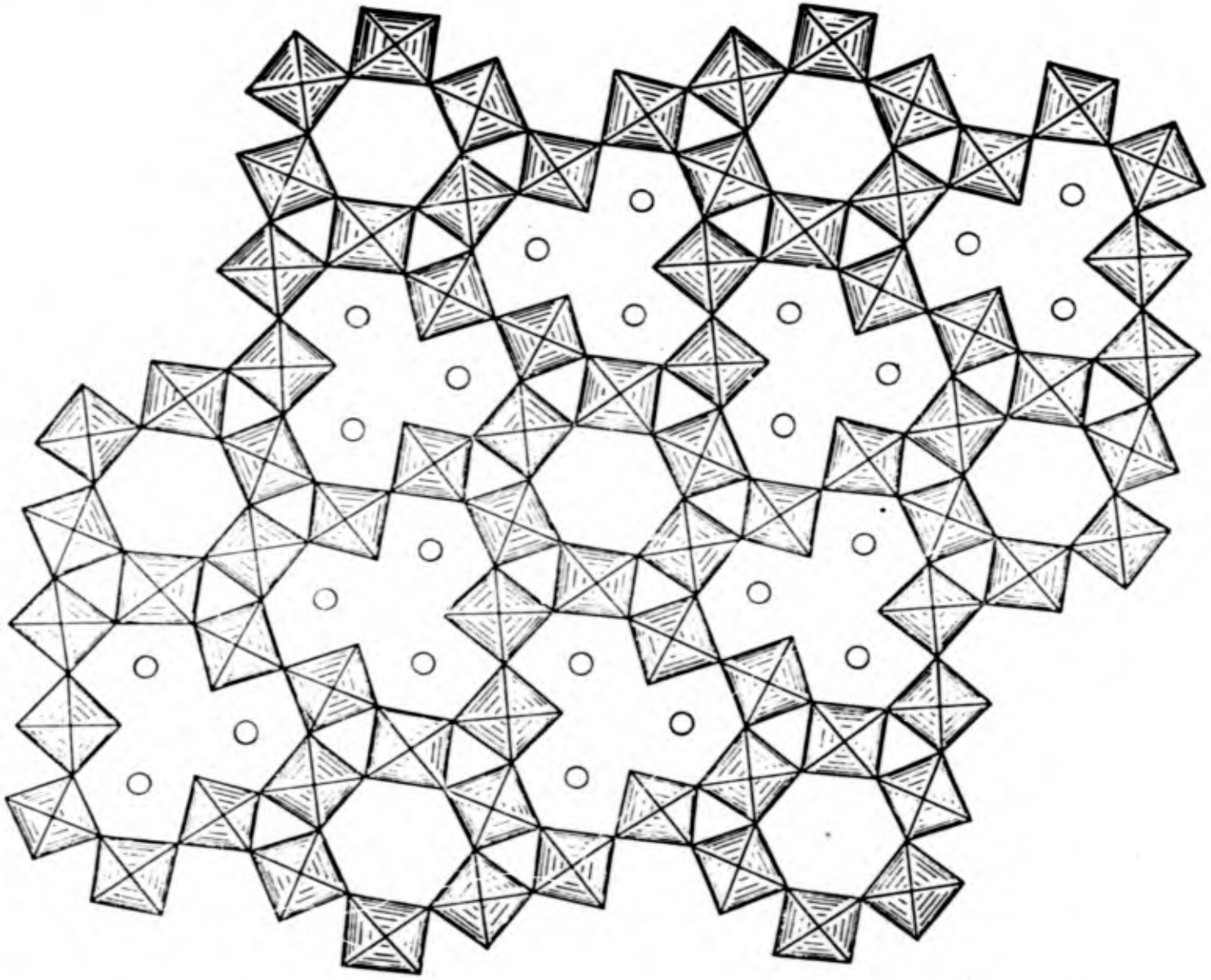

Fig. 1. The structure of $K_2W_4O_{13}$ projected along [001]. The potassium ions in the six-fold position are drawn as circles.

# Derivation of the Radial Distribution Function for Crystalline Materials from X-Ray Powder Data

PER-ERIK WERNER

In order to show the approximations and discuss the reliability of the radial distribution function applied to crystal powder data, this function is derived here and discussed in somewhat greater detail than is usual in the literature.

Consider a crystal powder containing $N_o$ atoms, having every possible orientation, scattering monochromatic X-rays. Assume there is only one kind of atom. Later the equations will be extended to cover the more general case.

According to Debye the coherent radiation

$$(1) \qquad I = I_e \cdot f^2 \cdot \sum_{p=1}^{N_o} \sum_{q=1}^{N_o} \frac{\sin(kr_{pq})}{kr_{pq}} \qquad \text{where } k = \frac{4\pi\sin\theta}{\lambda}$$

f is the atomic scattering factor and $r_{pq}$ is the magnitude of the vector separating the atoms p and q.

$$I_e = I_o \frac{e^4}{R^2 m^2 c^4} \cdot \frac{(1+\cos^2\theta)}{2}$$

is the X-ray intensity from a Thomson electron if $I_o$ is the intensity of the unpolarized primary beam. R is the distance between the electron and the observation point (the camera radius). It is presupposed that r and $\lambda$ are of the same order of magnitude and are both small compared to R.

Introduce a spherically symmetrical function g(r), such that $4\pi r^2 g(r)dr$ atoms lie in a spherical shell at distances between r and r+dr from the centre of an arbitrary atom.

$$(2) \qquad I = I_e f^2 N_o \Big[ 1 + \int_0^\infty 4\pi t^2 g(r) \frac{\sin(kr)}{kr} dr \Big]$$

$$(p=q)$$

In order to achieve convergence it is assumed that at large r

$$4\pi r^2 g(r) \rightarrow 4\pi r^2 g_o(r)$$

where $g_o(r)$ is the average atom density.

Expression (2) can be transformed to

$$(3) \quad I = I_e \cdot f^2 \cdot N_o\left[1 + \int_o^\infty 4\pi r^2[g(r)-g_o(r)]\frac{\sin(kr)}{kr}dr + \int_o^\infty 4\pi r^2 g_o(r)\frac{\sin(kr)}{kr}dr\right]$$

The second integral gives the radiation from the sample if the atoms were randomly spread out. For every k, big enough to be measured, this integral may be neglected. Therefore eq(3) may be rewritten.

$$(4) \quad k\left[\frac{I}{I_e N_o f^2} - 1\right] = \int_o^\infty 4\pi r[g(r) - g_o(r)]\sin(kr)dr$$

The Fourier integral theorem written in general form

$$f(x) = \frac{2}{\pi}\int_o^\infty \sin(xy)dy \int_o^\infty f(t)\sin(yt)dt$$

may be used in the following way. Put x = t = r and y = k, then

$$f(r) = \frac{2}{\pi}\int_o^\infty \sin(kr)dk \int_o^\infty f(r)\sin(kr)dr$$

Introduce $h(k) = \int_o^\infty f(r)\sin(kr)dr$ I.e.

$$f(r) = \frac{2}{\pi}\int_o^\infty h(k)\sin(kr)dr$$

Put $h(k) = k\left[\frac{I}{I_e N_o f^2} - 1\right]$ and $f(r) = 4\pi r[g(r)-g_o(r)]$

Eq(4) can now be transformed to

$$(5) \qquad 4\pi r[g(r) - g_o(r)] = \frac{2}{\pi}\int_o^\infty k\left[\frac{I}{I_e N_o f^2} - 1\right]\sin(kr)dk$$

or

$$(6) \qquad 4\pi r^2[g(r) - g_o(r)] = \frac{2r}{\pi}\int_o^\infty k\left[\frac{I}{I_e N_o f^2} - 1\right]\sin(kr)dk$$

The intensity I is composed of two parts

$$I = I_p + I_t$$

where $I_p$ = the peak intensity

and $I_t = I_e N_o f^2\left[1 + e^{-Bk^2}\right]$ is the diffuse temperature scattering.

Therefore eq (6) can be written as

$$(7) \qquad 4\pi r^2[g(r) - g_o(r)] = \frac{2r}{\pi}\int_o^\infty \frac{kI_p}{I_e N_o f^2}\sin(kr)dk - \frac{2r}{\pi}\int_o^\infty k\, e^{-Bk^2}\sin(kr)dk$$

The second integral may be solved in the following way

$$\int_o^\infty \underbrace{\sin(kr)}_{v}\cdot\underbrace{k\, e^{-Bk^2}}_{u'}\,dk = \underbrace{\int_o^\infty \underbrace{\sin(kr)}_{v}\ \underbrace{\frac{e^{-Bk^2}}{-2B}}_{u}}_{0} -$$

$$- \int_o^\infty \underbrace{\frac{e^{-Bk^2}}{-2B}}_{u}\ \underbrace{r\cos(kr)}_{v'}\,dk = \frac{r}{2B}\int_o^\infty e^{-Bk^2}\,\frac{(e^{ikr} - e^{-ikr})}{2}\,dk =$$

$$= \frac{r}{4B}\int_o^\infty e^{-(\sqrt{B}k - \frac{ir}{2\sqrt{B}})^2 - \frac{r^2}{4B}}\cdot\frac{d(\sqrt{B}k - \frac{ir}{2\sqrt{B}})}{\sqrt{B}} +$$

$$+ \frac{r}{4B} \int_0^\infty e^{-(\sqrt{B}k + \frac{ir}{2\sqrt{B}})^2 - \frac{r^2}{4B}} \cdot \frac{d(\sqrt{B}k + \frac{ir}{2\sqrt{B}})}{\sqrt{B}} =$$

$$= \frac{r}{2B^{3/2}} \cdot e^{-\frac{r^2}{4B}} \underbrace{\int_0^\infty e^{-x^2} dx}_{\frac{\sqrt{\pi}}{2}} = \frac{r\sqrt{\pi}}{4B^{3/2}} \cdot e^{-\frac{r^2}{4B}}$$

(Ch.-J. de La Vallée Poussin, Cours d'Analyse Infinitésimale, I. p. 239, Guathier-Villars, Paris 1954.)

As can be seen this value decreases strongly with increasing r. For not too small r-values the second integral in eq (7) may be neglected. I.e.

$$(8) \qquad r[g(r) - g_o(r)] = \frac{1}{2\pi^2} \int_0^\infty \frac{kI_p}{I_e N_o f^2} \sin(kr)dk$$

The total intensity P in a powder diffraction line is $I_p \cdot \Delta A$ where $\Delta A$ is the area of the complete reflecting circle.

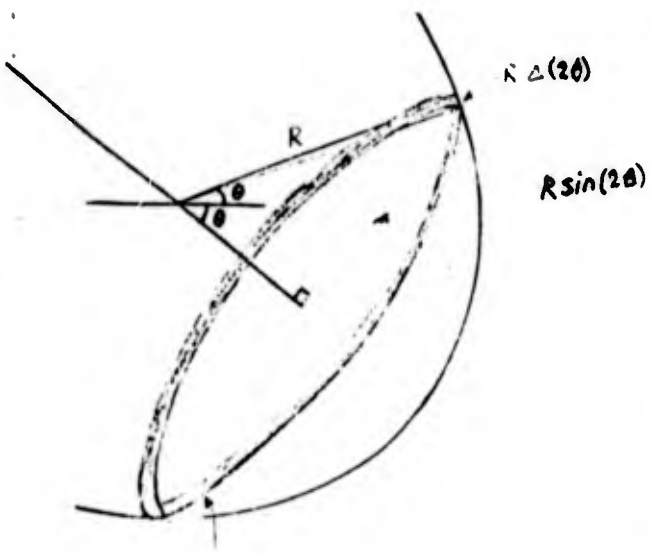


The reflecting circle

The circumference = $2\pi R \sin(2\theta)$

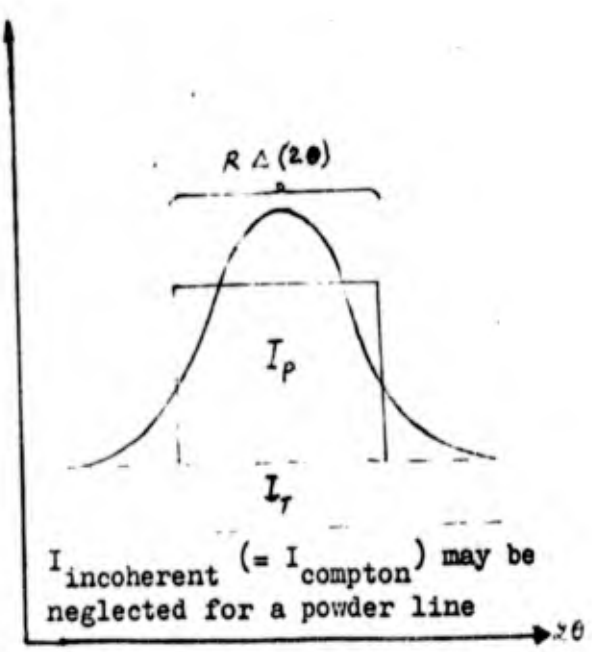

From this follows

(9) $$P = I_p \cdot \Delta A = I_p \cdot 2\pi R \sin(2\theta) \cdot R\,\Delta(2\theta)$$

$$dk = \frac{2\pi \cos\theta\, d(2\theta)}{\lambda}, \quad kdk = \frac{4\pi^2}{\lambda^2} \sin(2\theta)\, d(2\theta)$$

which, introduced into eq (9), gives

(10) $$P = I_p \frac{R^2\lambda^2}{2\pi} k\Delta k$$

Eq (8) can now be written

(11) $$r[g(r) - g_o(r)] = \frac{1}{\pi} \sum_{o}^{\infty} \frac{P \sin(kr)}{I_e N_o f^2 R^2 \lambda^2}$$

If more than one kind of atom is present it is possible to introduce an approximation for the atomic scattering factors. Put

(12) $$f_m = K_m \cdot f_e$$

where $f_m$ is the atomic scattering factor for the m:th atom, $K_m$ is the number of effective electrons in the atom and $f_e$ is the electronic scattering factor for a Thomson electron. Eq (11) may then be transformed to

(13) $$r[\rho(r) - \rho_o(r)] = \frac{1}{\pi} \sum_{o}^{\infty} \frac{P \sin(kr)}{I_e N_o f^2 R^2 \lambda^2}$$

where $\rho(r)$ is the electron distribution function analogous to the function $g(r)$. (See above.)

For a powder ring

(14) $$\frac{P}{I_o} = \frac{N^2 e^4 \lambda^3 V}{8m^2 c^4} \frac{[1 + \cos^2(2\theta)]}{\sin\theta} \cdot p'' \cdot F^2$$

(Int. Tab. Vol. II, 314) and for an electron

$$\frac{I_e}{I_o} = \frac{e^4}{R^2 m^2 c^4} \frac{[1 + \cos^2(2\theta)]}{2} \tag{15}$$

(Int. Tab. Vol. II, 237)

Therefore eq (13) can be written

$$r[\rho(r) - \rho_o(r)] = \sum_0^\infty \frac{N \cdot p'' \cdot |F|^2 \sin(kr)}{u f^2 k} \tag{16}$$

where N is the number of unit cells per unit volume, p" is the multiplicity factor, and u is the number of atoms per unit cell.

For a Guinier camera

$$PLG = \frac{1 + \cos^2(2\alpha)\cos(2\theta)}{[1 + \cos^2(2\alpha)] \sin\theta \sin(3\theta)} \tag{17}$$

if the angle between the Guinier camera and the primary beam is $30^\circ$.

P = the polarization factor

L = the Lorentz factor

G = the geometrical factor

$\alpha = 13^\circ 24'$ for a quartz monochromator

(K. Sagel, Tabellen zur Röntgenanalyse (1958) 78-79)

If the observed relative intensity in a powder line is denoted $I(\theta)$ and if the absorption factor $A(\theta)$ is equal to $\frac{1}{2\mu}$ or negligible, and a convergence factor $e^{\frac{-(\beta \sin^2\theta_i)}{\lambda^2}}$ is introduced, it is possible to approximate eq (16) as

$$r[\rho(r)-\rho_o(r)] = K_i \sum_{i=1}^{n} \frac{[1+\cos^2(2\alpha)]\sin\theta_i[3-4\sin^2\theta_i]}{1+\cos^2(2\alpha)[1-2\sin^2\theta_i]} \cdot e^{-(\frac{\beta \sin^2\theta_i}{\lambda^2})} \cdot I(\theta_i) \cdot \sin\left[\frac{4\pi \sin\theta_i}{\lambda} \cdot r\right] \tag{18}$$

where K is an arbitrary scale factor. The radial distribution function is placed on an arbitrary scale.

For other camera techniques the PLG factors and therefore eq (18) must be changed. The PLG factors needed are easily found in Tabellen zur Röntgenanalyse (1958), K. Sagel.

The termination-of-series errors in the summation process may be illustrated with two periodic waves. The upper limit gives a wave of a short wavelength which can seriously affect the positions of the maxima if the intensities for high θ-values are not negligible. Therefore it is sometimes favourable to replace the Guinier camera by another camera. The radiation used should be of as short wavelength as possible.

The lower limit introduced does not seem to be very serious. It may be discussed as a long periodic wave which affects the amplitudes more than the positions of the maxima in the distribution function.

Programs for the radial distribution function eq (18) has been made for the computers CDC 3200 and IBM 1800.

BLANK PAGE

# The crystal structure of $(Mo_{0.3}V_{0.7})_2O_5$ of R-$Nb_2O_5$ type and a Comparison with the Structures of $V_2O_5$ and $V_2MoO_8$

LARS KIHLBORG

Institute of Inorganic and Physical Chemistry, University of Stockholm, Stockholm, Sweden

ABSTRACT

$(Mo_{0.3}V_{0.7})_2O_5$ represents the molybdenum rich limit (at 650°C) of a range of solid solution extending from $V_2O_5$ along the line $(Mo_xV_{1-x})_2O_5$ in the Mo-V-O system. There are, however, discontinuities withtin this range associated with symmetry changes. This phase has been studied by single crystal diffraction methods. The dimensions of the monoclinic unit cell are a = 11.809 Å, b = 3.652 Å, c = 4.174 Å, $\beta$ = 90.57°, and the space group is C2.

The structure is of the same type as that of R-$Nb_2O_5$ and can be considered as composed of $MO_6$ octahedra coupled in the same way as in $V_2O_5$, although the distortion of the metal atoms within the octahedra follows a different pattern. This distortion, as reflected in the considerable divergence of the M - O bond lengths, is intermediate in magnitude between that in $V_2O_5$ and $MoO_3$. Molybdenum and vanadium atoms are randomly distributed over the metal atom positions.

The structure is also closely related to that of $V_2MoO_8$.

---

In the course of an investigation of the phases formed in the system V-Mo-O [1] it has been observed that molybdenum may replace vanadium in $V_2O_5$. This replacement gives rise to a range of solid solution, $(Mo_xV_{1-x})_2O_5$, extending at 650°C to the composition $(Mo_{0.3}V_{0.7})_2O_5$ approximately. To a first approximation the unit cell dimensions vary gradually within this interval but a closer examination of the powder

patterns and comparison with single crystal photographs revealed that the symmetry has changed from orthorhombic for $V_2O_5$ to monoclinic for $(Mo_{0.3}V_{0.7})_2O_5$. According to preliminary results, this transition occurs at a composition of about $x = 0.20$ and is probably associated with the occurrence at this composition of a phase giving a more complex powder pattern. Further studies of these problems are in progress.

This article presents a structure determination of a crystal with a composition close to the molybdenum-rich limit. A short communication of the investigations reported below was given at the Seventh International Congress of Crystallography[2].

## EXPERIMENTAL

The crystal studied was selected from a sample prepared by heating a mixture of $MoO_3$, $V_2O_5$ and $V_2O_3$ of gross composition $Mo_{0.3}V_{0.7}O_{2.5}$ in a sealed silica tube at 650°C for 2 days. The powder pattern of this sample showed the lines (Table 1) of a phase which could be indexed on the basis of a monoclinic unit cell with the dimensions given in Table 2. A few additional weak lines could be assigned to $VOMoO_4$ [3] and it seems therefore probable that the monoclinic phase contained slightly less molybdenum than indicated by the gross composition and that its formula should be approximately $(Mo_{0.28}V_{0.72})_2O_5$.

The crystal was shaped like a somewhat truncated parallelepiped with the dimensions 0.0204 mm (along a), 0.0636 mm (along b), and 0.0053 mm (along c). Integrated Weissenberg photographs were recorded of the h0l, h1l and h2l layer lines using CuKα radiation and multiple film technique. The relative intensities of the reflections were measured by means of a densitometer. These values were corrected for the effect of absorption (crystal assumed to be bounded by 7 planes; $\mu = 496$ cm$^{-1}$) and the usual Lp-correction was applied. These calculations as well as the subsequent structure factor calculations, least squares refinement and calculations of interatomic distances were performed on a computer of type FACIT EDB by means of the programs No.

6015, 6016, 6019, 6023 and 6030 [4] (the Lp-program written by B. Lundberg is not listed in Ref. 4). The atomic scattering factors listed in International Tables[5] were used, namely, for neutral oxygen and vanadium the values given in Table 3.3.1 A and for molybdenum those given in Table 3.3.1 B. The real part of the dispersion correction[5] was applied to these values.

## DETERMINATION AND REFINEMENT OF THE STRUCTURE

Systematic extinction was observed for all reflections hkl with $h+k = 2n+1$. Together with the observed Laue symmetry 2/m this led to the three possible space groups C2/m (No. 12), C2 (No. 5) and Cm (No. 8).

The fact that the crystal under investigation represented one end of a range of solid solution (cf. above) the other limit of which is $V_2O_5$ suggested a close relationship between the crystal structures. The space group of $V_2O_5$ is Pmnm (No. 59)[6,7] or possibly $Pmn2_1$ (No. 31)[7] which, on the other hand, implies a basic difference between the two structures.

A model was tried in which the arrangement of $MO_6$ octahedra was the same as in $V_2O_5$ but in which the distortion of the metal atoms from the centres of these octahedra was different to account for the different symmetry. Structure factor calculations and least squares refinement proved this model to be correct. The structure is shown in Fig. 1 together with that of $V_2O_5$. Completely random distribution of molybdenum and vanadium atoms over the metal atom positions had to be assumed since these positions were crystallographically equivalent and no indication of a superstructure had been observed on the X-ray photographs. Because of the uncertainty in the exact composition of the crystal (cf. above) three different Mo:V ratios were tested, viz. M = (0.33 Mo + 0.67 V), (0.30 Mo + + 0.70 V), and (0.27 Mo + 0.73 V). The results, obtained by least squares refinement, differed only insignificantly however.

The space group Cm was not consistent with the structure model but the remaining two, C2/m and C2, were both possible. Least squares refinement was carried out for both alternatives, namely (I) 1 M and 2 O in positions 4i, and 1 O in 2a of space group C2/m and (II) 1 M and 2 O in 4c and 1 O in 2a of space group C2. The final R-values (based on observed reflections only) were about the same for both alternatives, viz. 0.071 and 0.070, respectively, but the final y coordinates of O(1) and O(2) in alternative II differed by 7.4σ and 5.1 σ, respectively (σ = the corresponding standard deviation) from the values 0 and ½ at which they are fixed by symmetry in alternative I. The temperature factors obtained were also less divergent in alt. II than in alt. I and, particularly, they were much lower for atoms O(1) and O(2) in alt. II. It was thus evident that the structure is best described in the non-centrosymmetric space group C2 and the final parameters for this case are given in Table 2.

Weights in the least squares procedure were calculated according to Cruickshank's formula, $w = 1/(A + F_o + C \cdot F_o^2)$, where the following values were chosen for the parameters, A = 18, C = 0.012. The final weight analysis is given in Table 3. The observed and calculated structure factors are listed in Table 4.

## DISCUSSION

The structure of $(Mo_{0.3}V_{0.7})_2O_5$ turns out to be isotypic with that recently suggested by Gruehn for R-$Nb_2O_5$ on the basis of powder diffraction data [6]. The unit cell dimensions given for R-$Nb_2O_5$ are (the a and c axes interchanged here), a = $12.7_9$ Å, b = $3.82_6$ Å, c = $3.98_3$ Å, $\beta = 90.7_5°$. The space group was assumed to be (A2/m =) C2/m and the following atomic coordinates were reported (the numbering of the atoms changed here to become analogous with that in Table 2).

| | x | y | z |
|---|---|---|---|
| Nb | 0.146 | 0 | 0.07 |
| O(1) | 0.16 | 0 | 0.5 |
| O(2) | 0.18 | 0.5 | 0 |
| O(3) | 0 | 0 | 0 |

A comparison with Table 2 emphasizes the similarity between the two structures. The discussion below, therefore, applies also to R-$Nb_2O_5$.

The coordination of oxygen atoms around vanadium in $V_2O_5$ may be described either as five- or sixfold since the sixth V-O bond is considerably longer than the other five[7,8]. If the coordination is regarded as six-fold the structure may be described as built up of octahedra sharing edges and corners as visualized in Fig. 1b. Comparison with Fig. 1a indicates that the coupling of the octahedra is the same in $(Mo_{0.3}V_{0.7})_2O_5$. The structures can thus be described as built of edge sharing octahedra which form zig-zag chains that run in the b direction. These chains are mutually connected by corner sharing between octahedra in adjacent chains. Alternatively, they may be regarded as consisting of slabs of $ReO_3$-type, two octahedra thick, which extend infinitely in the bc plane; these, in turn, are interconnected by edge-sharing between component octahedra. The latter is a description in terms of a shear structure[9] introduced by Magnéli[10] and later developed by Andersson[11].

The difference between the two structures becomes significant when the distortions of the metal atoms from the centres of the octahedra are considered. These displacements occur predominantly along the direction of the c axis. It is seen in Fig. 1 that in $V_2O_5$ all metal atoms within an $ReO_3$-type slab are displaced in the same direction while in $(Mo_{0.3}V_{0.7})_2O_5$ they are shifted pairwise in opposite directions. The reason for this interesting difference between the two structures is not understood and is being further investigated. In both structures the metal atoms in a pair of octahedra sharing edges are displaced in opposite directions which, of course, is energetically most favourable from a purely electrostatic point of view.

It is interesting to compare these two structures with that of $V_2MoO_8$[12] shown in Fig. 2. Here the slabs of $ReO_3$ type have a thickness of three octahedra instead of two but the interconnection

of the slabs remains the same. Homologous series of structures is a term introduced by Magnéli for this type of structural relationship[10]. Considering the off-center displacements of the metal atoms $V_2MoO_8$ forms an intermediate between the above mentioned structures since the displacement within the middle octahedra of each slab goes in both directions; it alternates between +z and -z when going in the direction of the b axis which is therefore doubled (cf. Fig. 2). Both types of relative displacement within neighbouring octahedra are thus present simultaneously in this structure.

The M-O distances which are given in Table 5 can be grouped together in three short, two intermediate and one long bond. There is thus a marked tendency towards five-fold coordination although not as pronounced as in $V_2O_5$. The range of the M-O distances is seen to be intermediate between those in $V_2O_5$ and $MoO_3$. All close O-O distances have normal values ranging from 2.48 (± 6) Å (along the shared edge) to 2.97 (± 2) Å. The Nb-O distances in R-$Nb_2O_5$ as given by Gruehn[6] range from 1.7 to 2.3 Å which indicates a slightly smaller distortion in that structure than in the isostructural $(Mo_{0.3}V_{0.7})_2O_5$.

* * *

The work reported in this article forms a part of a research program sponsored in part by the Swedish Natural Science Research Council and in part by the European Research Office, United States Army, Frankfurt am Main, Germany. Grants for the use of computers were received from the Computer Division of the National Swedish Rationalization Agency (Kungl. Statskontoret).

I am indebted to Professor A. Magnéli for valuable comments on the manuscript.

REFERENCES


1. Kihlborg, L. To be published.
2. Kihlborg, L. and Eick, H.A. Acta Cryst. 21 (1966) A 59.
3. Eick, H.A. and Kihlborg, L. Acta Chem. Scand. 20 (1966) 722.
4. IUCr World List of Crystallographic Computer Programs, 2nd ed. A. Oosthoek's Uitgevers Mij. N.V., Utrecht 1966.
5. International Tables for X-ray Crystallography, Vol. III, The Kynoch Press, Birmingham 1962.
6. Gruehn, R. J. Less-Common Metals 11 (1966) 119.
7. Byström, A., Wilhelmi, K.-A. and Brotzen, O. Acta Chem. Scand. 4 (1950) 1119.
8. Bachmann, H.G., Ahmed, F.R. and Barnes, W.H. Z. Krist. 115 (1961) 110.
9. Wadsley, A.D. Revs. Pure and Appl. Chem. (Australia) 5 (1955) 165.
10. Magnéli, A. Acta Cryst. 6 (1953) 495.
11. Andersson, S. Bull. Soc. Chim. France 1965, 1088.
12. Eick, H.A. and Kihlborg, L. Acta Chem. Scand. 20 (1966) 1658.
13. Hambling, P.G. Acta Cryst. 6 (1953) 98.
14. Kihlborg, L. Arkiv Kemi 21 (1963) 357.

Table 1. X-ray powder diffraction data for $(Mo_{0.3}V_{0.7})_2O_5$, CuKα radiation. (λ = 1.54051 Å)

| I | $d_{obs}$ Å | $\sin^2\theta_{obs}$ x $10^5$ | hkl | $(\sin^2\theta_{obs}-\sin^2\theta_{calc})$ x $10^5$ |
|---|---|---|---|---|
| w | 5.894 | 1708 | 200 | + 6 |
| w+ | 4 169 | 3414 | 001 | + 9 |
| st | 3.487 | 4878 | 110 | + 5 |
| w | 3.419 | 5074 | $\bar{2}01$ | +14 |
| w | 3.392 | 5157 | 201 | + 2 |
| w+ | 2.952 | 6810 | 400 | + 3 |
| st | 2.678 | 8270 | 111 | +32 |
| | | | 310 | - 7 |
| | | | $\bar{1}11$ | -16 |
| vw | 2.420 | 10131 | $\bar{4}01$ | +13 |
| vw | 2.087 | 13621 | 002 | 0 |
| w | 1.9685 | 15311 | 600 | - 6 |
| vw | 1.9638 | 15384 | 202 | -34 |
| m | 1.8270 | 17775 | 020 | -15 |
| w | 1.7980 | 18353 | $\bar{5}11$ | -17 |
| w | 1.7944 | 18426 | $\bar{1}12$ | -20 |
| vw | 1.7458 | 19466 | 220 | -26 |
| vw | 1.7117 | 20250 | $\bar{4}02$ | +12 |
| w | 1.6738 | 21178 | 021 | -17 |
| w | 1.6086 | 22927 | 221 | -18 |
| w+ | 1.5533 | 24589 | 420 | - 9 |
| m | 1.5316 | 25293 | 710 | - 2 |
| vw | 1.4583 | 27898 | $\bar{4}21$ | -10 |
| w | 1.4583 | 28461 | $\bar{5}12$ | - 7 |
| vw | 1.4415 | 28551 | $\bar{7}11$ | +17 |

Table 1, cont.

| | | | | |
|---|---|---|---|---|
| m | 1.3386 | 33110 | 620 | + 3 |
| w | 1.2722 | 36659 | 621 | + 4 |
| vw | 1.2541 | 37724 | 403 | -15 |
| vw | 1.2488 | 38046 | $\bar{4}22$ | +17 |
| vw | 1.2109 | 40460 | $\bar{8}02$<br>130 | -11<br>+ 6 |
| vw | 1.1809 | 42545 | 911<br>10,0,0 | +17<br>- 1 |
| w | 1.1633 | 43841 | $\bar{1}31$<br>330 | + 6<br>-16 |
| vw | 1.1235 | 47000 | 622 | -13 |
| vw | 1.1214 | 47175 | $\bar{3}31$ | -16 |
| vw | 1.1197 | 47325 | 331 | - 9 |

Table 2. The crystal structure of $(Mo_{0.3}V_{0.7})_2O_5$.

Space group: C2 (No. 5)

Unit cell dimensions *: a = 11.809 (± 2) Å
b = 3.652 (± 1) Å
c = 4.174 (± 1) Å
$\beta$ = 90.57 (± 2) °

Unit cell content: 2 $M_2O_5$, M = $(Mo_{0.28}V_{0.72})$,
Mo/V ratio approximative (see text).

| Atom | Position | x ± σ(x) | y ± σ(y) | z ± σ(z) | B ± σ(B) |
|---|---|---|---|---|---|
| M | 4c | .14892± .00025 | 0 | .10034± .00076 | 0.441 ± .038 |
| O(1) | 4c | .1446 ± .0015 | .0651 ± .0088 | .4934 ± .0042 | 1.09 ± .32 |
| O(2) | 4c | .1792 ± .0013 | .5518 ± .0102 | .9953 ± .0037 | 0.51 ± .26 |
| O(3) | 2a | 0 | .002 ± .034 | 0 | 1.73 ± .47 |

* $\lambda[CuK\alpha_1]$ = 1.54051 Å, a[KCl, 25°C] = 6.29228 Å [13].

Table 3. Weight analysis obtained in the last cycle of refinement.
$\Delta = ||\underline{F}_{obs}| - |\underline{F}_{calc}||$, $\underline{w}$ = weighting factor.
The $\underline{w}\Delta^2$ values have been normalized.

| Interval sin θ | Number of independent reflections | $\overline{\underline{w}\Delta^2}$ | Interval $\lvert\underline{F}_{obs}\rvert$ | Number of independent reflections | $\overline{\underline{w}\Delta^2}$ |
|---|---|---|---|---|---|
| 0.00–0.46 | 26 | 0.71 | 0 – 16 | 3 | 0.47 |
| 0.46–0.58 | 21 | 0.84 | 16 – 24 | 7 | 1.75 |
| 0.58–0.67 | 15 | 1.49 | 24 – 32 | 29 | 1.19 |
| 0.67–0.74 | 15 | 0.82 | 32 – 40 | 32 | 1.11 |
| 0.74–0.79 | 13 | 0.51 | 40 – 48 | 19 | 1.04 |
| 0.79–0.84 | 11 | 1.20 | 48 – 56 | 18 | 0.60 |
| 0.84–0.89 | 10 | 0.99 | 56 – 64 | 14 | 0.86 |
| 0.89–0.93 | 7 | 1.28 | 64 – 72 | 7 | 0.76 |
| 0.93–0.97 | 15 | 0.82 | > 72 | 10 | 0.73 |
| 0.97–1.00 | 6 | 2.94 | | | |

Table 4. Observed and calculated structure amplitudes and calculated phase angles (expressed as a fraction of one cycle). $\Delta = \left| |F_{obs}| - |F_{calc}| \right|$ The values of $\Delta \sqrt{w}$ have been normalized.

| h | k | l | $\|F_{obs}\|$ | $\|F_{calc}\|$ | $\Delta\sqrt{w}$ | α |
|---|---|---|---|---|---|---|
| - 2 | 0 | 3 | 59.3 | 60.4 | 0.24 | 0.00000 |
| - 6 | 0 | 3 | 38.3 | 37.6 | 0.19 | 0.50000 |
| - 2 | 0 | 4 | 32.8 | 31.6 | 0.35 | 0.00000 |
| - 6 | 0 | 4 | 27.6 | 28.8 | 0.38 | 0.50000 |
| - 10 | 0 | 3 | 30.4 | 26.4 | 1.24 | 0.00000 |
| - 12 | 0 | 3 | 31.0 | 31.5 | 0.15 | 0.50000 |
| - 4 | 0 | 5 | 32.9 | 35.7 | 0.83 | 0.00000 |
| - 14 | 0 | 2 | 24.9 | 27.0 | 0.69 | 0.00000 |
| - 10 | 0 | 4 | 25.6 | 29.7 | 1.31 | 0.00000 |
| 0 | 0 | 5 | 34.6 | 34.8 | 0.05 | 0.50000 |
| 4 | 0 | 5 | 30.9 | 34.4 | 1.08 | 0.00000 |
| 8 | 0 | 4 | 32.7 | 32.4 | 0.09 | 0.50000 |
| 4 | 0 | 4 | 37.8 | 39.0 | 0.31 | 0.00000 |
| 2 | 0 | 3 | 50.3 | 48.8 | 0.38 | 0.50000 |
| 4 | 0 | 3 | 50.3 | 55.7 | 1.34 | 0.00000 |
| 8 | 0 | 3 | 54.3 | 55.3 | 0.25 | 0.50000 |
| 0 | 0 | 2 | 74.9 | 70.6 | 0.89 | 0.00000 |
| 2 | 0 | 2 | 74.2 | 80.6 | 1.30 | 0.50000 |
| 6 | 0 | 2 | 71.4 | 76.7 | 1.11 | 0.00000 |
| 8 | 0 | 2 | 45.7 | 41.5 | 1.10 | 0.50000 |
| 12 | 0 | 2 | 42.2 | 46.5 | 1.18 | 0.00000 |
| 12 | 0 | 3 | 34.9 | 38.1 | 0.94 | 0.00000 |
| 12 | 0 | 1 | 49.4 | 41.8 | 1.91 | 0.00000 |
| 10 | 0 | 1 | 32.2 | 29.4 | 0.86 | 0.50000 |
| 8 | 0 | 1 | 32.3 | 28.7 | 1.08 | 0.50000 |
| 6 | 0 | 1 | 81.7 | 83.9 | 0.43 | 0.00000 |
| 2 | 0 | 1 | 65.5 | 72.4 | 1.52 | 0.50000 |
| 0 | 0 | 1 | 88.9 | 92.5 | 0.65 | 0.00000 |
| 2 | 0 | 0 | 42.8 | 41.8 | 0.27 | 0.50000 |
| 4 | 0 | 0 | 81.4 | 87.6 | 1.20 | 0.50000 |
| 6 | 0 | 0 | 93.0 | 96.0 | 0.54 | 0.00000 |
| 8 | 0 | 0 | 21.5 | 23.4 | 0.64 | 0.00000 |
| 10 | 0 | 0 | 57.1 | 55.2 | 0.45 | 0.50000 |
| 14 | 0 | 0 | 38.9 | 34.0 | 1.35 | 0.00000 |
| 2 | 0 | - 1 | 37.8 | 33.0 | 1.35 | 0.00000 |
| 4 | 0 | - 1 | 57.9 | 58.2 | 0.08 | 0.50000 |
| 6 | 0 | - 1 | 34.6 | 30.2 | 1.29 | 0.00000 |
| 8 | 0 | - 1 | 45.4 | 38.7 | 1.76 | 0.00000 |
| 10 | 0 | - 1 | 28.1 | 24.5 | 1.14 | 0.50000 |
| 14 | 0 | - 1 | 31.6 | 28.2 | 1.04 | 0.00000 |
| 2 | 0 | - 2 | 56.6 | 52.3 | 1.01 | 0.00000 |
| 4 | 0 | - 2 | 64.2 | 63.0 | 0.27 | 0.50000 |
| 8 | 0 | - 2 | 59.1 | 53.2 | 1.38 | 0.00000 |
| 12 | 0 | - 2 | 32.5 | 28.9 | 1.10 | 0.50000 |
| 14 | 0 | - 2 | 23.0 | 27.0 | 1.34 | 0.00000 |
| 6 | 0 | - 3 | 41.1 | 37.6 | 0.96 | 0.50000 |
| 8 | 0 | - 3 | 30.3 | 27.8 | 0.79 | 0.00000 |
| 10 | 0 | - 3 | 30.4 | 26.4 | 1.24 | 0.00000 |
| 12 | 0 | - 3 | 32.1 | 31.5 | 0.18 | 0.50000 |
| 0 | 0 | - 1 | 89.5 | 92.5 | 0.56 | 0.00000 |
| - 9 | - 1 | 3 | 51.5 | 51.2 | 0.06 | 0.99140 |
| - 5 | - 1 | 3 | 50.4 | 52.1 | 0.43 | 0.49258 |
| - 3 | - 1 | 3 | 55.1 | 57.2 | 0.50 | 0.98005 |
| - 1 | - 1 | 3 | 32.1 | 29.3 | 0.84 | 0.01844 |
| - 5 | - 1 | 4 | 32.6 | 27.0 | 1.66 | 0.48810 |
| - 3 | - 1 | 4 | 42.7 | 46.7 | 1.09 | 0.00068 |
| - 3 | - 1 | 5 | 38.2 | 45.8 | 2.15 | 0.98709 |
| - 1 | - 1 | 5 | 24.5 | 24.1 | 0.11 | 0.49053 |
| 1 | - 1 | 2 | 72.7 | 77.7 | 1.05 | 0.99676 |
| 1 | - 1 | 1 | 15.3 | 14.9 | 0.16 | 0.39697 |
| 1 | - 1 | 2 | 32.1 | 32.1 | 0.00 | 0.50914 |
| 1 | - 1 | 3 | 56.8 | 62.5 | 1.35 | 0.48776 |
| 1 | - 1 | 4 | 37.5 | 39.9 | 0.69 | 0.50287 |
| 1 | - 1 | 5 | 25.3 | 26.6 | 0.44 | 0.48443 |
| 3 | - 1 | 5 | 35.4 | 45.7 | 3.02 | 0.98771 |
| 3 | - 1 | 4 | 30.1 | 30.9 | 0.25 | 0.99848 |
| 3 | - 1 | 3 | 28.1 | 22.8 | 1.67 | 0.95108 |
| 3 | - 1 | 2 | 36.8 | 31.5 | 1.52 | 0.49923 |
| 3 | - 1 | 1 | 30.3 | 34.7 | 1.37 | 0.56429 |
| 5 | - 1 | 1 | 38.7 | 38.8 | 0.03 | 0.01121 |
| 5 | - 1 | 2 | 52.2 | 52.2 | 0.00 | 0.01328 |
| 5 | - 1 | 3 | 51.7 | 49.0 | 0.67 | 0.00406 |
| 7 | - 1 | 1 | 35.0 | 33.6 | 0.41 | 0.02294 |
| - 9 | - 1 | 4 | 35.4 | 37.3 | 0.57 | 0.99811 |
| 9 | - 1 | 2 | 44.0 | 38.6 | 1.43 | 0.50651 |
| 9 | - 1 | 1 | 36.8 | 35.9 | 0.26 | 0.51621 |
| 11 | - 1 | 3 | 32.6 | 35.5 | 0.90 | 0.00038 |
| 13 | - 1 | 2 | 37.0 | 31.8 | 1.48 | 0.98893 |
| 13 | - 1 | 1 | 42.7 | 40.0 | 0.72 | 0.00210 |
| 13 | - 1 | 0 | 50.1 | 46.6 | 0.88 | 0.99055 |
| 11 | - 1 | 0 | 47.3 | 41.3 | 1.55 | 0.48016 |
| 7 | - 1 | 0 | 78.9 | 81.8 | 0.59 | 0.98928 |
| 3 | - 1 | 0 | 66.1 | 68.0 | 0.42 | 0.44782 |
| 1 | - 1 | - 1 | 69.8 | 72.7 | 0.62 | 0.01759 |
| 5 | - 1 | - 1 | 49.4 | 47.7 | 0.42 | 0.48853 |
| 7 | - 1 | - 1 | 56.9 | 53.6 | 0.78 | 0.01352 |
| 11 | - 1 | - 1 | 47.3 | 43.9 | 0.88 | 0.49914 |
| 11 | - 1 | - 2 | 56.9 | 48.4 | 2.00 | 0.48582 |
| 9 | - 1 | - 2 | 45.5 | 37.7 | 2.03 | 0.99632 |
| 7 | - 1 | - 2 | 48.1 | 44.8 | 0.85 | 0.98482 |
| 5 | - 1 | - 2 | 68.9 | 65.7 | 0.67 | 0.49066 |
| 1 | - 1 | - 2 | 74.2 | 77.7 | 0.73 | 0.99676 |
| 3 | - 1 | - 3 | 56.1 | 57.2 | 0.27 | 0.98005 |
| 5 | - 1 | - 3 | 51.4 | 52.1 | 0.19 | 0.49258 |
| 9 | - 1 | - 3 | 52.6 | 51.2 | 0.34 | 0.99140 |
| - 10 | - 2 | 3 | 27.1 | 21.4 | 1.82 | 0.96353 |
| - 8 | - 2 | 3 | 31.3 | 27.3 | 1.23 | 0.03437 |
| - 6 | - 2 | 3 | 35.0 | 32.4 | 0.75 | 0.50190 |
| - 2 | - 2 | 3 | 51.1 | 50.1 | 0.23 | 0.00519 |
| - 2 | - 2 | 4 | 27.9 | 29.8 | 0.60 | 0.02536 |
| - 6 | - 2 | 4 | 27.2 | 29.2 | 0.66 | 0.53376 |
| 0 | - 2 | 4 | 26.6 | 23.3 | 1.05 | 0.56142 |
| 0 | - 2 | 2 | 50.0 | 44.5 | 1.38 | 0.94102 |
| 2 | - 2 | 1 | 33.7 | 33.0 | 0.74 | 0.00283 |
| 2 | - 2 | 2 | 51.1 | 52.7 | 0.39 | 0.49021 |
| 2 | - 2 | 2 | 60.9 | 61.1 | 0.03 | 0.48574 |
| 2 | - 2 | 3 | 41.0 | 40.3 | 0.20 | 0.49094 |
| 4 | - 2 | 4 | 31.6 | 36.9 | 1.60 | 0.02218 |
| 4 | - 2 | 3 | 42.2 | 44.0 | 0.50 | 0.98658 |
| 4 | - 2 | 2 | 20.0 | 14.6 | 1.87 | 0.03743 |
| 4 | - 2 | 1 | 15.1 | 11.8 | 1.20 | 0.59228 |
| 6 | - 2 | 1 | 61.9 | 65.1 | 0.71 | 0.99637 |
| 6 | - 2 | 2 | 53.3 | 57.7 | 0.38 | 0.97422 |
| 6 | - 2 | 3 | 23.5 | 21.1 | 0.79 | 0.98750 |
| 8 | - 2 | 3 | 44.4 | 46.1 | 0.45 | 0.47776 |
| 8 | - 2 | 2 | 34.3 | 35.7 | 0.41 | 0.49496 |
| 8 | - 2 | 1 | 24.4 | 21.4 | 1.00 | 0.43355 |
| 10 | - 2 | 1 | 27.9 | 29.5 | 0.52 | 0.53116 |
| 10 | - 2 | 3 | 15.4 | 15.5 | 0.04 | 0.95923 |
| 12 | - 2 | 2 | 37.5 | 40.7 | 0.92 | 0.99307 |
| 12 | - 2 | 1 | 34.5 | 35.4 | 0.28 | 0.98642 |
| 12 | - 2 | 0 | 20.1 | 14.4 | 1.99 | 0.97680 |
| 10 | - 2 | 0 | 46.8 | 45.4 | 0.38 | 0.48789 |
| 8 | - 2 | 0 | 22.4 | 18.9 | 1.18 | 0.01520 |
| 6 | - 2 | 0 | 70.3 | 66.3 | 0.84 | 0.97065 |
| 4 | - 2 | 0 | 56.2 | 59.3 | 0.74 | 0.47196 |
| 2 | - 2 | 0 | 23.4 | 25.8 | 0.83 | 0.44461 |
| 10 | - 2 | - 1 | 27.2 | 25.7 | 0.49 | 0.53845 |
| 8 | - 2 | - 1 | 36.3 | 37.1 | 0.24 | 0.03629 |
| 6 | - 2 | - 1 | 31.6 | 22.9 | 2.63 | 0.99417 |
| 4 | - 2 | - 1 | 47.9 | 51.9 | 1.02 | 0.52024 |
| 2 | - 2 | - 1 | 27.3 | 23.6 | 1.20 | 0.01912 |
| 0 | - 2 | - 1 | 61.5 | 65.0 | 0.78 | 0.00283 |
| 2 | - 2 | - 2 | 43.4 | 45.2 | 0.48 | 0.02631 |
| 4 | - 2 | - 2 | 47.8 | 47.2 | 0.18 | 0.47616 |
| 8 | - 2 | - 2 | 44.0 | 45.4 | 0.37 | 0.00730 |
| 12 | - 2 | - 2 | 24.4 | 26.8 | 0.79 | 0.51194 |
| 8 | - 2 | - 3 | 28.4 | 27.3 | 0.35 | 0.03437 |
| 6 | - 2 | - 3 | 30.2 | 32.4 | 0.69 | 0.50190 |

Table 5. Metal oxygen distances.

| $(Mo_{0.3}V_{0.7})_2O_5$ | | | | | $V_2O_5$ (8) | $MoO_3$ (14) |
|---|---|---|---|---|---|---|
| Atoms | Coordinates | | | Distance (in Å) | Distance (in Å) | Distance (in Å) |
| M - | .149 | 0 | .100 | | | |
| - O(1) | .145 | .065 | .493 | 1.659 ± 18 | 1.585 | 1.671 |
| - O(2) | .179 | -.448 | -.005 | 1.733 ± 36 | 1.780 | 1.734 |
| - O(3) | 0 | .002 | 0 | 1.804 ± 3 | 1.878 | 1.948 |
| - O(2) | .321 | .052 | .005 | 2.081 ± 16 | 1.878 | 1.948 |
| - O(2) | .179 | .552 | -.005 | 2.094 ± 36 | 2.021 | 2.251 |
| - O(1) | .145 | .065 | -.507 | 2.544 ± 18 | 2.785 | 2.332 |

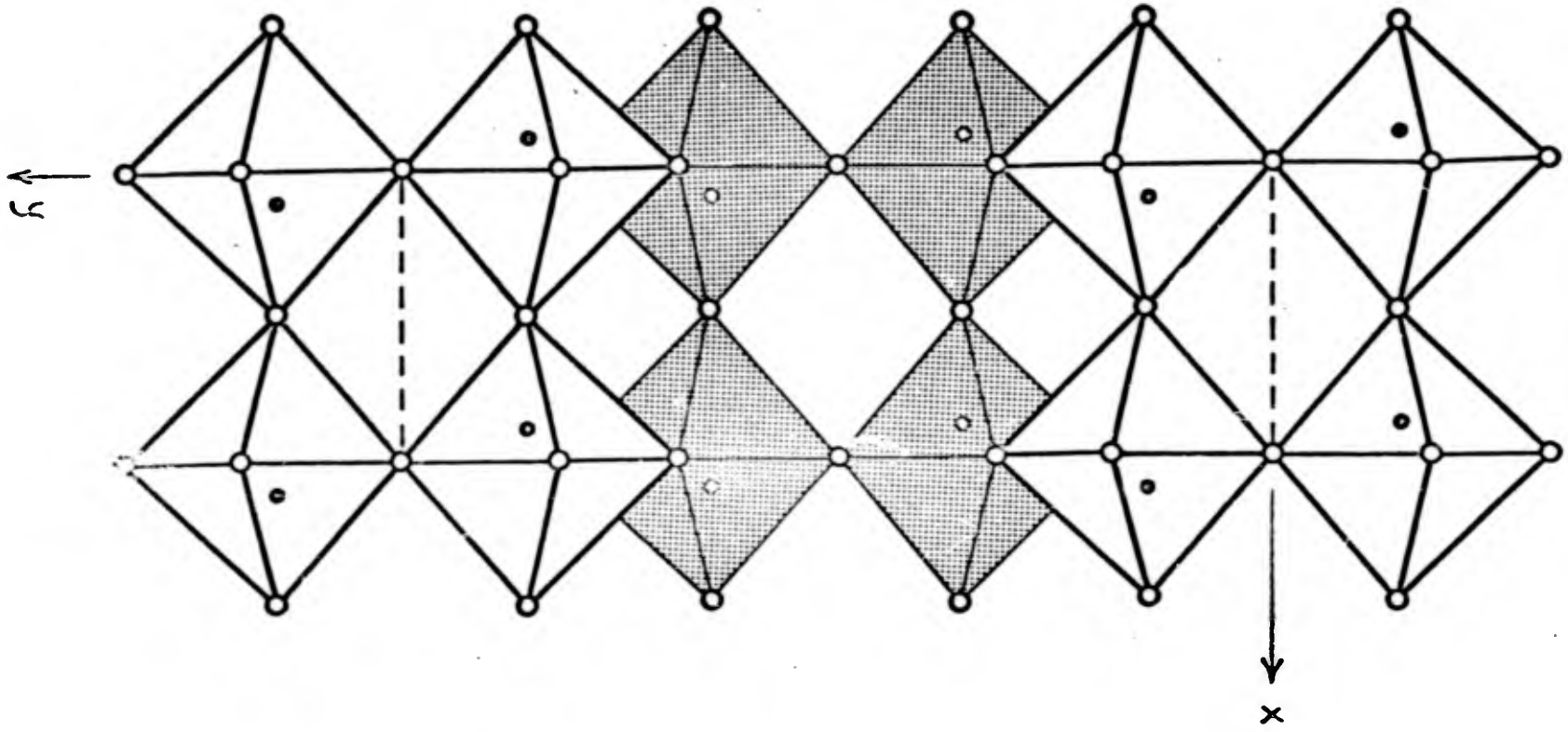


Fig. 1a. The structure of $(Mo_{0.3}V_{0.7})_2O_5$ visualized as built up of $MO_6$ octahedra at two levels (light and shaded, respectively). These polyhedra share corners with crystallographically identical ones above and below the positions of the metal atoms inside the octahedra are indicated by dots.

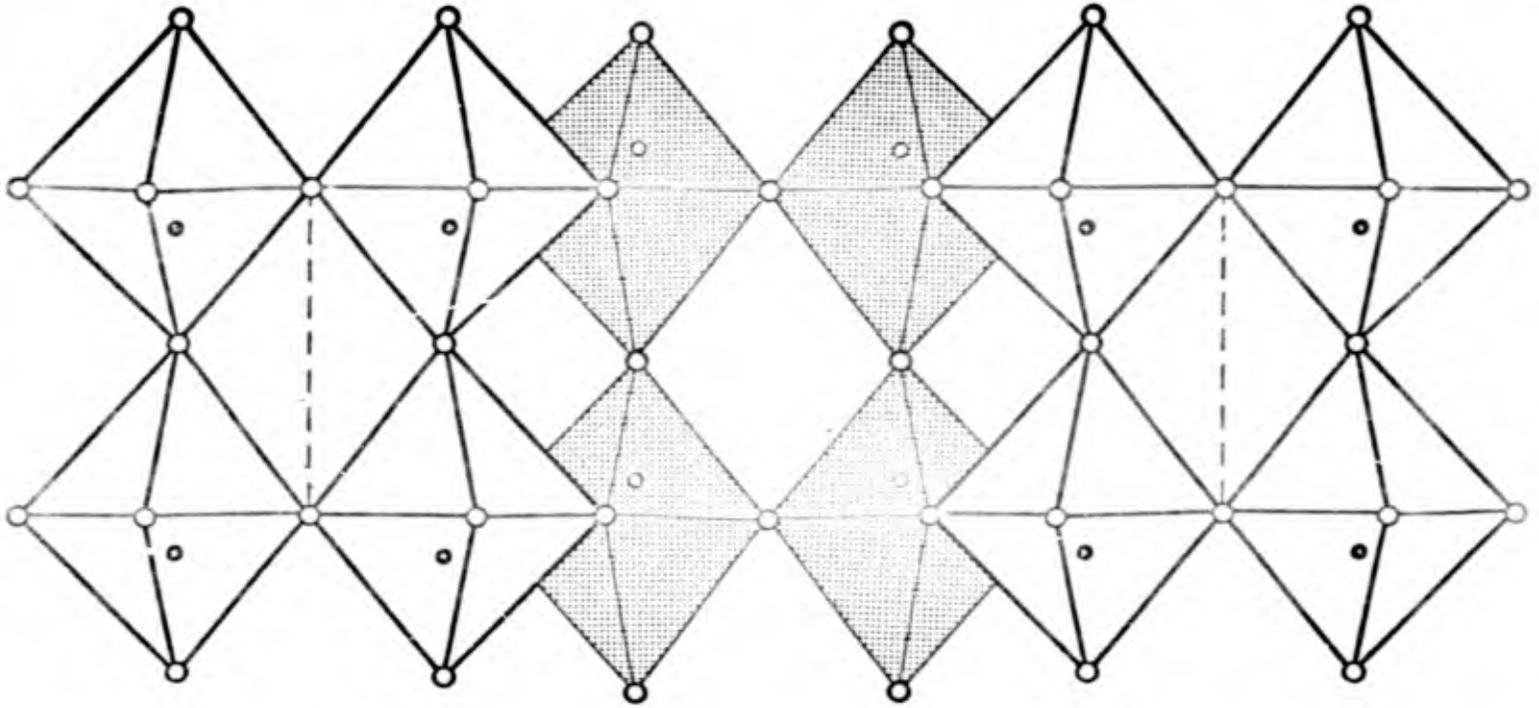

Fig. 1b. The structure of $V_2O_5$ visualized as built up of $MO_6$ octahedra at two levels (light and shaded, respectively). These polyhedra share corners with crystallographically identical ones above and below the positions of the metal atoms inside the octahedra are indicated by dots.

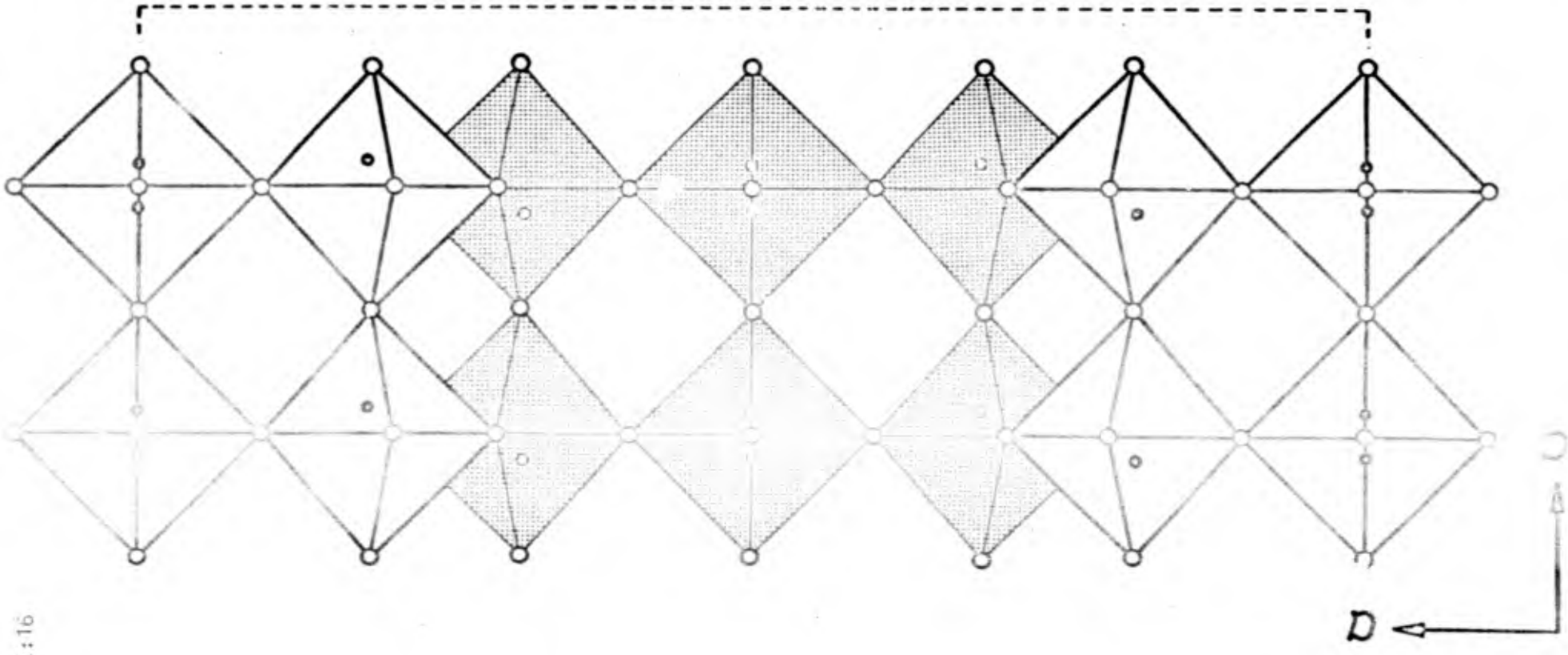


III:16

Fig. 2. The structure of $V_2MoO_8$ presented analogously with those in Fig. 1. In the octahedra containing two dots the metal atoms are situated alternatingly at the two positions in the strings of octahedra running along the line of sight. The dashed line indicates a repeat distance.

# The Crystal Structure of $NaMe_2^{IV}(PO_4)_3$, $Me^{IV}$ = Ge, Ti, Zr

LARS-OVE HAGMAN and PEDER KIERKEGAARD

Institute of Inorganic and Physical Chemistry, University of Stockholm, Stockholm, Sweden

The crystal structure of $NaZr_2(PO_4)_3$, a representative of an extensive group of isomorphous mixed phosphates containing alkali metals and germanium, titanium, zirconium or hafnium, has been determined from three-dimensional X-ray data. The space group is $R\bar{3}/c$ and the dimensions of the hexagonal unit cell for the three members of the series studied by the present authors are

| | | |
|---|---|---|
| $NaZr_2(PO_4)_3$ | $a$ = 8.8043 ± 2 Å | $c$ = 22.7585 ± 9 Å |
| $NaTi_2(PO_4)_3$ | $a$ = 8.4924 ± 5 Å | $c$ = 21.7788 ± 15 Å |
| $NaGe_2(PO_4)_3$ | $a$ = 8.1123 ± 4 Å | $c$ = 21.5133 ± 11 Å |

The crystals are built up of $MeO_6$ octahedra and $PO_4$ tetrahedra which are linked by corners to form a three-dimensional network. The sodium atoms are octahedrally surrounded by oxygen atoms. A discussion of the structure is given.

Studies on metal phosphates and in particular on transition metal phosphates have been conducted at this Institute for several years[1]. In connection with an investigation now in progress of the detailed superstructure of $ZrP_2O_7$ [2] it was found of interest to analyze the atomic arrangement of zirconium phosphates less complex in structure. The mixed phosphate $NaZr_2(PO_4)_3$ was selected for such an investigation.

Within the present study the compounds $NaZr_2(PO_4)_3$, $NaTi_2(PO_4)_3$ and $NaGe_2(PO_4)_3$ have been synthesized and found to be isomorphous. Sljukić *et al.* have prepared mixed zirconium and hafnium phosphates of all the alkali metals $AMe_2^{IV}(PO_4)_3$ [3]. The X-ray data reported by these authors suggest that all these compounds are isostructural.

## EXPERIMENTAL

Preparations of the crystals. A mixture of sodium metaphosphate (12.5 g, British Drug Houses, p.a.) and metal dioxide (1.2 g $ZrO_2$, Schering-Kahlbaum, p.a., 1.0 g $GeO_2$, Fairmont, p.a. or 0.75 g $TiO_2$, Merck, p.a.) was heated in a platinum crucible for 24 hours at 1200°C.[4] The products thus obtained were crystalline and gave good X-ray powder patterns but did not contain single crystals well suited for collecting extensive X-ray data. Good crystals could, however, be obtained after tempering in platinum crucible for several weeks at 1100°C, or according to a method given by Matković *et al.*[5] by crystallization from a melt of boric acid. The crystals thus obtained were found to consist of colourless, rectangular prisms.

Chemical analysis. A sample of the zirconium compound was fused with sodium potassium carbonate in a platinum crucible. After leaching with boiling water the amount of phosphorus in the solution was determined gravimetrically as $Mg_2P_2O_7$ [6]. The residue, insoluble in water, was in turn fused with sodium hydrogen sulphate in a platinum crucible. After dissolving in hot water the amount of zirconium was determined gravimetrically as $ZrO_2$ [6]. The following data were obtained:

| | Calc. for $NaZr_2(PO_4)_3$ | Obs. |
|---|---|---|
| $ZrO_2$ | 50.26 | 48.5 weight % |
| $P_2O_5$ | 43.43 | 45.1 |
| $Na_2O$ | 6.31 | 6.4 (residue) |

X-ray data collecting and treatment. The powder patterns of the three mixed sodium-transition metal phosphates prepared within this study could all be interpreted assuming a hexagonal (rhombohedral) unit cell. Accurate values of the cell dimensions were calculated from Guinier-Hägg powder photographs taken with strictly monochromatic $CuK\alpha_1$ radiation ($\lambda$ = 1.54056 Å) with potassium chloride ($a$ = 6.29228 Å)[7] added to the specimens as an internal standard. The hexagonal unit cell dimensions refined by the method of least-squares are (25°C):

| | | |
|---|---|---|
| $NaZr_2(PO_4)_2$ | $a_H$ = 8.8043 ± 2 | Å |
| | $c_H$ = 22.7585 ± 9 | Å |
| $NaTi_2(PO_4)_2$ | $a_H$ = 8.4924 ± 5 | Å |
| | $c_H$ = 21.7788 ± 15 | Å |
| $NaGe_2(PO_4)_3$ | $a_H$ = 8.1123 ± 4 | Å |
| | $c_H$ = 21.5133 ± 11 | Å |

The value of 3.20 $g/cm^3$ for the density of $NaZr_2(PO_4)_3$, found from the apparent loss of weight in benzene, corresponds to six formula units in the unit cell ($\rho_{calc}$ = 3.18 $g/cm^3$).

Crystals of all the three compounds were studied by taking rotation and Weissenberg photographs which confirmed the presence of strict isomorphism. Complete three-dimensional data were collected for $NaZr_2(PO_4)_3$ using CuK radiation. The crystal used was a rectangular prism measuring 1.07 x $10^{-4}$ $mm^3$. Multiple film technique was used for the Weissenberg photographs. The relative intensities were estimated visually by comparison with an intensity scale obtained by photographing a reflection with different exposure times. A correction for absorption was included in the computation of the $F^2$ values. (The linear absorption coefficient $\mu$ = 234.1 $cm^{-1}$.)[8]

In the first stages of this structural study the computational work was performed using the computers Facit EDB and TRASK. The limited capacity of these machines made it necessary to conduct the structural refinement with the unit cell described as monoclinic (C2/c). All the final calculations, however, made use of the computer CD 3600. This allowed the final structural refinement to be performed with the hexagonal description of the structure.

## STRUCTURE DETERMINATION

The Weissenberg data, which confirmed the hexagonal (rhombohedral) symmetry of the crystal, showed the Laue symmetry to be $\bar{3}m$. The reflections systematically absent are hkil with $-h+k+l \neq 3n$ and $h\bar{h}0l$ with $l \neq 2n$. This is characteristic of the space groups $R\bar{3}c$ (No. 167) and $R\bar{3}c$ (No. 161). A test for piezoelectricity gave no effect. The structural investigation was thus undertaken assuming the atomic arrangement to be in accordance with the higher symmetry $R\bar{3}c$.

In the space group $R\bar{3}c$ (hexagonal axes) the following point positions exist:

$(000;\ \frac{1}{3},\frac{2}{3},\frac{2}{3};\ \frac{2}{3},\frac{1}{3},\frac{1}{3})+$

6(a) $(0,0,\frac{1}{4};\ 0,0,\frac{3}{4})$

6(b) $(0,0,0;\ 0,0,\frac{1}{2})$

12(c) $\pm(0,0,z;\ 0,0,\frac{1}{2}+z)$

18(d) $(\frac{1}{2},0,0;\ 0,\frac{1}{2},0;\ \frac{1}{2},\frac{1}{2},0;\ \frac{1}{2},0,\frac{1}{2};\ 0,\frac{1}{2},\frac{1}{2};\ \frac{1}{2},\frac{1}{2},\frac{1}{2})$

18(e) $\pm(x,0,\frac{1}{4};\ 0,x,\frac{1}{4};\ x,x,\frac{1}{4})$

36(f) $\pm(x,y,z;\ \bar{y},x-y,z;\ y-x,\bar{x},z;\ \bar{y},\bar{x},\frac{1}{2}+z;\ x,x-y,\frac{1}{2}+z;\ y-x,y,\frac{1}{2}+z)$

From calculations of the Patterson projection P(pvw) and section P(0vw) and subsequent calculations of the electron density distributions in $\rho(pyz)$ and $\rho(0yz)$ the positions of the twelve zirconium, the eighteen phosphorus and the six sodium atoms - found to be situated in 12(c), 18(e) and 6(b) - in the unit cell could easily be determined with moderate accuracy. Starting from these data it was possible to make three-dimensional electron density calculations and find the positions of the 72 oxygen atoms situated in 2x36(f) point positions. At the electron density calculations and subsequent refinement atomic scattering curves for unionized atoms were used. The real part of the anomalous dispersion correction[9] was applied to the scattering curves.

A refinement of the coordinates so obtained was then performed by means of the least-squares method. The starting values of the individual isotropic temperature factors used in the program, were zero for all of the atoms. Initially all 296 of the independent reflections measured were included in the calculations, but after a few cycles, eight strong, low-angle reflections were omitted as suffering from extinction. The refinement was considered as complete when the parameter shifts were less than 5 % of the standard deviations, at which stage the discrepancy index R was 0.089. Hughes' weighting function $w = 1/h^2|F_{obs},min|^2$ for $|F_{obs}| \leq h|F_{obs},min|$ and $w = 1/|F_{obs}|^2$ for $|F_{obs}| > |F_{obs},min|$ with $h = 4.0$ was used in the refinement. A weight analysis obtained in the final cycle is given in Table 4.

A list of the observed and calculated structure factors is given in Table 5. A three-dimensional difference synthesis calculated over the unique part of the unit cell at points 0.2 Å apart showed very small maxima and minima. The largest maximum in this synthesis has a magnitude of about 20 % of the heights of the oxygen peaks in the electron density functions. Thus, from this calculation as well as from a computation of the interatomic distances (cf. Table 6), which were found to be within the normal range, further evidence was obtained that the atomic parameters arrived at in the final cycle of refinement and listed in Table 7 should present an adequate description of the structure. Also an attempt to improve the structure by lowering the symmetry to R3c was unsuccessful.

## DESCRIPTION AND DISCUSSION OF THE STRUCTURE

The crystal structure of $NaZr_2(PO_4)_3$ thus derived may be described in terms of $PO_4$ tetrahedra and $ZrO_6$ octahedra which are linked by corners to a three-dimensional network (cf. Fig. 1). Every oxygen atom thus belongs simultaneously within a $PO_4$ group and a $ZrO_6$ group. The sites of the sodium atoms are in the strongly distorted octahedra formed by the triangular faces of two $ZrO_6$ octahedra stacked on top of each other as illustrated in Fig. 2. The groups $O_3ZrO_3NaO_3ZrO_3$ thus formed may be considered as major structural units of the atomic arrangement. Such groups are mutually linked in the c direction by $PO_4$ tetrahedra in such a way that empty trigonal prisms of oxygen atoms are formed. The endless columns resulting from this linking are also connected normal to the c direction by the $PO_4$ tetrahedra (cf. Fig. 1).

All the interatomic distances are of normal lengths (cf Table 6). The $PO_4$ tetrahedra are nearly regular. The P-O distances are comparable to those found by Furberg[10] in $H_3PO_4$ and also by Cruickshank[11] and Kierkegaard[12] in several phosphate structures.

Rather few zirconium oxygen compounds have been found to contain $ZrO_6$ octahedra, more frequent coordination numbers of oxygen around this metal being seven (e.g. in $ZrO_2$, monoclinic[12], and $Zr_4(OH)_6(CrO_4)_5 \cdot 2H_2O$ [14]) or eight (e.g. in $ZrO_2$, cubic[15], $Zr(SO_4)_2 \cdot 4H_2O$ [16], $Zr(IO_3)_4$ [17] and $ZrOCl_2 \cdot 8H_2O$ [18]). The Zr-O distances of the somewhat distorted octahedra (Fig. 3b) of $NaZr_2(PO_4)_3$ (2.048 and 2.084 Å) are somewhat shorter than the value 2.097 Å reported for $BaZrO_3$ [18] of perovskite type structure.

The six-fold coordination of oxygen around sodium (Fig. 3c) represents a heavily distorted octahedron with O-Na-O angles of 66.0° and 114.0°.

Acknowledgements. This investigation has been sponsored in part by the Swedish Natural Science Research Council and in part by the European Research Office, United States Army, Frankfurt am Main, Germany. Permission for the use of the computers Facit EDB, TRASK and CD 3600 was granted by the Computer Division of the National Swedish Rationalization Agency.

The authors sincerely thank Professor Arne Magnéli for his encouraging and stimulating interest and for all facilities placed at their disposal. They are also indebted to Mr. Lars Tallbacka for his willing help in the measurement of the piezoelectric effect.

REFERENCES


1. Kierkegaard, P. Arkiv Kemi 19 (1962) 51.
2. Levi, G.R. and Peyronell, G. Z. Krist. 92 (1935) 190.
3. Sljukić, M. Matković, B. and Prodić, B. Croat. Chem. Acta 39 (1967) 145.
4. Gmelin's Handbuch, 8 ed. System No. 42, 410 Verlag Chemie, Weinheim/Bergstrasse 1958.
5. Matković, B., Sljukić, M. and Prodić, B. Croat. Chem. Acta 38 (1967) 69.
6. De Hevesy, G. and Kimura, Angew. Chem. 38 (1925) 775.
7. Hambling, P.G. Acta Cryst. 6 (1953) 98.
8. International Tables for X-Ray Crystallography, Vol. III, Birmingham 1962.
9. Dauben, C.H. and Tempelton, D.H. Acta Cryst. 8 (1955) 841.
10. Furberg, S. Acta Chem. Scand. 9 (1955) 1557.
11. Cruickshank, D.W.J. Acta Cryst. 17 (1964) 671.
12. Nord, A.G. and Kierkegaard, P. Acta Chem. Scand. 22 (1968)
13. McCullough, J.D. and Trueblood, K.N. Acta Cryst. 12 (1959) 507.
14. Lundgren, G. Arkiv Kemi 13 (1958) 59.
15. Passerini, L. Gazz. Chim. Ital. 60 (1930) 672.
16. Singer, J. and Cromer, D.T. Acta Cryst. 12 (1959) 719.
17. Larson, A.C. and Cromer, D.T. Acta Cryst. 14 (1961) 128.
18. Clearfield, A. and Vaughan, P.A. Acta Cryst. 9 (1956) 555.
19. Megav, H.D. Proc. Phys. Soc. 58 (1946) 133.

Table 1. X-Ray Powder Data of $NaGe_2(PO_4)_3$. CuKα radiation.
($\lambda$CuKα = 1.54056)

| h | k | l | Obs. | Calc. | Delta | $D_{obs}$ | $I_o$ |
|---|---|---|---|---|---|---|---|
| 0 | 1 | 2 | 1697 | 1715 | -18 | 5.91 | s |
| 1 | 0 | 4 | 3237 | 3253 | -16 | 4.28 | vs |
| 1 | 1 | 0 | 3601 | 3606 | -5 | 4.06 | vs |
| 1 | 1 | 3 | 4752 | 4760 | -8 | 3.53 | vs |
| 0 | 2 | 4 | 6835 | 6860 | -25 | 2.95 | vs |
| 1 | 1 | 6 | 8201 | 8221 | -20 | 2.69 | vs |
| 2 | 1 | 1 | 8537 | 8543 | -6 | 2.64 | s |
| 0 | 1 | 8 | 9391 | 9407 | -16 | 2.51 | m |
| 2 | 1 | 4 | 10450 | 10466 | -16 | 2.38 | s |
| 3 | 0 | 0 | 10801 | 10819 | -18 | 2.34 | vs |
| 2 | 0 | 8 | 13009 | 13013 | -4 | 2.14 | m |
| 1 | 1 | 9 | 13971 | 13990 | -19 | 2.06 | m |
| 2 | 2 | 0 | 14434 | 14425 | 9 | 2.03 | m |
| 2 | 1 | 7 | 14694 | 14696 | -2 | 2.01 | w |
| 3 | 0 | 6 | 15429 | 15434 | -5 | 1.96 | m |
| 2 | 2 | 3 | 15569 | 15579 | -10 | 1.95 | w |
| 3 | 1 | 2 | 16145 | 16140 | 5 | 1.92 | m |
| 1 | 2 | 8 | 16613 | 16619 | -6 | 1.89 | s |
| 0 | 2 | 10 | 17617 | 17628 | -11 | 1.84 | s |
| 0 | 0 | 12 | 18469 | 18461 | 8 | 1.79 | m |
| 2 | 2 | 6 | 19041 | 19040 | 1 | 1.77 | s |
| 0 | 4 | 2 | 19744 | 19747 | -3 | 1.73 | s |
| 2 | 1 | 10 | 21229 | 21235 | -6 | 1.67 | vs |
| 1 | 3 | 7 | 21883 | 21909 | -26 | 1.65 | m |
| 3 | 2 | 1 | 22969 | 22968 | 1 | 1.61 | w |
| 3 | 1 | 8 | 23828 | 23832 | -4 | 1.58 | s |
| 3 | 2 | 4 | 24892 | 24891 | 1 | 1.54 | s |
| 4 | 1 | 0 | 25250 | 25244 | 6 | 1.53 | s |
| 2 | 3 | 5 | 26059 | 26045 | 14 | 1.51 | vw |
| 0 | 1 | 14 | 26323 | 26329 | -6 | 1.50 | m |
| 0 | 4 | 8 | 27416 | 27438 | -22 | 1.47 | m |
| 1 | 3 | 10 | 28450 | 28447 | 3 | 1.44 | s |
| 3 | 0 | 12 | 29272 | 29280 | -8 | 1.42 | w |
| 2 | 3 | 8 | 30989 | 31040 | -51 | 1.38 | w |
| 3 | 1 | 11 | 31134 | 31139 | -5 | 1.38 | vw |
| 4 | 0 | 10 | 32065 | 32054 | 11 | 1.36 | s |
| 0 | 5 | 4 | | | | | |
| 1 | 1 | 15 | 32446 | 32451 | -5 | 1.35 | s |
| 3 | 3 | 0 | | | | | |
| 1 | 2 | 14 | 33558 | 33542 | 16 | 1.33 | m |
| 3 | 2 | 10 | 35684 | 35660 | 24 | 1.29 | m |
| 2 | 4 | 4 | | | | | |
| 5 | 1 | 4 | 39350 | 39317 | 33 | 1.23 | m |
| 3 | 1 | 14 | 40767 | 40754 | 13 | 1.21 | w |
| 2 | 1 | 16 | 41235 | 41234 | 1 | 1.20 | vw |
| 0 | 0 | 18 | 41550 | 41536 | 14 | 1.19 | w |
| 6 | 0 | 0 | 43270 | 43270 | 0 | 1.17 | m |

Table 2. X-Ray Powder Data of $NaTi_2(PO_4)_3$. $CuK\alpha_1$ radiation.
($\lambda CuK\alpha_1 = 1.54056$)

| h | k | l | Obs. | Calc. | Delta | $D_{obs}$ | $I_o$ |
|---|---|---|---|---|---|---|---|
| 0 | 1 | 2 | 1606 | 1597 | 9 | 6.08 | s |
| 1 | 0 | 4 | 3099 | 3098 | 1 | 4.38 | vs |
| 1 | 1 | 0 | 3295 | 3291 | 4 | 4.24 | vs |
| 1 | 1 | 3 | 4420 | 4417 | 3 | 3.66 | vs |
| 2 | 0 | 2 | 4895 | 4888 | 7 | 3.48 | vw |
| 0 | 2 | 4 | 6388 | 6389 | -1 | 3.05 | vs |
| 1 | 1 | 6 | 7803 | 7804 | -1 | 2.76 | vs |
| 2 | 1 | 1 | | | | | |
| 2 | 1 | 4 | 9700 | 9680 | 20 | 2.47 | s |
| 3 | 0 | 0 | 9883 | 9872 | 11 | 2.45 | m |
| 2 | 0 | 8 | 12383 | 12394 | -11 | 2.19 | m |
| 1 | 1 | 9 | 13403 | 13423 | -20 | 2.10 | w |
| 2 | 1 | 7 | 13810 | 13808 | 2 | 2.07 | vw |
| 2 | 2 | 3 | 14276 | 14289 | -13 | 2.04 | w |
| 3 | 0 | 6 | 14364 | 14376 | -12 | 2.03 | m |
| 1 | 3 | 1 | | | | | |
| 1 | 2 | 8 | 15665 | 15684 | -19 | 1.95 | s |
| 1 | 3 | 4 | 16256 | 16262 | -6 | 1.91 | s |
| 0 | 2 | 10 | 16908 | 16897 | 11 | 1.87 | s |
| 2 | 2 | 6 | 17684 | 17666 | 18 | 1.83 | m |
| 2 | 1 | 10 | 20184 | 20188 | -4 | 1.71 | s |
| 1 | 3 | 7 | 20401 | 20390 | 11 | 1.71 | m |
| 3 | 1 | 8 | 22278 | 22266 | 12 | 1.63 | s |
| 3 | 2 | 4 | 22838 | 22843 | -5 | 1.61 | s |
| 4 | 1 | 0 | 23027 | 23035 | -8 | 1.61 | m |
| 4 | 1 | 3 | 24175 | 24161 | 14 | 1.57 | m |
| 0 | 4 | 8 | 25582 | 25557 | 25 | 1.52 | s |
| 0 | 1 | 14 | | | | | |
| 1 | 3 | 10 | 26793 | 26769 | 24 | 1.49 | s |
| 4 | 1 | 6 | 27587 | 27539 | 48 | 1.47 | m |
| 3 | 0 | 12 | 27898 | 27886 | 12 | 1.46 | w |
| 5 | 0 | 12 | 28914 | 28906 | 8 | 1.43 | s |
| 2 | 0 | 14 | | | | | |
| 3 | 1 | 11 | 29443 | 29425 | 18 | 1.42 | m |
| 0 | 5 | 4 | | | | | |
| 1 | 2 | 14 | 32188 | 32196 | -8 | 1.36 | m |
| 3 | 3 | 6 | 34163 | 34130 | 33 | 1.32 | w |
| 5 | 1 | 1 | | | | | |
| 1 | 5 | 5 | 37106 | 37132 | -26 | 1.26 | w |
| 4 | 2 | 8 | 38764 | 38778 | -14 | 1.24 | w |
| 3 | 1 | 14 | | | | | |
| 6 | 0 | 0 | 39497 | 39489 | 8 | 1.23 | m |

Table 3. X-Ray Powder Data of $NaZr_2(PO_4)_3$. CuKα radiation. (λCuKα = 1.54056)

| h | k | l | Obs. | Calc. | Delta | $D_{obs}$ | $I_o$ |
|---|---|---|---|---|---|---|---|
| 0 | 1 | 2 | 1488 | 1479 | 9 | 6.31 | s |
| 1 | 0 | 4 | 2862 | 2853 | 9 | 4.55 | vs |
| 1 | 1 | 0 | 3073 | 3062 | 11 | 4.39 | vs |
| 1 | 1 | 3 | 4104 | 4093 | 11 | 3.80 | vs |
| 0 | 2 | 4 | 5921 | 5915 | 6 | 3.17 | vs |
| 1 | 1 | 6 | 7194 | 7186 | 8 | 2.87 | vs |
| 2 | 1 | 1 | 7262 | 7259 | 3 | 2.86 | s |
| 0 | 1 | 8 | 8353 | 8352 | 1 | 2.67 | m |
| 2 | 1 | 4 | 8983 | 8977 | 6 | 2.57 | s |
| 3 | 0 | 0 | 9188 | 9185 | 3 | 2.54 | vs |
| 2 | 0 | 8 | 11411 | 11414 | -3 | 2.28 | m |
| 2 | 2 | 0 | 12260 | 12247 | 13 | 2.20 | m |
| 1 | 1 | 9 | 12338 | 12341 | -3 | 2.19 | m |
| 1 | 0 | 10 | 12478 | 12476 | 2 | 2.18 | m |
| 2 | 1 | 7 | 12753 | 12757 | -4 | 2.16 | w |
| 3 | 0 | 6 | 13305 | 13309 | -4 | 2.11 | s |
| 3 | 1 | 2 | 13711 | 13726 | -15 | 2.08 | w |
| 1 | 2 | 8 | 14487 | 14476 | 11 | 2.02 | s |
| 1 | 3 | 4 | 15118 | 15100 | 18 | 1.98 | s |
| 0 | 2 | 10 | 15528 | 15538 | -10 | 1.95 | s |
| 3 | 1 | 5 | 16122 | 16131 | -9 | 1.92 | w |
| 2 | 2 | 6 | 16372 | 16371 | 1 | 1.90 | vs |
| 0 | 0 | 12 | 16497 | 16496 | 1 | 1.90 | w |
| 0 | 4 | 2 | 16772 | 16787 | -15 | 1.88 | m |
| 4 | 0 | 4 | 18160 | 18162 | -2 | 1.81 | w |
| 2 | 1 | 10 | 18615 | 18599 | 16 | 1.79 | vs |
| 1 | 3 | 7 | 18889 | 18881 | 8 | 1.77 | m |
| 3 | 2 | 1 | 19491 | 19506 | -15 | 1.74 | vvw |
| 3 | 1 | 8 | 20603 | 20599 | 4 | 1.70 | s |
| 3 | 2 | 4 | 21229 | 21224 | 5 | 1.67 | s |
| 4 | 1 | 0 | 21470 | 21432 | 38 | 1.66 | vs |
| 2 | 2 | 9 | 21522 | 21526 | -4 | 1.66 | vw |
| 2 | 3 | 5 | 22287 | 22255 | 32 | 1.63 | m |
| 4 | 1 | 3 | 22425 | 22463 | -38 | 1.63 | m |
| 0 | 1 | 14 | 23492 | 23473 | 19 | 1.59 | m |
| 0 | 4 | 8 | 23657 | 23661 | -4 | 1.58 | m |
| 1 | 3 | 10 | 24724 | 24723 | 1 | 1.55 | s |
| 3 | 2 | 7 | 25000 | 25004 | -4 | 1.54 | vw |
| 4 | 1 | 6 | 25560 | 25556 | 4 | 1.52 | s |
| 3 | 0 | 12 | 25686 | 25681 | 5 | 1.52 | w |
| 2 | 0 | 14 | 26538 | 26535 | 3 | 1.50 | s |
| 2 | 3 | 8 | 26726 | 26722 | 4 | 1.49 | w |

| h | k | l | Obs. | Calc. | Delta | $D_{obs}$ | $I_o$ |
|---|---|---|---|---|---|---|---|
| 3 | 1 | 11 | 27132 | 27129 | 3 | 1.48 | vw |
| 0 | 5 | 4 | 27344 | 27347 | -3 | 1.47 | m |
| 3 | 3 | 0 | 27550 | 27556 | -6 | 1.47 | m |
| 4 | 0 | 10 | 27791 | 27785 | 6 | 1.46 | m |
| 3 | 3 | 3 | 28580 | 28587 | -7 | 1.44 | vw |
| 1 | 1 | 15 | 28846 | 28836 | 10 | 1.43 | m |
| 1 | 2 | 14 | 29603 | 29597 | 6 | 1.42 | s |
| 1 | 0 | 16 | 30300 | 30346 | -46 | 1.40 | m |
| 4 | 1 | 9 | 30706 | 30711 | -5 | 1.39 | vw |
| 3 | 2 | 10 | 30851 | 30846 | 5 | 1.39 | m |
| 3 | 3 | 6 | 31675 | 31680 | -5 | 1.37 | m |
| 5 | 1 | 1 | 31744 | 31752 | -8 | 1.37 | w |
| 1 | 3 | 13 | 32603 | 32627 | -24 | 1.35 | vw |
| 5 | 1 | 4 | 33481 | 33471 | 10 | 1.33 | s |
| 2 | 4 | 7 | 34186 | 34189 | -3 | 1.32 | vvw |
| 1 | 5 | 5 | 34506 | 34502 | 4 | 1.31 | vw |
| 3 | 1 | 14 | 35726 | 35720 | 6 | 1.29 | m |
| 2 | 1 | 16 | 36463 | 36470 | -7 | 1.28 | w |
| 6 | 0 | 0 | 36731 | 36741 | -10 | 1.27 | m |
| 0 | 0 | 18 | 37104 | 37116 | -12 | 1.26 | w |
| 5 | 1 | 7 | 37245 | 37251 | -6 | 1.26 | w |
| 2 | 5 | 2 | 38216 | 38220 | -4 | 1.25 | w |
| 4 | 3 | 4 | 39613 | 39594 | 19 | 1.22 | w |
| 5 | 2 | 0 | 39797 | 39803 | -6 | 1.22 | m |
| 2 | 4 | 10 | 40042 | 40032 | 10 | 1.22 | m |
| 6 | 0 | 6 | 40872 | 40865 | 7 | 1.20 | w |
| 2 | 3 | 14 | 41858 | 41844 | 14 | 1.19 | m |
| 5 | 1 | 10 | 43102 | 43093 | 9 | 1.17 | vw |
| 5 | 2 | 6 | 43925 | 43927 | -2 | 1.16 | m |
| 2 | 5 | 8 | 45103 | 45093 | 10 | 1.15 | m |
| 1 | 5 | 11 | 45502 | 45499 | 3 | 1.14 | w |
| 1 | 6 | 4 | 45710 | 45718 | -8 | 1.14 | w |
| 3 | 0 | 18 | 46319 | 46301 | 18 | 1.13 | w |
| 4 | 1 | 15 | 47213 | 47207 | 6 | 1.12 | w |
| 3 | 2 | 16 | 48707 | 48717 | -10 | 1.10 | w |
| 4 | 4 | 0 | 48970 | 48988 | -18 | 1.10 | w |

Table 4. Weight analyses obtained in the final cycle of the least-squares refinement of $NaZr_2(PO_4)_3$

| Interval sin θ | Number of independent reflections | $\overline{w \Delta^2}$ | Interval $F_{obs}$ | Number of independent reflections | $\overline{w \Delta^2}$ |
|---|---|---|---|---|---|
| 0.0000-0.4642 | 30 | 1.36 | 0.0- 23.1 | 28 | 0.14 |
| 0.4642-0.5848 | 36 | 0.98 | 23.1- 31.3 | 29 | 0.47 |
| 0.5848-0.6694 | 30 | 0.58 | 31.3- 52.2 | 29 | 1.22 |
| 0.6694-0.7368 | 35 | 0.80 | 52.2- 63.4 | 29 | 1.06 |
| 0.7368-0.7937 | 27 | 1.02 | 63.4- 82.5 | 29 | 1.61 |
| 0.7937-0.8434 | 22 | 0.47 | 82.5- 99.6 | 29 | 1.28 |
| 0.8434-0.8879 | 36 | 0.85 | 99.6-115.5 | 28 | 1.14 |
| 0.8879-0.9283 | 23 | 1.13 | 115.5-143.3 | 30 | 1.18 |
| 0.9283-0.9655 | 30 | 0.97 | 143.3-192.1 | 28 | 0.61 |
| 0.9655-1.0000 | 19 | 1.84 | 192.1-345.3 | 29 | 1.29 |

**Table 5.** Observed and calculated structure factors. The 5 columns within each group contain the values $h$, $k$, $l$, $F_c$ and $k|F_o|$. The reflections deleted from the final cycles in the least-squares refinement are marked with an *.

Table 6. Interatomic distances and estimated standard deviations ($\pm \sigma$) in Å.

| | | | |
|---|---|---|---|
| Zr - O | Zr - 3 $O_1$ | = | 2.048 ± 13 |
| | Zr - 3 $O_2$ | = | 2.084 ± 12 |
| P - O | P - 2 $O_1$ | = | 1.516 ± 13 |
| | P - 2 $O_2$ | = | 1.546 ± 13 |
| Na - O | Na - 6 $O_2$ | = | 2.538 ± 12 |
| | Na - 6 $O_1$ | = | 3.689 ± 13 |
| O - O | $O_1$ - 4 $O_2$ | = | 2.48 ± 2 ; 2.52 ± 2 |
| | ($O_2$ - 4 $O_2$) | = | 2.94 ± 2 ; 3.01 ± 2 |
| | $O_1$ - 4 $O_1$ | = | 2.50 ± 2 ; 2 x 2.96 ± 2 |
| | | | 3.21 ± 2 |
| | $O_2$ - 3 $O_2$ | = | 2.52 ± 2 ; 2 x 2.761 ± 2 |

Additional distances

Zr - Na(Na-2Zr) = 3.315 ± 2
Zr - 3 P(P-2Zr) = 3.444 ± 3
Zr - 3 P(P-2Zr) = 3.493 ± 5
P - 2 Na(Na-6P) = 3.667 ± 3

Table 7. The structure of $NaZr_2(PO_4)_3$.

Space group: $R\bar{3}/c$

Unit cell dimensions: $a = 8.8043 \pm 2$ Å

$c = 22.7585 \pm 9$ Å

$V = 1527.7$ Å$^3$

Cell content: 6 $NaZr_2(PO_4)_3$

6 Na in 6(b): $(0,0,0;\ 0,0,\frac{1}{2})$

12 Zr in 12(c): $\pm(0,0,z;\ 0,0,\frac{1}{2}+z)$

18 P in 18(e): $\pm(x,0,\frac{1}{4};\ 0,x,\frac{1}{4};\ \bar{x},\bar{x},\frac{1}{4})$

36 $O_1$ and 36 $O_2$ in 2x36(f): $\pm(x,y,z;\ \bar{y},x-y,z;\ y-x,\bar{x},z;\ \bar{y},\bar{x},\frac{1}{2}+z;\ x,x-y,\frac{1}{2}+z;\ y-x,y,\frac{1}{2}+z)$

Atomic parameters and isotropic temperature factors with estimated standard deviations ($\pm\sigma$).

| Atom | x | y | z | B Å$^2$ |
|---|---|---|---|---|
| Na | 0 | 0 | 0 | 4.20 ± 40 |
| Zr | 0 | 0 | 0.1456 ± 1 | 1.80 ± 7 |
| P | 0.2909 ± 6 | 0 | $\frac{1}{4}$ | 2.40 ± 10 |
| $O_1$ | 0.1860 ± 15 | -0.0144 ± 15 | 0.1949 ± 5 | 3.20 ± 20 |
| $O_2$ | 0.1913 ± 15 | 0.1683 ± 15 | 0.0866 ± 5 | 2.90 ± 20 |

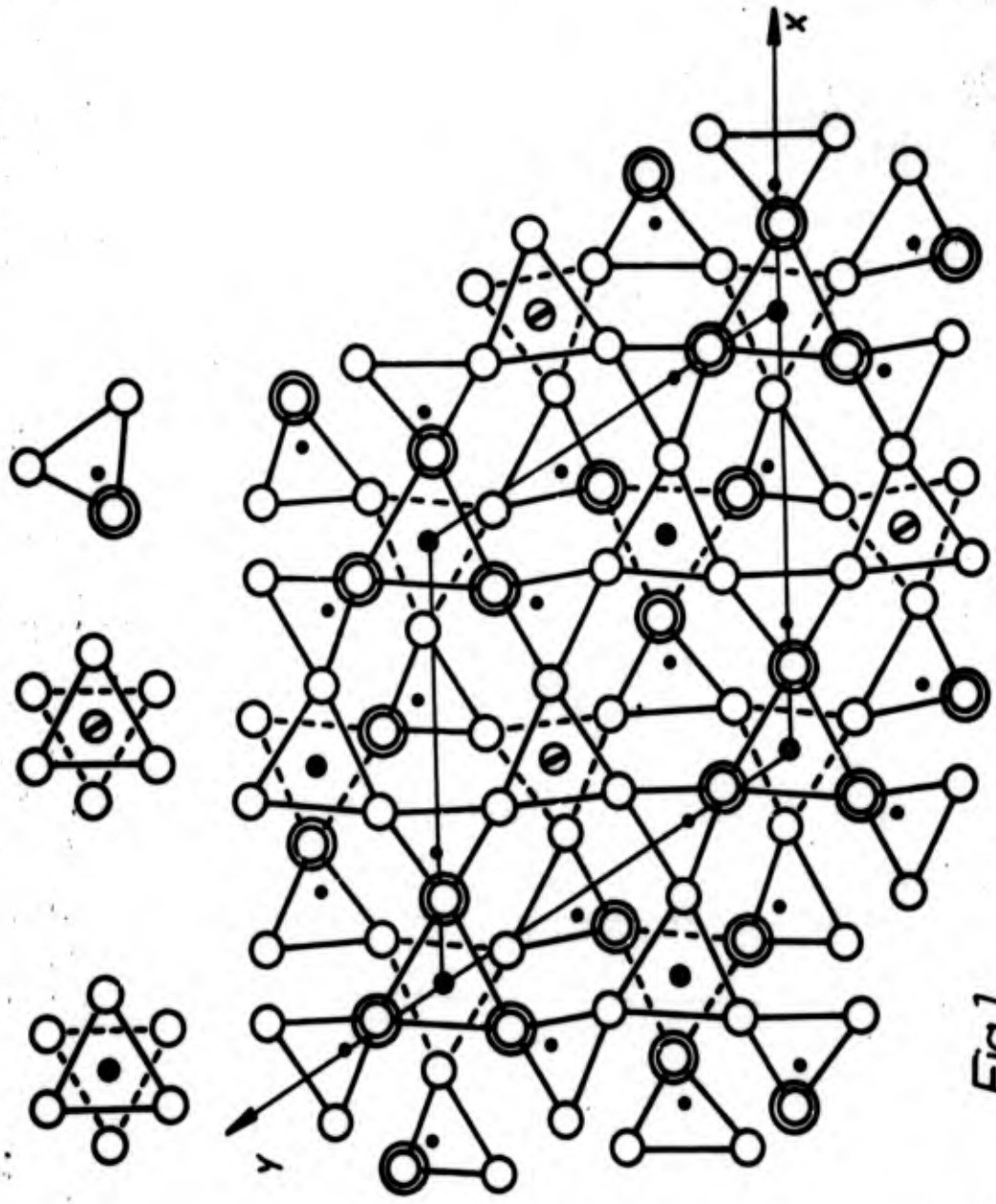


Fig.1.

**Fig. 1.** Schematic drawing showing the structure of $NaZr_2(PO_4)_3$. The structure viewed along [001] showing the contacts between $PO_4$ tetrahedra, $ZrO_6$ octahedra and $NaO_6$ octahedra. Only one third of the structure has been indicated (i.e. atoms with z parameters within the limits $0.00 \leq z \leq 0.33$).

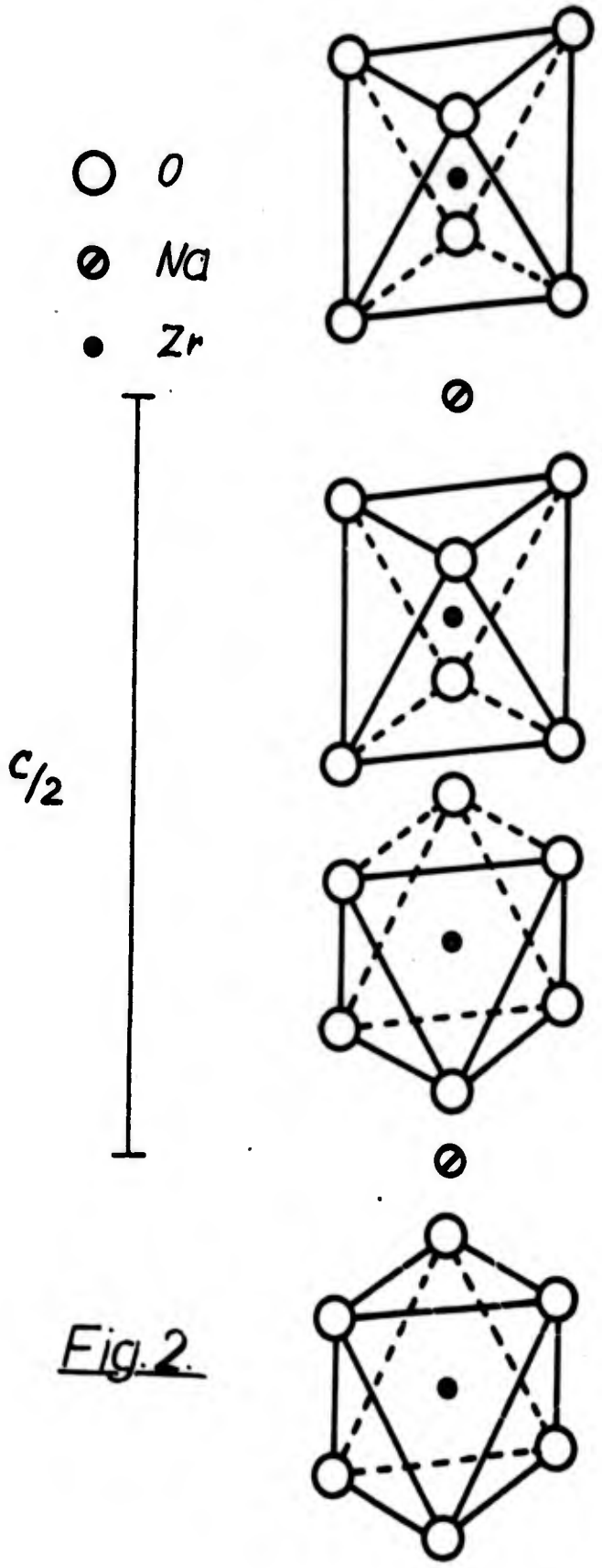


Fig. 2.

**Fig. 2.** Schematic drawing showing the sites of the sodium atoms between $ZrO_6$ octahedra in the structure of $NaZr_2(PO_4)_3$.

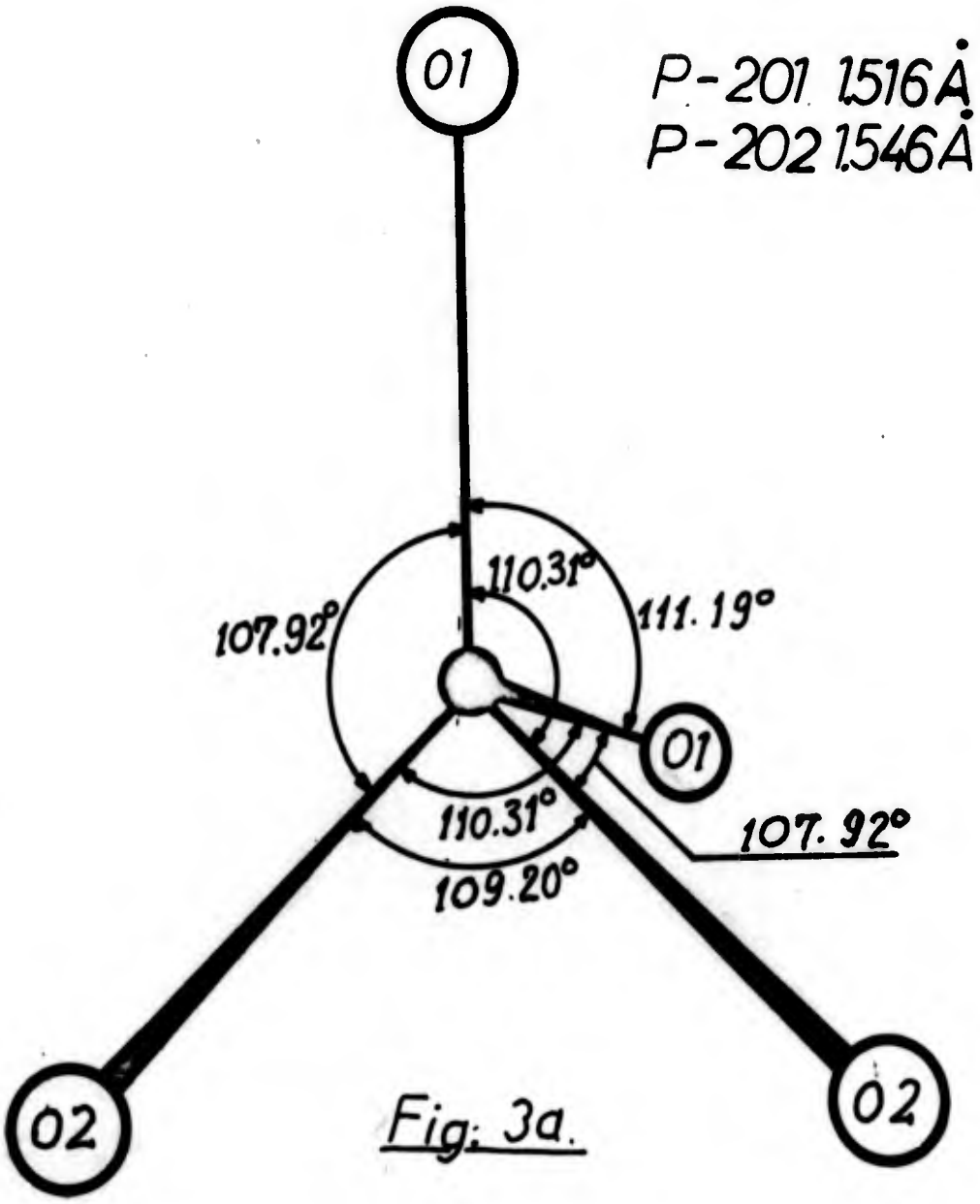


**Fig. 3a.** The $PO_4$ tetrahedron in the structure of $NaZr_2(PO_4)_3$.

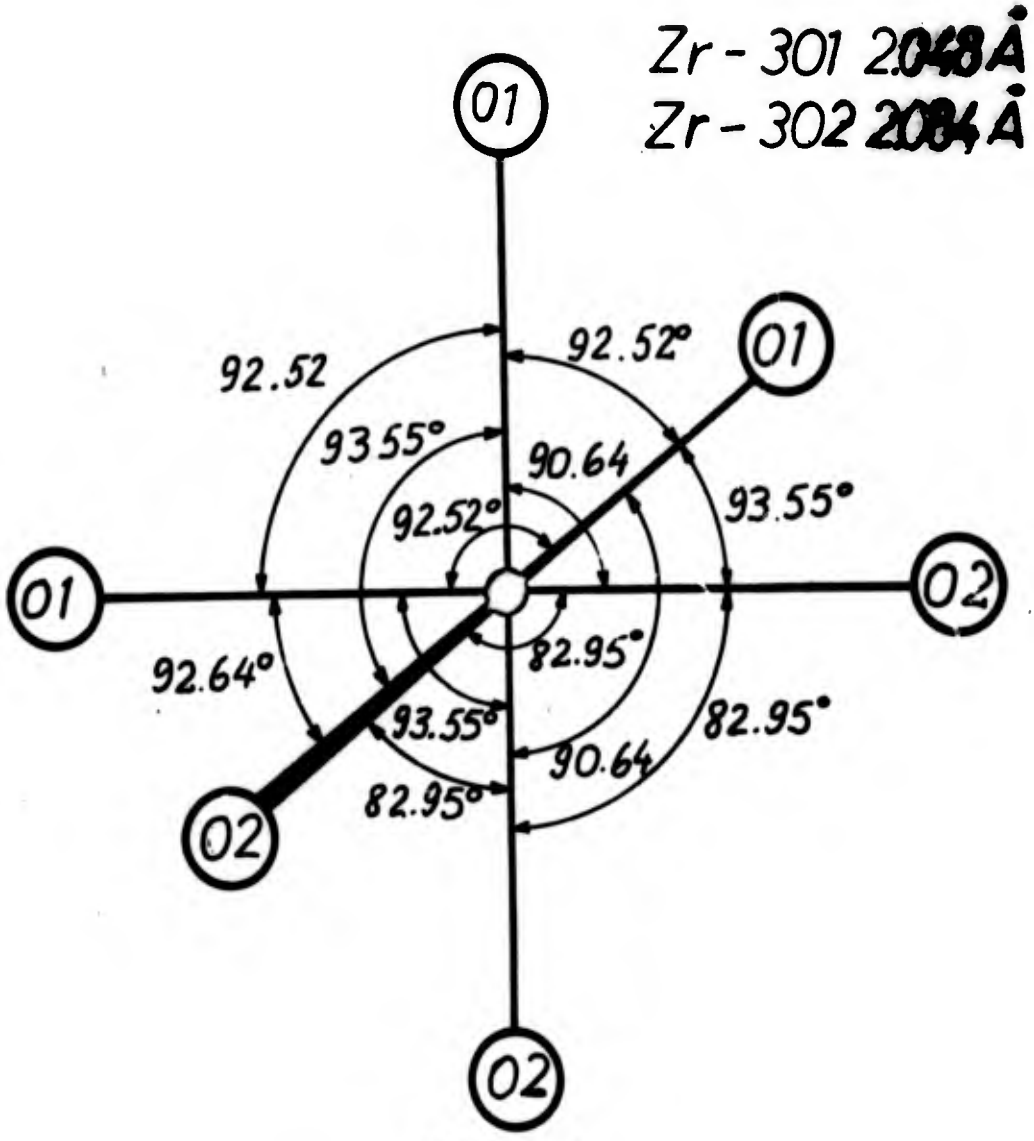


Fig.3b.

**Fig. 3b.** The $ZrO_6$ octahedron in the structure of $NaZr_2(PO_4)_3$.

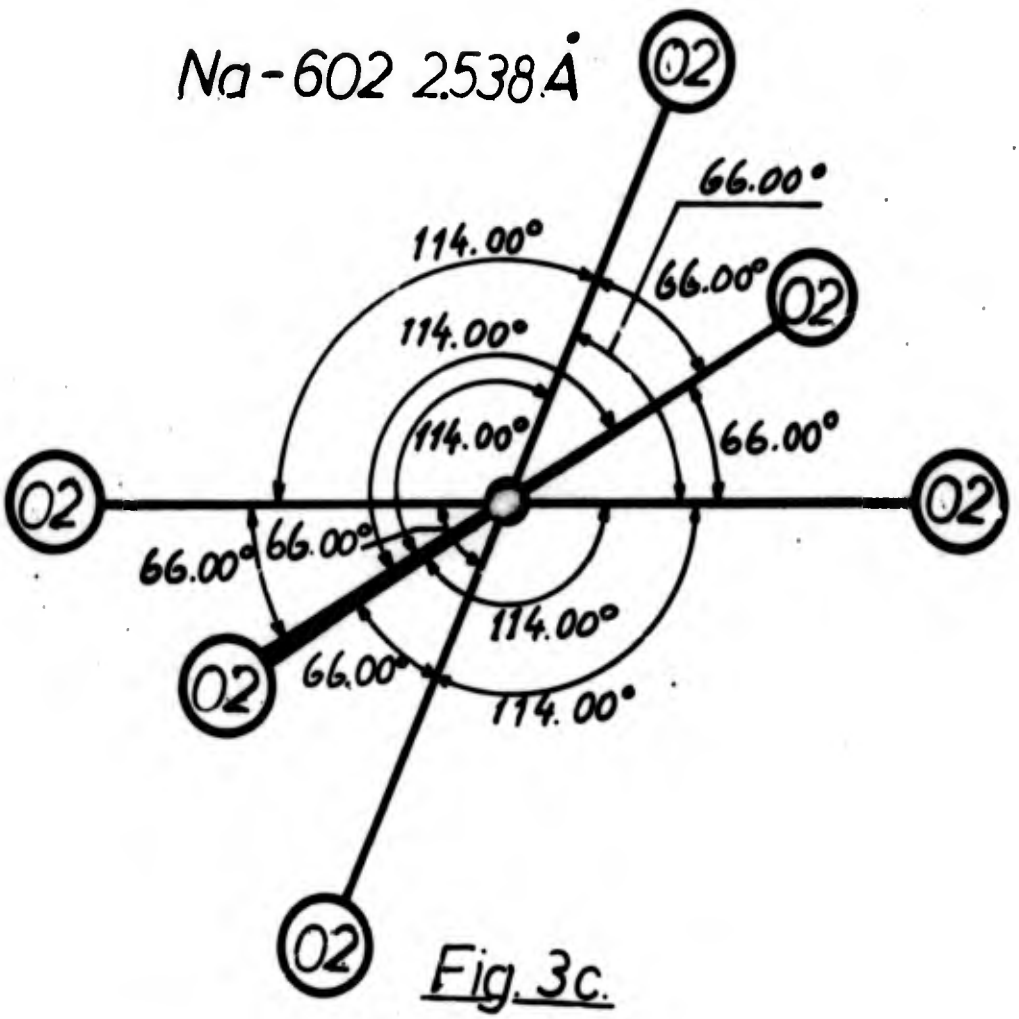


Fig. 3c.

Fig. 3c. The $NaO_6$ octahedron in the structure of $NaZr_2(PO_4)_3$.

# The Crystal Structure of a New Copper Wolfram Oxide, $Cu_3WO_6$

ELIZABETH GEBERT* and LARS KIHLBORG

Institute of Inorganic and Physical Chemistry, University of Stockholm, Stockholm Va, Sweden

The crystal structure of the previously unknown phase $Cu_3WO_6$ has been determined and refined from X-ray, single crystal diffractometer data. The symmetry is cubic, space group $Pa3$ - $T_h^6$ and the unit cell parameter is $a$ = 9.797 (±3) Å.

The structure can be described as built up of distorted $WO_6$ octahedra and $CuO_5$ triangular bipyramids, which share corners and edges in a rather complicated way. Each octahedron is linked to 6 bipyramids and each bipyramid to 4 octahedra and 6 other $CuO_5$ bipyramids.

Six $CuO_5$ bipyramids sharing edges form a staggered ring with 3 symmetry and one $WO_6$ group on either side of the ring closes the hole in the centre.

Interatomic distances and angles are given.

* *

While many ternary oxide systems involving transition metals have been extensively studied especially in recent years, rather little has been reported about the copper-wolfram-oxygen system. This is somewhat remarkable since the coordination chemistry of both these metals has drawn considerable attention and since there are inherent possibilities for interesting bonding features and physical properties in this system. There are a few papers in recent years reporting on "$CuWO_4$"[1,2], $Cu_xWO_3$ [3] and $Cu_xWO_{3+\delta}$ [4] but we have not found evidence in the literature for the existence of other intermediate phases in this system.

We have undertaken an investigation of this system by X-ray methods and in the course of this we have observed two phases, both prepared at about 800°C. A preliminary note about one of these, which we prefer to designate by the formula $CuWO_{4-x}$, but which is probably identical with the phases (phase) mentioned above, has recently been

---

* On leave from Argonne National Laboratory, Argonne, Ill., USA.

published in this journal.[5] Our studies on the second phase is reported in this article.

## EXPERIMENTAL

Mixtures of CuO and $WO_3$ of analytical grade were placed in platinum tubes which were evacuated, sealed and heated for 3-5 days at 800°C. Oxygen deficient samples were prepared by substituting $Cu_2O$ or $WO_2$ for part of the copper(II) or wolfram(VI) oxide, respectively.

The samples were examined microscopically and by taking X-ray powder patterns in a Guinier-type focussing camera using Cu$K\alpha_1$ radiation ($\lambda$ = 1.54051 Å) and KCl as an internal standard ($a$[KCl, 25°C] = 6.29228 Å.[6]) The density was determined pycnometrically on one sample in duplicate runs.

Single crystal photographs were recorded in a Weissenberg camera using Cu$K$ radiation. Data for the crystal structure determination were collected with a General Electric manual single crystal orienter equipped with a scintillation counter and using pulse height discrimination. Mo$K$ radiation filtered through a niobium foil and the $\theta - 2\theta$ scan technique was used in this case.

Diffractometer settings were made for 976 reflections with $h,k,l \geq 0$ and $\sin^2\theta \leq 0.20$ but after checking of the peak intensity the weakest reflections were rejected and only 653 were actually measured. The scan interval was calculated by the formula $\Delta(2\theta) = 1.65 \pm 1.0 \times \tan\theta$ (degrees), the scan velocity was 0.4 °/min in $2\theta$ and the background was counted one minute at the beginning and end of each scan interval. After averaging the measured values for symmetry equivalent reflections there remained a set of 234 non-equivalent intensity data which were used in the subsequent calculations.

## IDENTIFICATION AND CHARACTERIZATION OF $Cu_3WO_6$

The powder patterns of samples with gross compositions around $Cu_3WO_6$ indicated the presence of a new phase as a major component. The diffraction lines belonging to this phase could be indexed on the basis of a cubic unit cell with $\underline{a}$ = 9.79 Å, approximately. It has not yet been possible to prepare it in a completely pure state but all samples made in this composition region, including those of stoichiometric composition, contained at least traces of CuO and/or $CuWO_{4-x}$ as demonstrated by their powder patterns. The cell constant $\underline{a}$ calculated from the powder patterns of different samples by least squares refinement falls within the range 9.7936(±2) - 9.8005(±2) Å (the errors given within parentheses are single sigma values for each individual pattern). Although no obvious relation between the sample composition and the cell parameter has been found it cannot be excluded that these differences indicate the existence of a narrow homogeneity range for $Cu_3WO_6$.

A sample prepared from a mixture of 4 CuO and $WO_3$ showed faint lines of CuO in addition to those of the new phase. The density of this sample was found to be $\rho_{obs}$ = 6.62(±10) g $cm^{-3}$. The value calculated for $Cu_3WO_6$ using the observed cell parameter and assuming eight formula units per cell is $\rho_{calc}$ = 6.65 g $cm^{-3}$. Since the density of CuO is approximately 6.4 g $cm^{-3}$ a small amount of this compound as an impurity could not seriously affect the measured density value. It was therefore assumed that the unit cell content is $Cu_{24}W_8O_{48}$ which was proved to be correct by the subsequent structure analysis.

The $Cu_3WO_6$ phase was formed as black, octahedrally shaped crystals and one of these was selected from a sample of stoichiometric composition for use in the single crystal studies. The powder pattern is listed in Table 1.

## DETERMINATION AND REFINEMENT OF THE STRUCTURE

The Laue symmetry $\underline{m}3$ was evident in the Weissenberg photographs and from the observation of systematic absences of reflections the space group could be uniquely determined to be $\underline{Pa}3$ - $T_h^6$ (No. 205). The presence of both 8- and 24-fold positions in this space group was in accordance with the assumed composition and unit cell content.

A three-dimensional Patterson synthesis was calculated from the diffractometer data. Assuming the W atoms to occupy the 8-fold position ($x,x,x$) a positional parameter could easily be found which gave rise to W-W vectors that could explain all the strong maxima in this synthesis. The W position thus derived was used in a difference Fourier synthesis from which plausible locations of the copper atoms on one 24-fold position were obtained. After a least squares refinement of the W and Cu positions a second difference synthesis was calculated in which maxima corresponding to oxygen atoms were found. Least squares refinement of these atomic parameters could be successfully performed and the resulting final parameters are given in Table 2.

## DETAILS OF THE CALCULATIONS

Computers of the types CD 3200, CD 3600, IBM 360/50 and IBM 1800 were used for the calculations. Among the programs used on these machines the following more important ones may be mentioned; PIRUM for indexing of powder patterns and refinement of cell constants (written by P.-E. Werner, Stockholm), GIP for calculation of diffractometer settings (R. Norrestam, Stockholm), DRF for data reduction and Fourier summations (A. Zalkin, Berkeley, Calif., USA, modified by R. Liminga and J.-O. Lundgren, Uppsala), LALS for full matrix least squares refinement (Gantzel-Sparks-Trueblood, Univ. of Calif., modified by A. Zalkin, J.-O. Lundgren, R. Liminga and C.-I. Brändén), DISTAN for calculation of interatomic distances, angles and standard deviations thereof (A. Zalkin, modified by J.-O. Lundgren and R. Liminga), and ORTEP for making stereo drawings (C.K. Johnson, Oak Ridge, Tenn., USA).

The crystal selected for the data collection was relatively large but its extension varied only between 0.0107 cm and 0.0115 cm in all directions. Its shape could therefore be approximated by a sphere in the absorption correction of the intensities. A linear absorption coefficient $\mu = 397.5$ cm$^{-1}$ was used in these calculations.

The atomic scattering factors used were those given for unionized Cu and W in Ref. 7 and for O in Ref. 8. The complex anomalous dispersion parameters given by Cromer[9] were applied on the scattering factors of Cu and W.

Weights in the least squares refinement were calculated according to the formula $w = 1/(7000 + |F_{obs}| - 0.3|F_{obs}|^2 + 0.45|F_{obs}|^3)$. The weight analysis obtained in the last cycle is given in Table 3.

It became evident during the refinement that the strongest reflections suffered from extinction since the observed structure amplitudes for these were throughout smaller than the calculated values. The average of the quotient $|F_{obs}|/|F_{calc}|$ was 0.80 for the 30 strongest reflections and these were given zero weight in the last few cycles of refinement. The final values of $R = \Sigma||F_{obs}| - |F_{calc}||/\Sigma|F_{obs}|$ were 0.065 (the 30 strongest reflections omitted) and 0.120 (including the strong reflections).

The observed and calculated structure amplitudes are listed in Table 4.

## DESCRIPTION AND DISCUSSION OF THE STRUCTURE

The structure of $Cu_3WO_6$, illustrated in Fig. 1, is of a type which to our knowledge has not been reported previously. It is quite different from the cubic or pseudocubic alkaline earth wolframates of the same stoichiometry which have been known since long.[10] It can be considered as composed of distorted $WO_6$ octahedra and $CuO_5$ "trigonal" bipyramids (the trigonal symmetry is lost by distortion, cf. below). These polyhedra are joined by shared corners or edges in a rather intricate way. Each $WO_6$ octahedron is coupled to six $CuO_5$ groups, to three of these by corner-sharing and to the other three by edge-sharing. The $WO_6$ groups have no oxygen atoms in common although they occur pairwise in the structure with a separation of 3.97 Å between the wolfram atoms along the trigonal axes. Each $CuO_5$ bipyramid, on the other hand, shares one of the non-equatorial edges (1a-1c, Fig. 2) with a $WO_6$ octahedron and the three remaining corners with three other octahedra (Fig. 3a). It is also coupled to two other $CuO_5$ bipyramids by edge-sharing (1b-2a, 1c-2b) and to four additional bipyramids by corner-sharing (Fig. 3b).

Six mutually edge-sharing $CuO_5$ bipyramids form a ring with the point group symmetry $\bar{3}$ (Fig. 4) and such rings are centered on the equivalent positions 4a of this space group (0,0,0; $\frac{1}{2},\frac{1}{2},0$; $0,\frac{1}{2},\frac{1}{2}$; $\frac{1}{2},0,\frac{1}{2}$). The two $WO_6$ octahedra which form a "pair" (cf. above) both share three

corners with the same bipyramid ring and are situated on opposite sides of the plane (approximate, see below) of the ring on the trigonal axis. The three edges of each octahedron connecting the corners which are not shared with the ring are shared with three other edges in three other bipyramid rings and the $WO_6$ polyhedra may therefore be considered, formally, to act as a glue for the bipyramid rings.

Interatomic distances and bond angles are listed in Table 5. As was mentioned above, the octahedral coordination around wolfram is not regular but distorted so that only one of the threefold axes remains of the point group symmetry elements. This gives rise to three short and three long W-O bonds and may be looked upon as resulting from a displacement of the metal atom from the centre towards one of the octahedral faces. This 3+3 type coordination seems not to have been reported previously for any wolfram-oxygen compound in which the W-O distances have been determined with sufficient accuracy. Hexavalent wolfram is often tetrahedrally coordinated by oxygen but distorted octahedral coordination is also rather common. It occurs for example in $WO_3$ and in ternary oxides of the wolframite type (for instance $NiWO_4$ [11], $CdWO_4$ [12] and $CuWO_{4-x}$ [5]). In these latter cases the distortion gives rise to a group of four shorter and two longer bonds and can be regarded as reflecting a tendency towards four-coordination.

There is no doubt concerning the coordination number for copper in $Cu_3WO_6$. The distances to the five nearest oxygen atoms are within 2.25 Å while the sixth oxygen is 3.10 Å remote. The details of the coordination figure should be evident from Table 5 and Fig. 2. It is seen that the deviation from regularity is predominantly a relaxation of the trigonal symmetry giving rise to one short and two long edges in the equatorial plane.

The most common coordination around bivalent copper seems to be the four-fold, square planar arrangement with or without two more distant ligands completing a distorted octahedron. Five-fold coordination has also been observed in a number of structures, especially of metal-organic compounds. In most of these latter cases the coordination figure is best described as a square pyramid but in a few struc-

tures, including the present one, it must be regarded as a triangular bipyramid. These are $Cu_2(OH)AsO_4$ (olivenite)[13] and the isomorphous $Cu_2(OH)PO_4$ (libethenite)[14], $Cu_2O(SO_4)$ (dolerophanite)[15], $[Cr(NH_3)_6]$ $CuCl_5$[16] and $\mu_4$-oxohexa-$\mu$-chlorotetrakis(triphenylphosphine oxide) copper(II) [17]. In the first three only one half of the copper atoms are five-coordinated, the other half of them have 4+2 neighbours.

The shortest distance between copper atoms is that between the atoms situated in two bipyramids that share an edge, i.e. the distance between adjacent copper atoms in the rings. This distance, 2.990 (±3) Å, may be compared with the closest approach of metal atoms in CuO, where the three shortest distances are 2.9005 (±3), 3.0830 (±3) and 3.1734 (±4) Å according to a recent refinement[18]. The present value, which occur twice for each copper atom, is seen to be almost exactly the mean of the two shortest distances in CuO. Corresponding distances in $CuWO_{4-x}$ are 2.982 (±4) Å and 3.152 (±4) Å.[19]

The oxygen-oxygen distances are quite normal throughout. A shortening of the O-O distances along edges which are common to two polyhedra is a generally observed phenomenon in structures where there is no appreciable metal-metal interaction across these edges. This effect is noticeable also in this structure as the shortest edges within each polyhedron are those shared with other polyhedra. It is less pronounced for edges shared between two $CuO_5$ bipyramids than for those shared between a bipyramid and a $WO_6$ octahedron in accordance with the rules developed by Pauling from simple electrostatic arguments.

The "oxygen volume", $V_{cell}/n_O$, is 19.57 Å$^3$ which indicates that the oxygen lattice is a fairly open one. Corresponding values for structures with small cations in a close packed oxygen framework usually lie within the range 16.0 - 16.5 Å$^3$. The same thing is evident from the fact that the oxygen atoms have only nine oxygen near neighbours, lying within a distance of 3.10 and 2.92 Å, whereas the next nearest neighbours are not closer than 3.93 and 3.77 Å for O(1) and O(2), respectively.

This compound, which has crystallographically equivalent copper atoms in a somewhat unusual coordination with oxygen, should be studied by other methods, and investigations of its electric and magnetic pro-

perties have been started at this institute. In this connection a closer examination of possible non-stoichiometry will also be made. Preliminary measurements indicate that $Cu_3WO_6$ exhibits temperature independent paramagnetism over the temperature range 120-290°K with the value $\lambda_g \approx 4.5 \times 10^{-6}$ cgs units.[20]

Acknowledgements. This investigation has been financially supported in part by the Swedish Natural Science Research Council and in part by the European Research Office, United States Army, Frankfurt am Main, Germany. Permission for the use of the computers was granted by the Computer Division of the National Swedish Rationalization Agency.

## REFERENCES


1. Van Uitert, L.G., Rubin, J.J. and Bonner, W.A. J. Am. Ceramic Soc. 46 (1963) 512.
2. Clark, G.M. and Doyle, W.P. Spectrochim. Acta 22 (1966) 1441.
3. Conroy, L.E. and Sienko, M.J. J. Am. Chem. Soc. 79 (1957) 4048.
4. Sienko, M.J. and Weller, P.F. Inorg. Chem. 1 (1962) 324.
5. Gebert, E. and Kihlborg, L. Acta Chem. Scand. 21 (1967) 2575.
6. Hambling, P.G. Acta Cryst. 6 (1953) 98.
7. Cromer, D.T. and Waber, J.T. Acta Cryst. 18 (1965) 104.
8. Hanson, H.P., Herman, F., Lea, J.D. and Skillman, S. Acta Cryst. 17 (1964) 1040.
9. Cromer, D.T. Acta Cryst. 18 (1965) 17.
10. Steward, E.G. and Rooksby, H.P. Acta Cryst. 4 (1951) 503.
11. Keeling, Jr., R.O. Acta Cryst. 10 (1957) 209.
12. Chichagov, A.P., Ilyukhin, V.V. and Belov, N.V. Dokl. Akad. Nauk SSSR 166 (1966) 87.
13. Heritsch, H. Z. Krist. 99 (1938) 466.
14. Walitzi, E.M. Mineral. Petrogr. Mitt. 8 (1963) 614.
15. Flügel-Kahler, E. Acta Cryst. 16 (1963) 1009.
16. Mori, M., Saito, Y. and Watanabe, T. Bull. Chem. Soc. Japan 34 (1961) 295.
17. Bertrand, J.A. Inorg. Chem. 6 (1967) 495.
18. Norrby, L.-J. and Åsbrink, S. To be published.
19. Kihlborg, L. and Gebert, E. To be published.
20. Barvling, G. and Kihlborg, L. To be published.

Table 1. X-ray powder pattern of $Cu_3WO_6$. The values for the intensity of the lines have been obtained from rough visual estimation putting very strong = 10 and very faint = 1. $\lambda$ = 1.54051 Å. $\Delta = \sin^2\theta_{obs} - \sin^2\theta_{calc}$. $\sin^2\theta_{calc}$ based on $\underline{a}$ = 9.7989(± 2) Å calculated by least squares refinement.

| $\underline{I}$ | $\underline{h}^2+\underline{k}^2+\underline{l}^2$ | $\underline{d}_{obs}$ | $\sin^2\theta_{obs} \times 10^5$ | $\Delta \times 10^5$ |
|---|---|---|---|---|
| 9 | 3 | 5.660 | 1852 | -1 |
| 4 | 4 | 4.898 | 2473 | 1 |
| 10 | 5 | 4.385 | 3086 | -3 |
| 6 | 6 | 3.998 | 3711 | 3 |
| 4 | 8 | 3.455 | 4971 | 27 |
| 4 | 9 | 3.265 | 5566 | 4 |
| 6 | 11 | 2.954 | 6798 | 1 |
| 10 | 13 | 2.7199 | 8020 | -12 |
| 10 | 14 | 2.6206 | 8639 | -11 |
| 8 | 16 | 2.4496 | 9887 | 0 |
| 4 | 17 | 2.3766 | 10504 | 0 |
| 6 | 18 | 2.3096 | 11122 | 0 |
| 6 | 20 | 2.1906 | 12363 | 5 |
| 4 | 21 | 2.1384 | 12975 | 0 |
| 6 | 22 | 2.0900 | 13582 | -11 |
| 3 | 25 | 1.9595 | 15451 | 3 |
| 2 | 26 | 1.9208 | 16081 | 15 |
| 6 | 27 | 1.8850 | 16697 | 13 |
| 10 | 29 | 1.8194 | 17924 | 4 |
| 5 | 30 | 1.7888 | 18542 | 5 |
| 6 | 32 | 1.7317 | 19784 | 11 |
| 1 | 33 | 1.7057 | 20391 | 0 |
| 8 | 35 | 1.6562 | 21630 | 3 |
| 6 | 36 | 1.6323 | 22267 | 22 |
| 6 | 37 | 1.6105 | 22874 | 11 |
| 9 | 38 | 1.5895 | 23482 | 1 |

| $\underline{I}$ | $\underline{h}^2+\underline{k}^2+\underline{l}^2$ | $\underline{d}_{obs}$ | $\sin^2\theta_{obs}$ x $10^5$ | $\Delta$ x $10^5$ |
|---|---|---|---|---|
| 4 | 40 | 1.5494 | 24713 | -2 |
| 8 | 41 | 1.5307 | 25320 | -13 |
| 4 | 42 | 1.5119 | 25954 | 2 |
| 9 | 45 | 1.4614 | 27780 | -25 |
| 9 | 46 | 1.4454 | 28399 | -24 |
| 2 | 48 | 1.4140 | 29672 | 12 |
| 5 | 49 | 1.3998 | 30274 | -2 |
| 5 | 51 | 1.3725 | 31494 | -18 |
| 5 | 52 | 1.3590 | 32124 | -6 |
| 5 | 53 | 1.3462 | 32739 | -9 |
| 9 | 54 | 1.3337 | 33352 | -14 |
| 4 | 56 | 1.3098 | 34585 | -17 |
| 4 | 57 | 1.2984 | 35193 | -27 |
| 5 | 59 | 1.2756 | 36460 | 4 |
| 5 | 61 | 1.2546 | 37693 | 1 |
| 5 | 62 | 1.2444 | 38313 | 3 |
| 3 | 64 | 1.2248 | 39546 | 0 |
| 1 | 65 | 1.2149 | 40196 | 32 |
| 2 | 66 | 1.2062 | 40780 | -1 |
| 1 | 67 | 1.1967 | 41426 | 26 |
| 2 | 68 | 1.1880 | 42037 | 20 |
| 5 | 69 | 1.1795 | 42644 | 9 |
| 5 | 70 | 1.1710 | 43263 | 10 |
| 3 | 73 | 1.1468 | 45110 | 3 |
| 3 | 74 | 1.1389 | 45739 | 14 |
| 3 | 75 | 1.1314 | 46344 | 1 |
| 8 | 77 | 1.1169 | 47556 | -22 |
| 4 | 78 | 1.1098 | 48169 | -26 |

Table 2. The crystal structure of $Cu_3WO_6$.

Space-group: Pa3 - $T_h^6$

Unit cell parameter: a = 9.797 (± 3) Å

Unit cell content: 8 $Cu_3WO_6$

| Atom | Position | x | y | z | B |
|---|---|---|---|---|---|
| W | 8c | 0.11703 (±8) | 0.11703 (±8) | 0.11703 (±8) | 0.19 (±6) |
| Cu | 24d | 0.40443 (±28) | 0.24568 (±26) | 0.13762 (±24) | 0.69 (±6) |
| O(1) | 24d | 0.2193 (±13) | 0.3016 (±12) | 0.0891 (±12) | -0.13 (±19) |
| O(2) | 24d | 0.4446 (±15) | 0.4636 (±16) | 0.1953 (±16) | 0.33 (±24) |

The errors given are the calculated single sigma values.

Table 3. Weight analysis obtained in the last cycle of refinement. $\Delta = ||\underline{F}_{obs}| - |\underline{F}_{calc}||$, $\underline{w}$ = weighting factor. The $w\Delta^2$ values have been normalized.

| Interval sin θ | Number of independent reflections | $\overline{w\Delta^2}$ | Interval $\lvert\underline{F}_{obs}\rvert$ | Number of independent reflections | $\overline{w\Delta^2}$ |
|---|---|---|---|---|---|
| 0.000 - 0.209 | 24 | 1.411 | 0.0 - 57.2 | 20 | 1.707 |
| 0.209 - 0.263 | 22 | 0.502 | 57.2 - 72.7 | 20 | 0.943 |
| 0.263 - 0.301 | 22 | 0.732 | 72.7 - 89.1 | 21 | 1.167 |
| 0.301 - 0.332 | 24 | 1.160 | 89.1 - 102.1 | 20 | 0.638 |
| 0.332 - 0.357 | 20 | 1.213 | 102.1 - 119.2 | 21 | 0.926 |
| 0.357 - 0.379 | 24 | 1.044 | 119.2 - 135.7 | 20 | 0.409 |
| 0.379 - 0.400 | 20 | 1.290 | 135.7 - 154.4 | 20 | 0.738 |
| 0.400 - 0.418 | 13 | 0.661 | 154.4 - 178.8 | 21 | 1.079 |
| 0.418 - 0.434 | 21 | 1.216 | 178.8 - 205.1 | 20 | 0.944 |
| 0.434 - 0.450 | 13 | 0.769 | 205.1 - 260.2 | 21 | 1.449 |

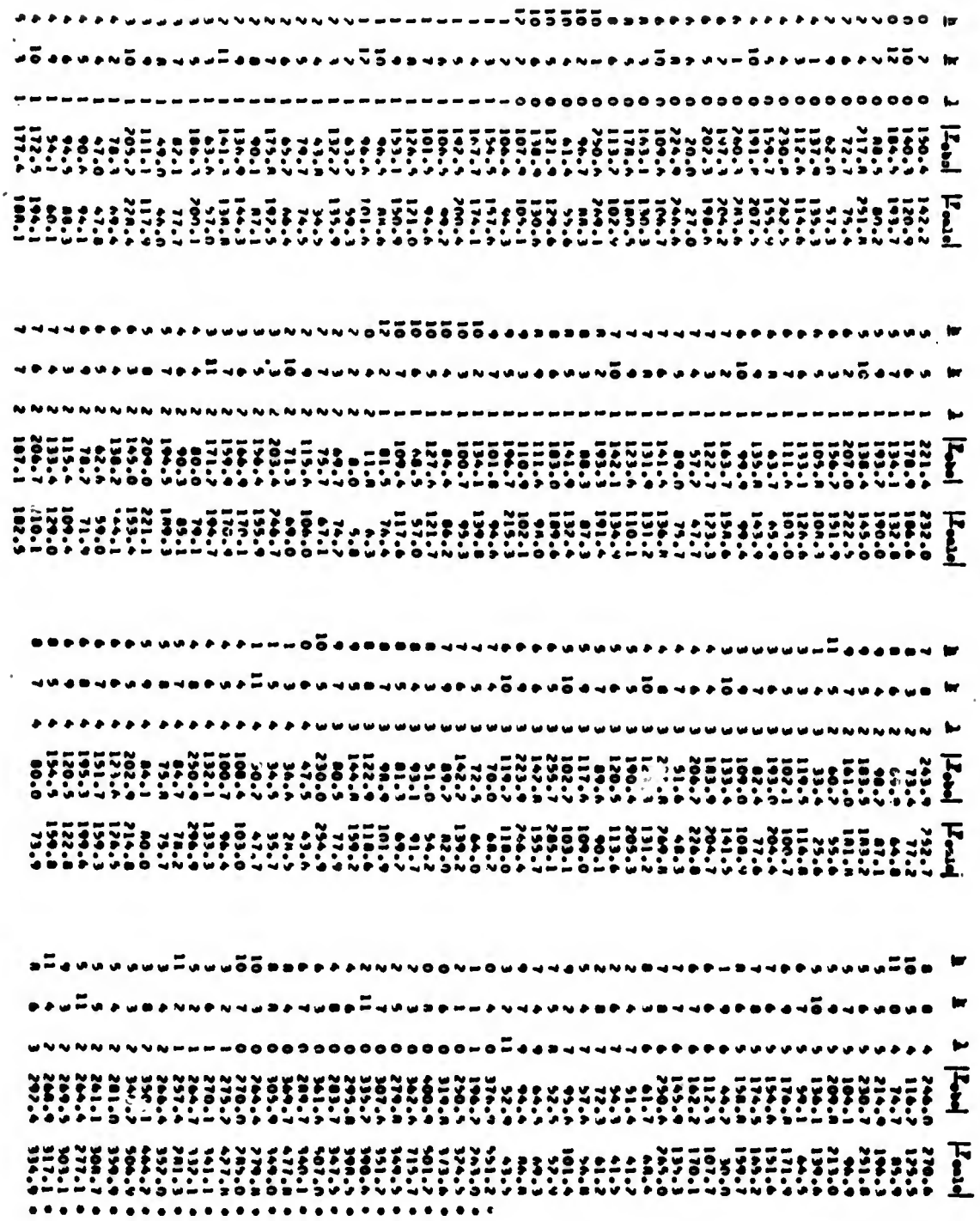

Table 4. Observed and calculated structure amplitudes for $Cu_3WO_6$. The strong reflections which were considered to suffer considerably from extinction and therefore were given zero weight are marked by an asterisk.

Table 5. Interatomic distances and angles in $Cu_3WO_6$

| | | | Distance between the oxygen atoms |
|---|---|---|---|
| **Within octahedra** | | | |
| W - O(2) (3x) | 1.791 (±16) Å | O(1)-W-O(1) (3x) 76.1 (±5)° | 2.57 (±2) Å |
| - O(1) (3x) | 2.085 (±12) | O(1)-W-O(2) (3x) 88.6 (±6) | 2.72 (±2) |
| | | O(1)-W-O(2) (3x) 89.3 (±6) | 2.73 (±2) |
| | | O(2)-W-O(2) (3x) 102.7 (±6) | 2.80 (±2) |
| | | O(1)-W-O(2) (3x) 161.0 (±6) | 3.82 (±2) |
| **Within bipyramids** | | | |
| Cu - O(1b) | 1.921 (±12) Å | O(1c)-Cu-O(1a) 81.1 (±7)° | 2.57 (±2) Å |
| - O(1c) | 1.953 (±13) | O(1c)-Cu-O(2b) 87.7 (±6) | 2.78 (±2) |
| - O(1a) | 2.002 (±12) | O(1c)-Cu-O(2a) 87.5 (±5) | 2.91 (±2) |
| - O(2b) | 2.060 (±15) | O(1b)-Cu-O(1a) 104.3 (±3) | 3.10 (±2) |
| - O(2a) | 2.243 (±16) | O(1b)-Cu-O(2b) 93.3 (±6) | 2.90 (±2) |
| | | O(1b)-Cu-O(2a) 83.4 (±5) | 2.78 (±2) |
| | | O(1a)-Cu-O(2a) 135.8 (±6) | 3.93 (±2) |
| | | O(1a)-Cu-O(2b) 136.3 (±6) | 3.77 (±2) |
| | | O(2a)-Cu-O(2b) 85.1 (±8) | 2.91 (±2) |
| | | O(1b)-Cu-O(1c) 170.8 (±5) | 3.86 (±2) |

**Between polyhedra**

| | | | |
|---|---|---|---|
| W - W | 3.970 (±1) Å | O(1) - Cu | 1.921 (±12) Å |
| - Cu (3x) | 3.090 (±3) | - Cu | 1.953 (±13) |
| - Cu (3x) | 3.420 (±3) | - Cu | 2.002 (±12) |
| - Cu (3x) | 3.516 (±3) | - W | 2.085 (±12) |
| - Cu (3x) | 3.648 (±3) | | |
| | | O(2) - W | 1.791 (±16) |
| Cu - W | 3.090 (±3) | - Cu | 2.060 (±15) |
| - W | 3.420 (±3) | - Cu | 2.243 (±16) |
| - W | 3.516 (±3) | | |
| - W | 3.648 (±3) | | |
| - Cu (2x) | 2.990 (±3) | | |
| - Cu (2x) | 3.219 (±4) | | |
| - Cu (2x) | 3.529 (±3) | | |

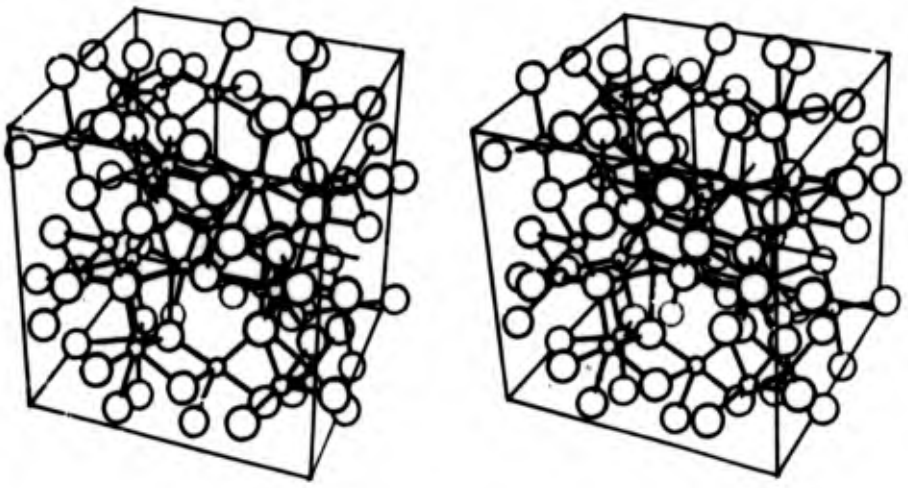

Figure 1. A stereo pair showing the $Cu_3WO_6$ structure. The metal atoms within one unit cell volume and their coordinating oxygen atoms are shown. The origin 0,0,0 is at the centre of the cube but is hidden behind an oxygen atom. The positive directions of the axes from this point are indicated forming a right-handed coordinate system with z vertical. Small spheres = W, medium spheres = Cu, large spheres = O atoms.

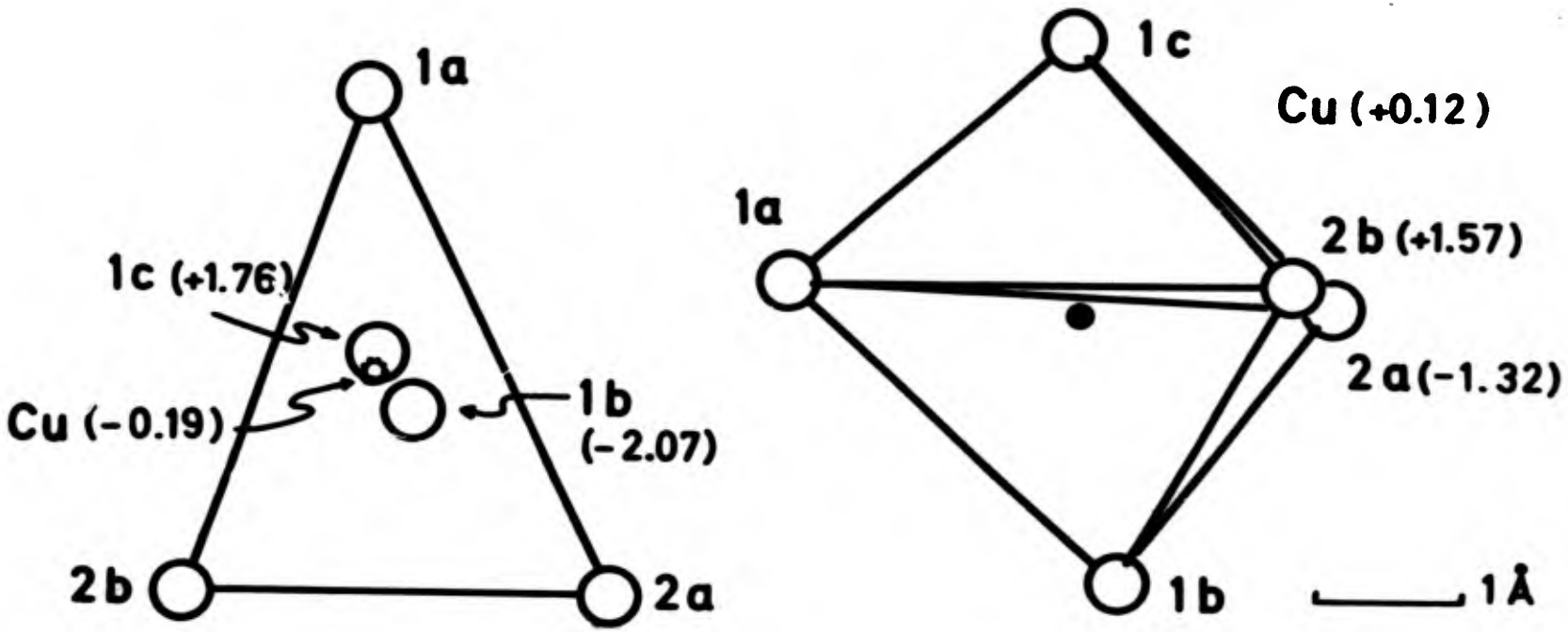


V:17

Fig. 2. The coordination of oxygen atoms around copper shown in two different projections. Left: Projection on the "equator" plane containing the oxygen atoms 1a, 2a and 2b. Right: Projection on the plane through 1a and the "poles" 1b and 1c. The values within parentheses are the distance in Å of the atoms above (+) or below (-) these planes.

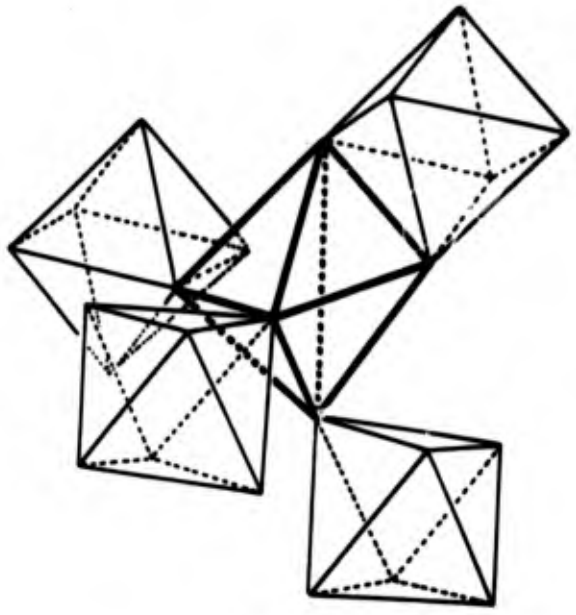

**Figure 3 a.** The arrangement of $WO_6$ octahedra around one $CuO_5$ triangular bipyramid.

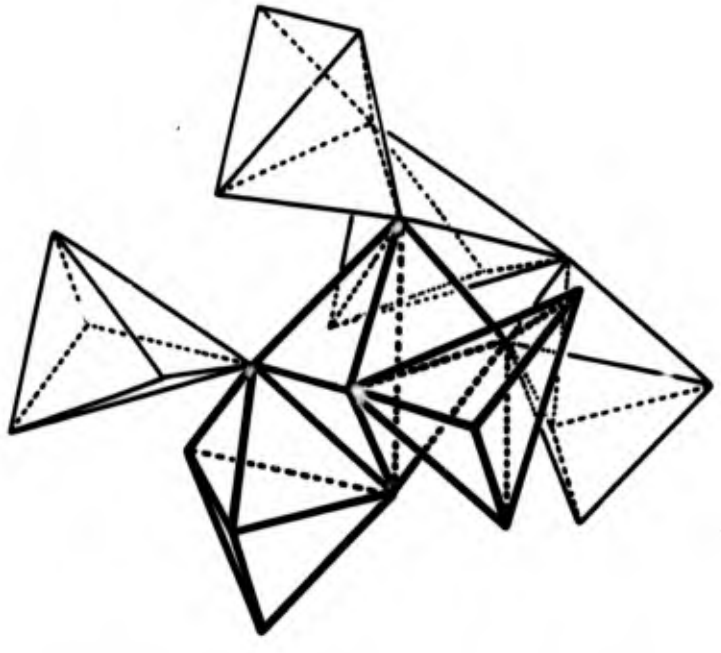

**Figure 3 b.** The arrangement of $CuO_5$ bipyramids around the same $CuO_5$ group as in Figure 3a. The two bipyramids which belong to the same bipyramid ring as the central one are also indicated by heavy lines.

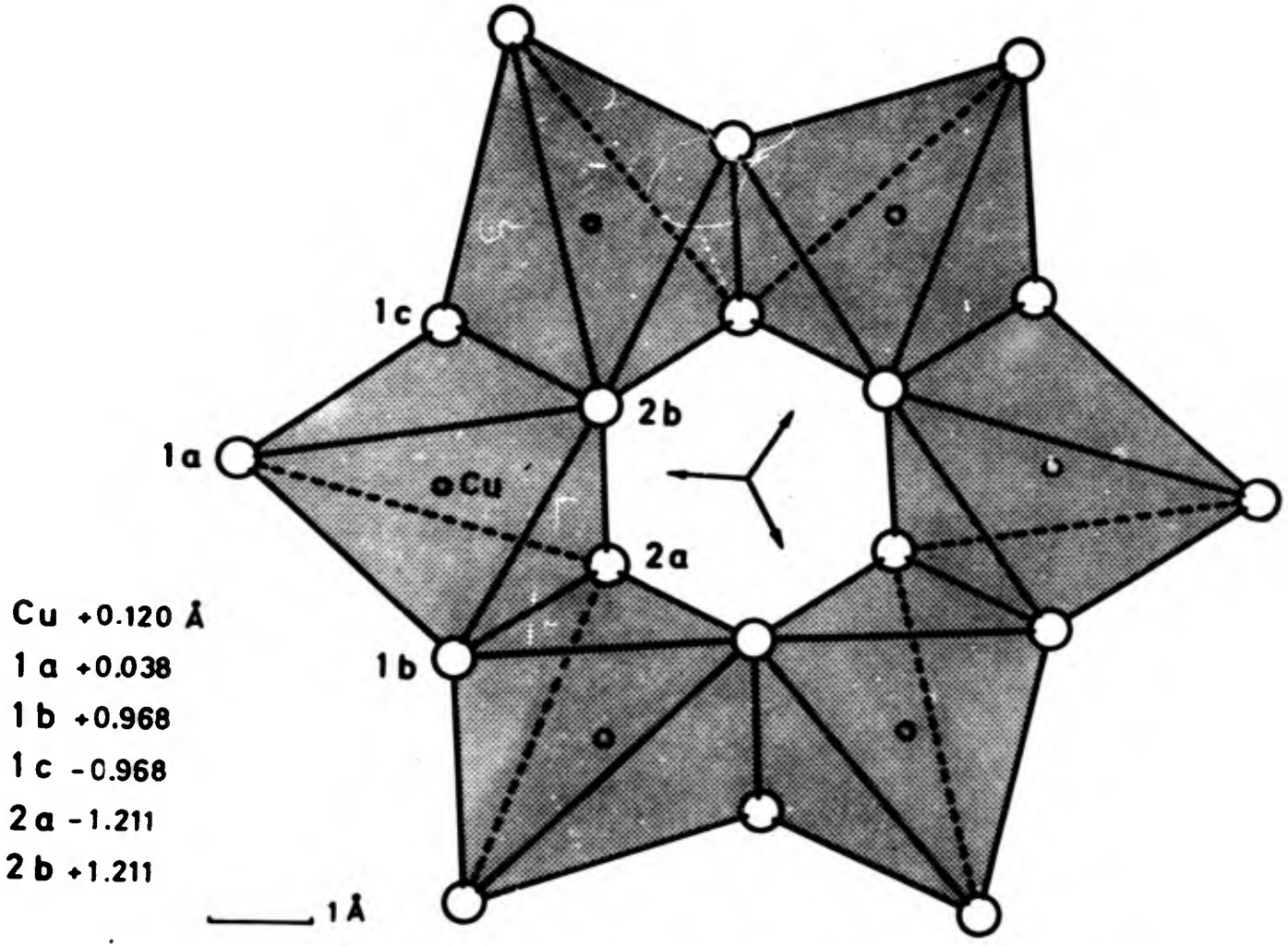


Figure 4. The arrangement of six $CuO_5$ triangular bipyramids forming a ring of symmetry $\bar{3}$ viewed along the trigonal axis. To the left are given the level of the indicated atoms above (+) or below (-) the plane through the inversion centre.

UNCLASSIFIED
Security Classification

## DOCUMENT CONTROL DATA - R & D

*(Security classification of title, body of abstract and indexing annotation must be entered when the overall report is classified)*

1. ORIGINATING ACTIVITY (Corporate author)
University of Stockholm
Institue of Inorganic and Physical Chemistry
Stockholm, Sweden

2a. REPORT SECURITY CLASSIFICATION
Unclassified

2b. GROUP

3. REPORT TITLE
Studies on Structural Relations in Crystalline and Vitreous Compounds

4. DESCRIPTIVE NOTES (Type of report and inclusive dates)
Final Technical Report March 67 - March 68

5. AUTHOR(S) (First name, middle initial, last name)
Peder Kierkegaard, et al.

6. REPORT DATE
March 1968

7a. TOTAL NO. OF PAGES
150

7b. NO. OF REFS
39

8a. CONTRACT OR GRANT NO.
DAJA37-67-C-0421

b. PROJECT NO.

c.
DA Accession No. 9320

d.

9a. ORIGINATOR'S REPORT NUMBER(S)

9b. OTHER REPORT NO(S) (Any other numbers that may be assigned this report)

10. DISTRIBUTION STATEMENT
Distribution of this document is unlimited

11. SUPPLEMENTARY NOTES

12. SPONSORING MILITARY ACTIVITY
US Army R&D Group (Europe)
APO New York 09757

13. ABSTRACT

Studies on the structural properties of crystalline and vitreous polymolybdates and polywolframates have been performed. Results obtained from X-ray studies on sodium dimolybdate and diwolframate are reported and discussed. Details of the structural investigation of dipotassium tetrawolframate are given. The research work has also comprised some studies on glasses and crystalline substances on arsenate molybdate (wolframate) basis containing alkali or silver atoms. Structural data are given for the crystalline compounds $NaZr_2(PO_4)_3$ and $U(PO_3)_4$. Studies on the structural conditions in the ternary oxide systems containing vanadium and molybdenum or wolfram have been performed. Description of the structures are given for the crystalline phases $(Mo_{0.93}V_{0.07})_5O_{14}$, $W_{0.375}V_{0.625}O_{2.5}$ and $W_{0.35}O_{0.65}O_{2.5}$. Preliminary results are given for investigations of copper wolfram oxides. X-ray investigations have been performed on the compounds $CuWO_{4-x}$ and $Cu_3WO_6$. The preparation and properties of amorphous molybdenum trioxide are described. A summary of the types of calculations carried out by computer within this research project is given. Apparatus and measuring techniques for studies or magnetic susceptibility of vitreous and crystalline specimens have been developed. Measurements over the temperature region 90°K-298°K have been performed on the crystalline compounds $MoOPO_4$ and $W_2O_3(PO_4)_2$ and glasses prepared from these phases. The crystals of $MoOPO_4$ have been found to be paramagnetic while the other compounds are diamagnetic.

DD FORM 1 NOV 68 1473 REPLACES DD FORM 1473, 1 JAN 64, WHICH IS OBSOLETE FOR ARMY USE.

UNCLASSIFIED
Security Classification

| 14. KEY WORDS | LINK A | | LINK B | | LINK C | |
|---|---|---|---|---|---|---|
| | ROLE | WT | ROLE | WT | ROLE | WT |
| Ceramics | | | | | | |
| Crystalline Compounds | | | | | | |
| Vitreous Compounds | | | | | | |
| X-ray Diffraction | | | | | | |